UNIVERSITY OF CALIFORNIA
RIVERSIDE

Host- and Cell-Specific Neuroprotective Responses to Chronic *Toxoplasma gondii* Infection

A Dissertation submitted in partial satisfaction
of the requirements for the degree of

Doctor of Philosophy

in

Microbiology

by

Kristina Victoria Bergersen

June 2022

Dissertation Committee
Dr. Emma H. Wilson, Chairperson
Dr. Meera G. Nair
Dr. Ansel Hsiao

The Dissertation of Kristina Victoria Bergersen is approved:

_____

_____

_____

Committee Chairperson

University of California, Riverside

ACKNOWLEDGMENTS

Chapter 2 of this dissertation is a reprint of the original research article as it appears in *Frontiers in Cellular and Infection Microbiology* (2021). I would like to acknowledge my co-authors on the manuscript for their contributions to the research conducted: Ashli Barnes, Dr. Danielle Worth, Dr. Clement David, and Dr. Emma H. Wilson. The Nanostring Bioinformatics team also deserves acknowledgment for their contributions to this publication. *Frontiers* is an open-access journal, and no permission was required to re-print this material. I have included the full citation at the bottom of this paragraph and at the end of the dissertation:

Bergersen, K. V., et al. "Targeted Transcriptomic Analysis of C57bl/6 and Balb/C Mice During Progressive Chronic Toxoplasma Gondii Infection Reveals Changes in Host and Parasite Gene Expression Relating to Neuropathology and Resolution." *Front Cell Infect Microbiol* 11 (2021): 645778. Print.

Dr. Clement David is credited for the generation of the Evans Blue staining data presented in Figure 12 (Chapter 3). I would additionally like to thank the following people who have contributed significantly to the generation of data material presented in Chapter 3: Bill Kavvathas, Dr. Byron D. Ford, and Dr. Emma H. Wilson. Dr. Frances Mercer graciously provided guidance and the HL-60 cells used for experiments in Chapter 4. In addition to funding awarded to Dr. Emma H. Wilson, the work in this dissertation was also supported in part by the Nanostring Mini Grant Fellowship.

At this time, I would like to thank the members of the University of California Riverside's Center for Glial Neuronal Interactions (CGNI) and the Genomics and School of Medicine Research COREs for all advice and use of equipment. I would like to thank the UCR Genomics, Microscopy, and School of Medicine Research COREs for all advice, use of equipment, and processing of samples where appropriate. I am also thankful to the UCSD IGM Genomics Center for sequencing of RNA samples. I sincerely appreciate all the work conducted by UCR's IACUC and the animal husbandry provided by Leslie Karpinski, Linda McCloud, Jennifer Johnson, and all the vivarium staff.

I would like to thank my PI Dr. Emma Wilson for her invaluable guidance and superb mentorship throughout my PhD journey. Thank you to my Dissertation and Qualifying Exam committee members, especially Dr. Meera Nair and Dr. Ansel Hsiao, without whom I would not have curated the caliber of research presented here. Thank you to all my current and previous lab mates (Edward Vizcarra, Zoe Figueroa, Emily Tabaie, Dr. Arzu Ulu, and Dr. Danielle Worth) and undergraduate students (especially Ashli Barnes, Bill Kavvathas, and Mike Akaraphanth) for all of the advice, support, and help with conducting the research experiments presented in this dissertation.

DEDICATION

This dissertation is dedicated to my amazing family (Eric, Ann, Jacob, and Emily Bergersen, John and Anthony Kruzic, and Kirstie Duncan) and my incredible fiancé Mike Calandrino, without whom I would not be where and who I am today. Thank you from the bottom of my heart for all of the unconditional love, support, stress relief, funny jokes, and genuine excitement throughout this crazy PhD journey. I would not have maintained my sanity throughout this process if it were not for each and every one of you. Your love and support mean the world to me, and I love you all beyond words.

ABSTRACT OF THE DISSERTATION

Host- and Cell-Specific Neuroprotective Responses to Chronic *Toxoplasma gondii* Infection

by

Kristina Victoria Bergersen

Doctor of Philosophy, Graduate Program in Microbiology
University of California Riverside, June 2022
Dr. Emma H. Wilson, Chairperson

Infection with the protozoan parasite *Toxoplasma gondii* leads to the formation of lifelong cysts inside neurons in the brain of its host, and it is estimated that approximately one third of the world's population is infected. Infection in the immunocompromised can cause severe clinical manifestations like neuropathology, toxoplasmic encephalitis, and death. While chronic infection can lead to severe clinical manifestations of disease, infection in immunocompetent hosts remains largely asymptomatic. This suggests there are neuroprotective mechanisms at work that preserve neuronal integrity and maintain a balanced brain environment during chronic infection, but these mechanisms remain largely unknown. The concept of neuroprotection has been demonstrated in other models of central nervous system (CNS) injury and infection such as ischemic stroke and experimental cerebral malaria through the work of neuroprotective molecules such as the NRG-1/ErbB4 signaling pathway and MSR1. In addition, innate and adaptive immune

cell responses to chronic Toxoplasma infection play a large role in balancing the fragile CNS environment and preventing clinical manifestations of disease.

This collective study identifies host- and parasite-specific transcriptional changes relating to infection-induced neuropathology and neuroprotective repair mechanisms in the CNS via targeted transcriptomic analysis. Through the employment of various techniques such as multi-parameter flow cytometry, single-cell RNA sequencing, and *in vivo* depletion experiments, it explores a population of functionally heterogenous neutrophils that play a protective role in the brain throughout chronic infection. Additionally, *in vitro* work using human neutrophil-like cells demonstrates cyst-specific responses tailored to chronic infection. Taken together, this overall study provides important insights into the dependence of neuroprotective mechanisms on host immune status, characterizes a protective chronic neutrophil population, and bridges the gap between neutrophil responses in murine and human models of chronic *T. gondii* infection.

TABLE OF CONTENTS

LIST OF TABLES

LIST OF FIGURES

Chapter 1: Introduction

Toxoplasma gondii, parasite life cycle, and infection

Toxoplasma gondii is a resilient parasite that infects ~ 10% of the population older than 6 years in the United States alone and more than 60% of populations in other countries worldwide (Prevention 2018). Infection with this protozoan parasite leads to a lifelong infection characterized primarily by the formation of cysts inside neurons of the brain, and it is estimated that one third of the world's population is infected (Montoya and Liesenfeld 2004). This parasite is capable of invading any nucleated cell, and in addition to its primary feline host, it has a wide array of intermediate hosts comprised of any warm-blooded animal including livestock and humans (Robert-Gangneux and Dardé 2012, Liu et al. 2015).

In its primary feline host, the parasite is capable of undergoing sexual reproduction characterized by the transition of fast-replicating sporozoites into dormant oocysts, which are excreted into the environment through feline feces (Dubey 1988). These oocysts are then ingested by other intermediate hosts such as mice and livestock (pigs, cows, sheep, etc.) where *T. gondii* undergoes only asexual reproduction. This asexual reproduction involves the lysing of oocysts, transition of free parasites into fast-replicating tachyzoites, rapid dissemination throughout the body until entry into the host brain or skeletal muscle, transition from fast-replicating tachyzoite to slow-replicating cyst-forming bradyzoite, and then formation of long-lasting cysts inside brain neurons or skeletal muscle cells (Dubey 1988). The formation of cysts inside neurons of the brain specifically has been shown to affect murine behavior and reduce their natural fear of feline predators (Berdoy,

Webster and Macdonald 2000, Boillat et al. 2020, Vyas et al. 2007). This change in behavior enables the ingestion of *T. gondii* tissue cysts by the primary feline host and allows for the start of sexual reproduction once again. While this is the preferred pathway of the parasite, the ability of *T. gondii* to infect any warm-blooded animal results in a multitude of "dead-end" infections in intermediate hosts including humans. Infection of human hosts occurs most commonly via the ingestion of *T. gondii* through consumption of infective tissue cysts in undercooked meat, ingestion of infective oocysts on unwashed fruits and vegetables or in contaminated water, and inhalation of infective oocysts present in cat litter (Dubey 1988, Baldursson and Karanis 2011, Meireles et al. 2015).

Clinical Toxoplasmosis

While infection with Toxoplasma is often asymptomatic due to a robust host immune response, infection in an immunocompromised host can result in serious clinical manifestations of disease including parasite reactivation in the brain, the onset of Toxoplasmic encephalitis, and death (Wang et al. 2017). Examples of commonly affected patients include those with HIV/AIDS, cancer, and organ transplant recipients (Pott and Castelo 2013, Lu et al. 2015, Da Cunha et al. 1994). In immunocompromised patients, the most common cause of disease is caused by latent reactivation of the cyst-form of the parasite in the brain which leads to neurological symptoms including headache, disorientation, and convulsions among others (Robert-Gangneux and Dardé 2012). While latent parasite reactivation is the most common cause of Toxoplasma-associated disease, acute infection with this parasite under immunocompromised conditions can also lead to severe disease involving multiple organs (Machala et al. 2015).

Importantly, while there are treatment strategies available for the acute stage of infection as reviewed by Dunay et. al (Dunay et al. 2018), the signs of Toxoplasma infection often go unnoticed, and there are no current treatments available for the chronic stage of infection despite promising studies in animal models (Schultz et al. 2014). The "gold-standard" treatment of acute Toxoplasmosis has long been a combination of sulfonamide and pyrimethamine drugs since successful mouse experiments were performed in the 1940s and 1950s (Sabin and Warren 1942, Eyles and Coleman 1953). While these treatments have been successfully utilized in the treatment of Toxoplasma infection in immunocompetent patients, the drugs are often contraindicated during pregnancy, and alternative, albeit sometimes less effective, treatment methods must be employed in pregnant women (Desmonts and Couvreur 1974, Daffos et al. 1988, Buonsenso et al. 2022).

Infection of women with *T. gondii* during pregnancy can result in congenital toxoplasmosis that is passed from mother to fetus (Vogel et al. 1996). Previous work has demonstrated varying levels of congenital toxoplasmosis severity depending on immune status of the mother and stage of pregnancy during time of infection (Thiébaut et al. 2007). While active infection of pregnant women can lead to serious congenital defects, pregnant women who are latently infected with Toxoplasma are unlikely to pass infection to the fetus (Desmonts and Couvreur 1974). While these clinical outcomes of *T. gondii* infection can lead to devastating consequences, the majority of infections in immunocompetent hosts remain asymptomatic due to a continuous robust and balanced immune response.

Immune response to infection

Following ingestion of *T. gondii*, there is a period of acute systemic infection lasting approximately one week characterized by rapid dissemination of the parasite throughout the body in its acute tachyzoite form (Montoya and Liesenfeld 2004). This process begins via the lysing of cysts in stomach acid and progression of the parasites into the small intestine of the host. Once in the small intestine, bradyzoites from the lysed cysts transition to the fast-replicating tachyzoite form of the parasite and infect intestinal epithelial cells (Liesenfeld et al. 1996). Following the infection of intestinal epithelial cells, the innate immune response is activated starting with neutrophil recruitment to the site of infection, and these cells are absolutely necessary to control acute infection (Bliss et al. 2001). These cells not only begin attacking the parasite directly (Abi Abdallah et al. 2012), but they also increase the immune response by amplifying other innate responses (Miranda et al. 2021) and recruiting other innate immune cells such as dendritic cells, macrophages, inflammatory monocytes, and natural killer (NK) cells to sites of infection (Sukhumavasi, Egan and Denkers 2007) to prevent the rapid spread of infection. These innate immune cells are also able to phagocytose some *T. gondii* parasites and kill them by sending them to lysosomal compartments for degradation (Sibley, Weidner and Krahenbuhl 1985).

Despite these early immune responses, *T. gondii* is very capable of evading the host immune response and can continue its rapid spread throughout the body. During this rapid dissemination, the parasite utilizes a multitude of techniques to hijack the host immune response. These techniques include infection of antigen presenting cells (APCs)

such as macrophages and dendritic cells, hijacking of these immune cell functions, and progression throughout the body in hiding within these cell types (Lüder et al. 1998, Lima and Lodoen 2019). Through these and the deployment of other parasite-dependent virulence factors (Hunter and Sibley 2012, Dupont, Christian and Hunter 2012, Du et al. 2014), the parasite is able to effectively evade the host immune response and travel to its environment of interest, the brain (Feustel, Meissner and Liesenfeld 2012).

Upon entry into the brain, *T. gondii* transitions from its fast-replicating tachyzoite form back into bradyzoite form in order to form dormant lifelong cysts. This transition allows *T. gondii* to evade immediate detection by the host immune response, and the parasite remains sequestered in dormant cyst form within neurons in the brain creating a lifelong infection (Tomita et al. 2013, Di Cristina et al. 2008). Neurons are the primary cell type infected in the brain, and they are the only cell type where cyst formation occurs and is maintained (Cabral et al. 2016). While cysts are less recognizable to the immune response, as a result of the foreign presence of *T. gondii* in the brain, an immune response involving both innate and adaptive cells is initiated (Dupont et al. 2012, Graham et al. 2020, Bergersen et al. 2021).

Resident CNS immune cells such as astrocytes and microglia initiate this immune response by secreting various chemokines and cytokines like CXCL1, IL-8, IL-17, and IL-33 to recruit peripheral immune cells as reviewed by Suzuki et. al (Kostic et al. 2017, Still et al. 2020, Suzuki 2002). Additionally, astrocytes are responsible for the activation of inflammatory cytokine production in the brain as a response to infection via the upregulation of STAT1 signaling (Hidano et al. 2016). During this process, APCs also

travel to the lymph node bearing parasite-specific antigen to activate *T. gondii*-specific T cell responses via MHC II antigen presentation (Lüder and Seeber 2001). This leads to the recruitment of innate immune cells like macrophages (Gazzinelli et al. 1993a) and neutrophils (Biswas et al. 2017) followed by adaptive *T. gondii*-specific T cells (Ploix et al. 2011), all of which are required to control parasite replication and maintain a balanced environment (McGovern and Wilson 2013, Sasai and Yamamoto 2019, Biswas et al. 2017).

The infiltration of peripheral immune cells into the immune-privileged infected brain requires migration across the blood brain barrier (BBB). As mentioned above, the recruitment of these cells to the CNS begins via the production of chemokines by brain-resident immune cells like microglia and astrocytes. In response to the production of IL-8 by CNS cells, neutrophils are recruited to the BBB via binding of the chemokine receptors CXCR1 and CXCR2 (Russo et al. 2014). Once neutrophils arrive at the BBB, they utilize various integrins such as VLA-4 and CD15 to "crawl" along the vasculature in response to upregulated VCAM-1 and are able to migrate into the brain parenchyma (Debierre-Grockiego et al. 2020, Nakayama et al. 2001). Other peripheral immune cells like macrophages and inflammatory monocytes are also recruited to the brain in a chemokine-dependent manner and also transmigrate across the BBB. Upon entry into the brain, neutrophils and other innate immune cells begin secreting early pro-inflammatory cytokines such as IL-6 and IL-12 to aid in T cell recruitment and stimulation of T cell responses (Yap, Pesin and Sher 2000, Cassatella et al. 1995, Gazzinelli et al. 1993b, Ge et al. 2014, Gazzinelli et al. 1994).

Adaptive T cells are recruited to the brain via the production of various cytokines, chemokines, and antigen presentation via MHC II as mentioned above. To enter the brain, parasite-specific activated T cells respond to the upregulation of VCAM1 on the vascular endothelial cells of the BBB via upregulation of the integrin VLA-4 (Sa et al. 2014). Once in the brain, adaptive CD4+ and CD8+ T cells are responsible for the majority of infection control via the production of the pro-inflammatory cytokine IFNγ as well as production of parasite-killing mechanisms such as granzymeB and perforin (Nishiyama et al. 2020, Landrith, Harris and Wilson 2015, Merritt et al. 2020, Suzuki, Conley and Remington 1989). Continuous peripheral inflammation of CD4+ and CD8+ T cells specifically is required to prevent uncontrolled parasite replication and potentially fatal pathology (Gazzinelli et al. 1992). This supports the absolute necessity of a constant immune pressure on the parasite by immune cells in the brain in order to control infection.

Regulation of CNS inflammation during infection

The necessity of constant immune pressure in order to control infection in the brain encourages a pro-inflammatory resistance to *T. gondii* infection, but this pro-inflammatory response can also result in devastating pathologies such as excessive inflammation and cell death if not mediated properly. *T. gondii* has been found to regulate multiple aspects of the host immune response to maintain a safe environment during chronic infection, thereby establishing a delicate balance between immune response to infection and parasite survival (Hwang et al. 2018). A vital aspect of regulation of inflammation in the brain during chronic infection is the production of an

equally strong anti-inflammatory response, which is regulated and induced by both host and parasite mechanisms. Immune cells involved in these mechanisms include alternatively activated macrophages and possibly neutrophils; and anti-inflammatory cytokine production including IL-10 and IL-27.

Macrophages and neutrophils are classically associated with the pro-inflammatory response to *T. gondii* infection through the production of IL-12, which recruits T cells to the brain and stimulates the production of IFNγ (Gazzinelli et al. 1993b). While these cells are important in the pro-inflammatory immune response to *T. gondii* infection, previous work has demonstrated that there are alternatively activated macrophages that are associated with an anti-inflammatory immune response during infection. These alternatively activated macrophages, also known as M2 macrophages, produce a chitinase called AMCase, which is capable of cyst lysis and is required for protective immunity during chronic infection (Nance et al. 2012). M2 macrophages also limit inflammation caused by proinflammatory cytokines TNFα and IL-1β through the production of IL-10 and TGFβ (Bogdan et al. 1992).

As mentioned above, neutrophils are prominent first responders to infection and are key producers of the pro-inflammatory cytokine IL-12 after being recruited to sites of infection via the IL-8/CXCR2 signaling pathway (Del Rio et al. 2001, Cassatella et al. 1995). Neutrophils are commonly associated with the pro-inflammatory response to *T. gondii* infection, but a secondary subset of neutrophils known as PMN-II's has been discovered in other disease models that is associated with more anti-inflammatory effects (Tsuda et al. 2004). These anti-inflammatory effects include production of the anti-

inflammatory cytokines IL-10 and IL-4 and the chemokine CCL2 and the blocking of IFNγ (Tsuda et al. 2004). The production of IL-10, IL-4, and CCL2 by this secondary subset of neutrophils helps to limit inflammation in these other models of disease, but the presence and role of these neutrophil subsets in regulating inflammation caused by *T. gondii* infection remain unknown.

In addition to alternative functions of immune cells to regulate inflammation, anti-inflammatory cytokine production is another mechanism employed to maintain a balanced CNS environment during infection. IL-10 is one of the many anti-inflammatory cytokines associated with limiting inflammation caused by *T. gondii* infection. This cytokine has been known to limit the functions of infiltrating T cells and natural killer (NK) cells during *T. gondii* infection (Neyer et al. 1997). Inflammation caused by these cells during infection can be devastating, as is shown in an IL-10 -/- model of infection. In this model, IL-10 -/- mice develop a lethal inflammatory phenotype during chronic infection caused by increased numbers of infiltrating macrophages and T cells, which also leads to an increase in pro-inflammatory cytokine production (Wilson et al. 2005). Despite the lethal inflammatory response induced by the presence of macrophages and T cells in IL-10 -/- mice, it has been demonstrated that the main producers of IL-10 during chronic infection in WT mouse models are in fact these very same infiltrating macrophages and CD4+ T cells (Wilson et al. 2005). IL-10 plays a vital role in the regulation of inflammation caused by CD4+ T cells in the brain, which occurs in a self-regulating manner (Brien et al. 2018). Following interaction between macrophages and T cells and the production of IFNγ, IL-10 is also produced by CD4+ T cells to limit

inflammation. Similarly, blockade of the IL-10 receptor IL-10R results in similar infiltration of CD4+ T cells and levels of pro-inflammatory cytokine production (Brien et al. 2018). These results demonstrate that IL-10 is completely vital to regulate levels of inflammation in the brain during chronic infection and to maintain the delicate balance established during infection.

The cytokine IL-27 is commonly associated with the promotion of Th1 differentiation in naïve CD4+ T cells. While this is the common perception of IL-27, recent evidence has been found that suggests an anti-inflammatory role for this cytokine and its receptor. IL-27 and its receptor WSX-1 have been found to limit the intensity of the CD4+ T cell pro-inflammatory response, as evidenced by the development of a lethal T cell-mediated inflammatory disease in WSX-1 -/- mice (Villarino et al. 2003). These mice succumb to infection due to excessive IFNγ production caused by CD4+ T cell infiltration into the brain during chronic infection. This demonstrates a role for IL-27 to limit inflammation caused by the immune response to *T. gondii* infection through interaction with its WSX-1 receptor. IL-27 also works together with IFNγ to limit pathology caused by *T. gondii* infection through the promotion of T-bet expression and CXCR3 in Treg cells at mucosal sites in the body, signifying its importance in regulation of inflammation by controlling the Th1 immune response (Hall et al. 2012).

Transcriptomic changes relating to neuropathology and regulation of infection

It is important to keep in mind the delicate balance between parasite control mechanisms and the maintenance of functional brain homeostasis during infection. There is still much

that is unknown about how the brain environment changes in response to infection, and one way to investigate this is by looking at infection-induced changes at the transcriptomic level. Previous data have reported broad transcriptomic changes in the brain of *T. gondii*-infected mice at both acute and chronic time points (Hu et al. 2020, Tanaka et al. 2013, Li et al. 2020, Schneider et al. 2019). However, these studies often focus on one specific time point in chronic infection, and they fail to explore transcriptomic changes that occur over the course of infection that are important to determine directional change. The parasite itself goes through genetic changes in order to convert from a fast-replicating tachyzoite during acute systemic infection to a cyst-forming bradyzoite during the early stage of chronic infection after crossing the blood brain barrier (Hong, Radke and White 2017, Radke et al. 2018, Feustel et al. 2012, Lachenmaier et al. 2011). At this early chronic stage, CNS-resident cells begin actively recruiting peripheral immune cells in response to the presence of the parasite, which is still transitioning from tachyzoite to bradyzoite to cyst. As infection progresses and reaches the mid-chronic stage, cyst numbers stabilize as the majority of parasites in the brain are now slow-replicating bradyzoites. At this point in chronicity, both innate and adaptive peripheral immune cells have been in the brain for some time and are constantly maintaining the balance between pro- and anti-inflammatory cytokine production. In addition, subtle neuropathology is commonly seen as noted by changes in morphology and function of both infected and non-infected neurons and changes in glia (Graham et al. 2020, David et al. 2016). Control of infection is maintained for the lifetime of the host and pathology at this stage can vary depending on the genetics of the parasite as well as

the background of the host (Mukhopadhyay, Arranz-Solís and Saeij 2020, Lilue et al. 2013, Denkers 1999, Liesenfeld et al. 1996, Lee and Kasper 2004). These changes in parasite phenotype, host immune response, and neuropathology have yet to be fully explored in the context of progressive chronic infection.

The lifelong presence of cysts within neurons and continuous neuroinflammation gives ample opportunity for *T. gondii* infection to initiate significant changes in the brain. Recent work has identified anatomical location of immune cells that could largely influence these changes, specifically the presence of inflammatory monocytes in the olfactory cortex which could lead to infection-induced behavioral changes (Schneider et al. 2019). Indeed, many studies have demonstrated significant alterations in rodent behavior including attraction to cat urine postulated to be parasite manipulation to maximize the chances of return to the definitive host (Boillat et al. 2020, Vyas et al. 2007, Berdoy et al. 2000). Additionally, infected mice also show significant changes in behavior in an elevated plus maze (David et al. 2016). Such changes may be related to direct and indirect modulation of neurotransmitters including imbalances in excitatory and inhibitory signaling and the production of dopamine (David et al. 2016, Brooks et al. 2015, Prandovszky et al. 2011, Ngô et al. 2017, Webster and McConkey 2010). However, the presence of the parasite is hard to unlink from the degree of neuroinflammation and any changes in host behavior is likely as much to do with cytokine signaling as the presence of the parasite (Boillat et al. 2020).

To address the complex interplay of infection, inflammation and neurochemistry, there have been several studies investigating transcriptional changes related to chronic CNS

Toxoplasma infection. RNAseq analysis of *in vitro* cultured neurons, astrocytes, fibroblasts and skeletal muscle cells tested infection-induced changes in cell -specific transcriptomes and indicated a host-cell dependent genetic basis for spontaneous cyst formation in neurons and skeletal muscle cells (Swierzy et al. 2017). A comprehensive transcriptomic and proteomic study of human brain tissue including those congenitally infected suggests *T. gondii* infection alters neurodevelopment, plasticity, and disease association in various neural and immune networks (Ngô et al. 2017). Although not as clinically relevant, murine studies are robust and have recently underlined the dominance of immune changes in the brain following infection with oocysts of the Pruqniaud strain revealing activated pathways of metabolism and biosynthesis at both acute and chronic stages of infection (Hu et al. 2020, Jia et al. 2013).

As with all infections, host genetic background plays an important role in disease and despite the ability of Toxoplasma to establish itself in almost all mammalian hosts, it has been known for some time that the development of disease is highly dependent on mouse strain, recently reviewed by Mukhopadhyay (Johnson et al. 2002, Blackwell, Roberts and Alexander 1993, Resende et al. 2008, Mukhopadhyay et al. 2020). Indeed, continuous culturing of Toxoplasma strains in vivo rely upon resistant and susceptible strains of mice to maintain virulence and cyst formation, something vitally important to maintain life cycle competency (Goerner et al. 2020). Thus, in the common lab strains of mice, C57Bl/6 are susceptible to disease with greater parasite burden and inflammation while BALB/c mice are resistant to encephalitis dependent on MHC presentation of the antigen GRA6 (Tanaka et al. 2013, Jia et al. 2013, Ngô et al. 2017, Li et al. 2020, Hu et al. 2020).

These striking differences may provide an opportunity to model disease processes in the brain however little direct comparisons of the kinetics of this host response have been conducted.

Neuroprotective and alternative mechanisms during infection and CNS disease

During chronic infection, despite cyst-containing neurons and brain inflammation caused by the recruitment of peripheral immune cells, Toxoplasma causes few clinical symptoms in the immunocompetent host. However, underlying changes in neurochemistry and significant changes in the health of neurons (David et al. 2016, Mendez et al. 2021) suggest a constant need to balance inflammation and protect against neuropathology. As stated previously, Toxoplasma infection of the brain leads to necessary inflammatory responses that are mediated and encouraged partially by CNS-resident microglia. Recent work utilizing a modified commonly used anti-depressant demonstrates inhibition of damaging pro-inflammatory responses and the return of a neuro-supportive environment during *in vitro* infection (Shinjyo et al. 2021). Additionally, exogenous treatment of *T. gondii*-infected mice with the drug resveratrol leads to neuroprotective effects that are mediated by purinergic signaling (Bottari et al. 2020). Recent studies to determine Toxoplasma-induced changes in immunological and neurological transcripts in the brain supports neurological changes but also reveals potential neuroprotective pathways (Bergersen et al. 2021). While exogenous treatment methods induce a more neuroprotective environment during infection, the recent research conducted during untreated chronic infection suggests that there are already endogenous neuroprotective

mechanisms at work to maintain brain homeostasis and prevent clinical disease. However, these endogenous neuroprotective mechanisms remain poorly understood.

The concept of neuroprotection and resolution of inflammation has been investigated in models of sterile CNS injury as well as a non-Toxoplasma model of infection including spinal cord injury, ischemic stroke, and experimental cerebral malaria. In CNS injury models, one of the mechanisms employed to maintain neuronal integrity is the signaling of the endogenous ligand Neuregulin 1 (NRG-1) through its main receptor ErbB4. NRG-1 is a ligand naturally produced by the body, particularly by neurons in the CNS, during brain development, and this ligand usually signals through its main receptor ERbB4 to aid in neuronal development and maintain mature neuron function (Falls 2003, Li et al. 2007, Cahill et al. 2013). In instances of CNS injury, this signaling pathway switches from maintaining homeostasis to providing protection. In a model of ischemic stroke, NRG-1 and ErbB4 regulate inflammation and reduce pro-inflammatory cytokine production by microglia through alternative activation of the NFκB pathway (Simmons et al. 2016). This signaling pathway also protects neuronal integrity and survival and protects against ischemia-induced damage (Xu et al. 2005). In other models of CNS injury such as spinal injury and epilepsy, NRG-1 and ErbB4 are also neuroprotective by encouraging a regulatory immune response and regulating glutamate activity (Alizadeh et al. 2018, Tan et al. 2011, Yu et al. 2015). In a cerebral malaria mouse model of infection, another Apicomplexan parasite, the NRG-1/ErbB4 pathway attenuates mortality associated with disease by inhibiting neuronal cell death through regulation of ErbB4-mediated AKT and STAT3 signaling (Solomon et al. 2014, Liu et al. 2018).

In addition to direct neuroprotective mechanisms such as NRG-1/ErbB4 signaling, there are other molecules that aid in neuroprotection in a more indirect manner. For instance, resolution of neuropathology in a model of ischemic stroke is supported by the functions of macrophage scavenger receptor 1 (MSR1). This scavenger receptor is commonly associated with clearance of debris during homeostasis. In a model of ischemic stroke, MSR1 functions in an indirectly neuroprotective manner through clearance of damage signals, debris, and revascularization of damaged tissue (Shichita et al. 2017). Further work has identified MSR1 and CD21 interactions as indirectly neuroprotective through CD21-dependent enhancement of DAMP signal clearance and TLR4 inhibition by MSR1 (Liu et al. 2021, Zou et al. 2021). In addition to increased MSR1 function in ischemic stroke, transcripts of this scavenger receptor are also significantly upregulated during Toxoplasma infection in a step-wise manner correlating with increasing chronicity (Bergersen et al. 2021). Expression and function of these directly and indirectly neuroprotective molecules contribute to neuroprotection in other models of CNS inflammation and infection and help maintain a balanced CNS environment. The neuroprotective functions of these pathways in other models of CNS inflammation and infection and their increased upregulation during chronic infection suggests potential neuroprotective activity in Toxoplasma infection.

Alternative role of neutrophils in models of disease

As mentioned previously, neutrophils are commonly thought of as one of the earliest host responses to infection, are one of the primary cell types responsible for the recruitment of other innate immune cells, and their presence is vital for control of acute Toxoplasma

infection (McGovern and Wilson 2013, Debierre-Grockiego et al. 2020, Petri et al. 2000, Bliss et al. 2001). Classical neutrophil responses during Toxoplasma infection include early production of the cytokine IL-12, production of reactive oxygen species (ROS), and recruitment of other immune cells (Sukhumavasi et al. 2007). In addition, neutrophils are capable of trapping and killing *T. gondii* tachyzoites through direct phagocytosis; degranulation, or the release of pre-formed toxic granules into the environment; and NETosis, where neutrophils create neutrophil extracellular traps (NETs) by expelling their inner components including DNA and granule proteins to trap and kill free parasites (Abi Abdallah et al. 2012, Naegelen et al. 2015, Miranda et al. 2021).

While T cells are thought to be the main immune modulator of chronic Toxoplasma infection, recent independent research groups have identified a small population of neutrophils present in the brain between 2- and 4wpi (Biswas et al. 2017, Schneider et al. 2019). Work by the Dunay group not only identifies neutrophils in the brain during chronic Toxoplasma infection, but also introduces the idea of alternative functions of these cells through the characterization of various pro-inflammatory and regulatory indicators including CD62-L expressed by these cells (Biswas et al. 2017). Additionally, this study demonstrates successful depletion of these neutrophils from the periphery and brain during chronic infection which leads to increased parasite burden in the CNS. This work collectively suggests there may be a more versatile role for neutrophils during chronic infection.

Previous literature focusing on potential alternative roles for neutrophils in non-Toxoplasma models describes two basic classes of these cells based on their differential

expression of markers such as the integrins CD15 and CD49d, pro- and anti-inflammatory cytokines, and various chemokines like CCL2 (Tsuda et al. 2004, Beyrau, Bodkin and Nourshargh 2012, Nakayama et al. 2001). The first is a "classical" pro-inflammatory subset that is associated with classical macrophage activation, increased granularity, NETosis, and the production of Th1 cytokines IL-12 and TNFα (Nakayama et al. 2001, Beyrau et al. 2012). The second class is considered "alternative" based on anti-inflammatory cytokine expression like IL-10 and IL-4, association with alternative macrophage activation, decreased granularity, and angiogenesis and vascular repair functions (Tsuda et al. 2004, Beyrau et al. 2012).

While earlier studies introduce the idea of alternative neutrophil functions, more recent works investigating neutrophils in homeostasis, tissue injury, and non-Toxoplasma models of infection have demonstrated a much broader range of previously undescribed heterogeneity and functions among these cells (Peiseler and Kubes 2019, Xie et al. 2020). This heterogeneity is dependent on a variety of factors, the first of which is age. Immature neutrophils in the bone marrow differ distinctly from mature cells in circulation, and aged neutrophils classified as CXCR4+ make up a completely separate subset (Xie et al. 2020, Massena et al. 2015, Biswas et al. 2017). An additional factor that determines neutrophil function and encourages heterogeneity is the differentiation between circulating and tissue-resident neutrophils as well as the tissue environment (Ballesteros et al. 2020). Finally, neutrophil heterogeneity is also dependent on the immune status of the host, and the presence of injury or infection will induce neutrophil differentiation specific to the responses required of them, whether that be classical

infection control mechanisms or more regulatory functions such as angiogenesis and tissue repair (Azcona et al. 2022, Binet et al. 2020, Christoffersson et al. 2012, Hou et al. 2019). Collectively, this newly-acquired appreciation of neutrophil heterogeneity paired with the discovery of these cells in the brain suggests a previously uncharacterized role in chronic Toxoplasma infection.

Human neutrophils and Toxoplasmosis

While extensive work has been done in murine models, less is known about the immune responses of human immune cells, specifically neutrophils, during chronic Toxoplasma infection. Due to the broad range of acute symptoms and the asymptomatic nature of chronic infection, many *in vivo* human studies are restricted to those of antibody detection to determine infection stage (Anuradha and Preethi 2014, Villard et al. 2016) and post-mortem studies where *T. gondii* has been detected (Hofman et al. 1993, Diaconu et al. 2016). Previous work has been conducted investigating the human immune response to infection as reviewed by Fisch et. al (Fisch, Clough and Frickel 2019), but research investigating specific immune cell functions in human infection must often be conducted *in vitro*. Previous work investigating the neutrophil-specific response to *T. gondii* demonstrates parasite-dependent release of NETs and destruction of acute tachyzoites by both murine and human neutrophils (Abi Abdallah et al. 2012). Furthermore, more recent work utilizing primary human neutrophils has shown that Toxoplasma infection leads to NET-dependent amplification of innate and adaptive

immune responses which can be seen upon re-exposure to tachyzoites in co-culture (Miranda et al. 2021). While this work demonstrates that neutrophils respond to the acute stage of *T. gondii*, whether these cells are capable of responding to the chronic cyst form of the parasite remains unknown.

Summary

This collective study identifies host- and parasite-specific transcriptional changes relating to infection-induced neuropathology and neuroprotective repair mechanisms in the CNS via targeted transcriptomic analysis. Through the employment of various techniques such as multi-parameter flow cytometry, single-cell RNA sequencing, and *in vivo* depletion experiments, it explores a population of functionally heterogenous neutrophils that play a protective role in the brain throughout chronic infection. Additionally, *in vitro* work using human neutrophil-like cells demonstrates cyst-specific responses tailored to the chronic stage of the parasite. Taken together, this study provides important insights into the dependence of neuroprotective mechanisms on host immune status, characterizes a protective chronic neutrophil population, and demonstrates conserved neutrophil responses in both murine and human models of chronic *T. gondii* infection.

Chapter 2: Targeted transcriptomic analysis of C57BL/6 and BALB/c mice during progressive chronic *Toxoplasma gondii* infection reveals changes in host and parasite gene expression relating to neuropathology and resolution

Abstract

Toxoplasma gondii is a resilient parasite that infects a multitude of warm-blooded hosts and results in a lifelong chronic infection requiring continuous responses by the host. Chronic infection is characterized by a balanced immune response and neuropathology that are driven by changes in gene expression. Previous research pertaining to these processes has been conducted in various mouse models, and much knowledge of infection-induced gene expression changes has been acquired through the use of high throughput sequencing techniques in different mouse strains and post-mortem human studies. However, lack of infection time course data poses a prominent missing link in the understanding of chronic infection, and there is still much that is unknown regarding changes in genes specifically relating to neuropathology and resulting repair mechanisms as infection progresses throughout the different stages of chronicity. In this paper, we present a targeted approach to gene expression analysis during *T. gondii* infection through the use of NanoString nCounter gene expression assays. Wild type C57BL/6 and BALB/c background mice were infected, and transcriptional changes in the brain were evaluated at 14, 28, and 56 days post infection. Results demonstrate a dramatic shift in both previously demonstrated and novel gene expression relating to neuropathology and resolution in C57BL/6 mice. In addition, comparison between BALB/c and C57BL/6 mice demonstrate initial differences in gene expression that evolve over the course of

infection and indicate decreased neuropathology and enhanced repair in BALB/c mice. In conclusion, these studies provide a targeted approach to gene expression analysis in the brain during infection and provide elaboration on previously identified transcriptional changes and also offer insights into further understanding the complexities of chronic *T. gondii* infection.

Introduction

Toxoplasma gondii is a resilient parasite that infects ~ 10% of the population older than 6 years in the United States alone and more than 60% of populations in other countries worldwide (Prevention 2018). Following a period of systemic infection and inflammation, the parasite is sequestered within neurons in the brain creating a lifelong infection. A requirement for continuous peripheral inflammation including CD4 and CD8 T cells is required to prevent uncontrolled parasite replication and potentially fatal pathology (Gazzinelli et al. 1992). Despite the presence of parasites and inflammation, infection is subclinical. However, infection in the immunocompromised can result in reactivation of the parasite, leading to Toxoplasmic encephalitis.

Previous data have reported broad transcriptomic changes in the brain of *T. gondii*-infected mice at both acute and chronic time points (Hu et al. 2020, Tanaka et al. 2013, Li et al. 2020, Schneider et al. 2019). However, these studies often focus on one specific time point in chronic infection, and they fail to explore transcriptomic changes that occur over the course of infection that are important to determine directional change. The parasite itself goes through genetic changes in order to convert from a fast-replicating tachyzoite during acute systemic infection to a cyst-forming bradyzoite during the early

stage of chronic infection after crossing the blood brain barrier (Hong et al. 2017, Radke et al. 2018, Feustel et al. 2012, Lachenmaier et al. 2011). At this early chronic stage, CNS-resident cells begin actively recruiting peripheral immune cells in response to the presence of the parasite, which is still transitioning from tachyzoite to bradyzoite to cyst. As infection progresses and reaches the mid-chronic stage, cyst numbers stabilize as the majority of parasites in the brain are now slow-replicating bradyzoites. At this point in chronicity, both innate and adaptive peripheral immune cells have been in the brain for some time and are constantly maintaining the balance between pro- and anti-inflammatory cytokine production. In addition, subtle neuropathology is commonly seen as noted by changes in morphology and function of both infected and non-infected neurons and changes in glia (Graham et al. 2020, David et al. 2016). Control of infection is maintained for the lifetime of the host and pathology at this stage can vary depending on the genetics of the parasite as well as the background of the host (Mukhopadhyay et al. 2020, Lilue et al. 2013, Denkers 1999, Liesenfeld et al. 1996, Lee and Kasper 2004). These changes in parasite phenotype, host immune response, and neuropathology have yet to be fully explored in the context of progressive chronic infection.

The lifelong presence of cysts within neurons and continuous neuroinflammation gives ample opportunity for *T. gondii* infection to initiate significant changes in the brain. Indeed, many studies have demonstrated significant alterations in rodent behavior including attraction to cat urine postulated to be parasite manipulation to maximize the chances of return to the definitive host (Boillat et al. 2020, Vyas et al. 2007, Berdoy et al. 2000). Additionally, infected mice also show significant changes in behavior in an

elevated plus maze (David et al. 2016). Such changes may be related to direct and indirect modulation of neurotransmitters including imbalances in excitatory and inhibitory signaling and the production of dopamine (David et al. 2016, Brooks et al. 2015, Prandovszky et al. 2011, Ngô et al. 2017, Webster and McConkey 2010). However, the presence of the parasite is hard to unlink from the degree of neuroinflammation and any changes in host behavior is likely as much to do with cytokine signaling as the presence of the parasite (Boillat et al. 2020).

To address the complex interplay of infection, inflammation and neurochemistry, there have been several studies investigating transcriptional changes related to chronic CNS Toxoplasma infection. RNAseq analysis of *in vitro* cultured neurons, astrocytes, fibroblasts and skeletal muscle cells tested infection-induced changes in cell -specific transcriptomes and indicated a host-cell dependent genetic basis for spontaneous cyst formation in neurons and skeletal muscle cells (Swierzy et al. 2017). A comprehensive transcriptomic and proteomic study of human brain tissue including those congenitally infected suggests *T. gondii* infection alters neurodevelopment, plasticity, and disease association in various neural and immune networks (Ngô et al. 2017). Although not as clinically relevant, murine studies are robust and have recently underlined the dominance of immune changes in the brain following infection with oocysts of the Pruqniaud strain revealing activated pathways of metabolism and biosynthesis at both acute and chronic stages of infection (Hu et al. 2020, Jia et al. 2013).

As with all infections, host genetic background plays an important role in disease and despite the ability of Toxoplasma to establish itself in almost all mammalian hosts, it has

been known for some time that the development of disease is highly dependent on mouse strain, recently reviewed by Mukhopadhyay (Johnson et al. 2002, Blackwell et al. 1993, Resende et al. 2008, Mukhopadhyay et al. 2020). Indeed, continuous culturing of Toxoplasma strains in vivo rely upon resistant and susceptible strains of mice to maintain virulence and cyst formation, something vitally important to maintain life cycle competency (Goerner et al. 2020). Thus, in the common lab strains of mice, C57Bl/6 are susceptible to disease with greater parasite burden and inflammation while BALB/c mice are resistant to encephalitis dependent on MHC presentation of the antigen GRA6 (Tanaka et al. 2013, Jia et al. 2013, Ngô et al. 2017, Li et al. 2020, Hu et al. 2020). These striking differences may provide an opportunity to model disease processes in the brain however little direct comparisons of the kinetics of this host response have been conducted.

In this study, we utilize a targeted approach to analysis of gene expression and investigate >1500 genes associated with neurological and immunological processes by direct counting of RNA transcripts without the need for amplification via NanoString technology (Geiss et al. 2008). We determine the changes in these host genes over time in parallel with changes in *T. gondii* developmental-specific genes. In addition, we compare side-by-side gene expression changes between susceptible (C57BL/6) and resistant (BALB/c) mouse strains to address possible pathological versus repair signatures of neuroinflammation. Results demonstrate a dramatic shift in both previously demonstrated and novel gene expression relating to neuropathology, inflammation, and

neuroinflammation as chronic infection progresses and reveals possible pathways of inflammation resolution.

Materials and Methods

Animals and Infections

Animals. All research was conducted in accordance with the Animal Welfare Act, and all efforts were made to minimize suffering. All protocols were approved by the Institutional Animal Care and Use Committee (IACUC) of the University of California, Riverside. Female WT C57BL/6 and BALB/c mice were obtained from Jackson Laboratories and were maintained in a pathogen-free environment in accordance with IACUC protocols at the University of California Riverside.

Infections. The ME49 strain of *T. gondii* was maintained in cyst form by continuous passaging in SW and CBA background mice. Female 6-8 week old WT C57BL/6 and WT BALB/c mice were infected with 10 ME49 cysts per mouse in 200µl of sterile 1x PBS solution via intraperitoneal (IP) injection. Naïve controls received 200µl of sterile 1x PBS solution via intraperitoneal (IP) injection. This infection protocol regularly leads to ~3000 cysts in the brains of infected mice by 4 weeks post infection (Goerner et al. 2020).

DNA Extraction and Parasite Burden Quantification

Parasite burden in brain was quantified as previously described (Goerner et al. 2020). Briefly, DNA from naïve and 2, 4, and 8-week infected half brains of C57BL/6 (n=4/group) and BALB/c (n=5/group) mice was extracted and purified using a High Pure PCR Template Prep Kit (Roche). DNA concentration of each sample was determined via

NanoDrop, and all DNA was normalized to 12.5ng/µl before amplification. Parasite burden was measured by amplifying the B1 gene of *T. gondii* by RT PCR.

RNA Extraction

RNA from brain lysate of naïve, 2 week infected, 4 week infected, and 8 week infected C57BL/6 and BALB/c mice (n=3 for all groups) was collected using Trizol extraction method. At each time point, mice were sacrificed and perfused intracardially with 20mL of sterile 1x PBS. Whole brain was dissected and homogenized in 1mL Trizol. Phase separation was completed by adding 200µl of chloroform and incubating at room temperature for 2-3 minutes. Samples were centrifuged at 12,000xg for 15 minutes at 4°C, and upper aqueous phase was collected followed by RNA precipitation using 500µl isopropyl alcohol. Samples incubated at room temperature for 10 minutes followed by centrifugation. RNA pellet was washed with 1mL of 75% ethanol twice. All supernatant was discarded and RNA pellet was dissolved in 100µl of nuclease free water. RNA concentration for each sample was determined using a NanoDrop 2000, and RNA samples normalized to a concentration of 10ng/µL in molecular grade water.

NanoString nCounter Gene Expression Assays and Analysis

Gene Expression Assays. nCounter gene expression assays (NanoString Technologies) were performed for each of the following NanoString panels: Neuropathology, Neuroinflammation, and Inflammation+CustomizedPLUS covering a total of 1530 targeted genes including 10 parasite-specific genes: *ROP18, GDA1/CD39, ADF, GRA12, SRS22A, TUBA1, SRS35A, SRS44, BAG1,* and *LDH2* (Geiss et al. 2008). *T. gondii* genes included in custom PLUS codeset were selected based on the percent expression in

tachyzoite and bradyzoite growth stages (90% expression in one stage and 0% in other stage) using previous studies differentiating growth stages and ToxoDB (Goerner et al. 2020). Briefly, panel codeset probes were hybridized with 150ng of total RNA per brain over 18hr at 65C according to NanoString protocol. Inclusion of a customized PLUS codeset in the Inflammation panel required additional Reporter and Capture Plus codesets to be added during the hybridization reaction (NanoString User Manual C0019-08). Hybridized RNA was then diluted in molecular grade water and loaded into nCounter SPRINT cartridge (NanoString), placed into nCounter SPRINT Profiler, and [quantified.] RNA-conjugated probes were counted via NanoString Sprint Profiler technology.

nSolver and Advanced Analysis. Results from each panel were merged into one data file for comparative analysis, normalized in nSolver following best practices, and analyzed using nSolver and Advanced Analysis software according to previously published protocols (Danaher et al. 2017). nSolver-generated heat maps were created using normalized (merged) data and agglomerative clustering, a bottom-up form of hierarchical clustering (NanoString User Manual C0019-08). For Advanced Analysis, normalized merged data was used (NanoString User Manual 10030-03). Differential expression (DE) analysis was performed to identify specific targets that exhibit significantly increased or decreased expression in response to naïve control values or, in the case of BALB/c C57BL/6 comparison, to C57BL/6 control values at each time point. Gene set analysis was run to determine the change in direction of regulation within each pre-defined gene set relative to naïve controls. Global significance scores, a summary T-statistic used to measure change (NanoString User Manual 10030-03) were calculated, and the directed

global significance scores were expressed via heatmap. Cell type profiling module analysis was conducted to determine the relative abundance in classically activated cell types during infection using genes assigned to each cell type: T cells (*CD3e, CD6, CD3g, TRAT1,* and *CD3d*), CD8+ T cells (*CD8a*), macrophages (*CD68* and *CD84*), and microglia (*GPR84, LRRC25, IRF8, NCF1, TNF, TLR2,* and *TNF.1*). NanoString cell type profiling is a validated method to measure relative abundance of up to 24 different immune cell types, with high concordance to flow cytometry (Danaher et al. 2017). Pathway analysis was also conducted to determine overall changes in pathways based on the first principal component of the targets within a pathway as annotated by NanoString (NanoString User Manual 10030-03). Direction of pathway change (up- or downregulated) was determined by cross referencing the pathway score with the corresponding volcano plot for that pathway. Summary pathway score plot colors are based on calculated scores and are represented as downregulation (blue) to upregulation (orange). Statistical significance was determined using R software. All data are available on Gene Expression Omnibus (GEO).

Separate Statistical Analyses. Normalized Log_2 scores for *T. gondii*-specific genes were used in fold changes analysis of tachyzoite-associated genes and bradyzoite-associated genes compared to naïve controls in Prism. In addition, results from cell type profiling modules were placed into Prism and evaluated at each time point. Violin plots were created in a similar fashion by analyzing normalized Log_2 scores of specific probes to show the rounded distribution of data. Statistical significance was determined by 2-tailed,

unpaired Student's *t*-test and One-Way ANOVA with multiple comparisons (p-value < 0.05).

Results

Chronic T. gondii infection stimulates a dramatic shift in gene expression as infection progresses from early to late chronic stages.

To determine broad transcriptomic changes that occur over the course of infection, RNA from infected C57BL/6 mouse brains was harvested at day 14, 28 and 56 days post infection (dpi) representing time points associated with transitionary, stable and late chronic infection respectively. RNA was hybridized with NanoString panel-specific codesets using two panels of genes specific for inflammation and neuropathology, and RNA-conjugated probes were counted via NanoString Sprint Profiler technology. Resulting gene expression changes compared to calculated control z-scores are demonstrated in **Figure 1**. Merged data analysis of NanoString neuropathology, neuroinflammation, inflammation, and a Toxoplasma-specific custom codeset probes using basic nSolver software demonstrate dramatic shifts in gene expression (**Fig. 1A**). The majority of genes relating to neuropathology, neuroinflammation, and inflammation switch completely from low expression (blue) compared to control z-scores in an uninfected state to high expression (orange) by late chronic infection, signifying an 8-10 fold change in expression. This significant switch is seen almost in entirety by the mid-chronic stage of infection when cysts are prevalent in the brain. Contrastingly, a multitude of gene expression changes are still occurring at the early chronic stage correlating with tachyzoite entry and active cyst formation (Dupont et al. 2012, Cabral et

al. 2016, Mendez and Koshy 2017). Biological replicates in each time point generally exhibit close clustering with 14dpi showing the greatest variation in line with a transitioning state between acute and chronic infection (**Fig. 1B**).

Consistent with a powerful infection in an otherwise immune privileged site, differential expression analysis reveals that at all timepoints, the majority of genes significantly altered by infection are upregulated as compared to naïve controls (**Fig. 1C-E; Supplemental Table 1**). At 14dpi, the majority of genes that experience changes in expression undergo significant upregulation despite CNS infection not being fully established. At this early stage, many genes exhibit fold changes up to 7-fold (*CCL5, CD74*) and this only increases at later chronic timepoints, reaching up to 8-fold change at 28dpi and up to 10-fold change at 56dpi.

Comparison of genes that are significantly altered as determined by differential expression analysis reveals both conserved gene expression changes across all timepoints as well as time point-specific changes (**Fig. 1E**). At 28dpi (light green), there are 202 genes that have significant changes in expression (22% of total) that are specific to this mid-chronic stage of infection. This number is significantly greater than the stage-specific changes seen at 14dpi (dark blue; 4 genes = 0.4%) and 56dpi (dark purple; 11 genes = 1.2%). There are no shared differentially expressed genes (DEGs) between the early (14dpi) and late (56dpi) chronic stages and very few shared genes (light blue, 4 genes = 0.4%) between the early (14dpi) and mid- (28dpi) chronic stages of infection. Consistent with establishment of infection, mid- (28dpi) and late (56dpi) chronic stages share a far greater number of DEGs (light purple, 237 genes = 26% of total), signifying a

similar infection phenotype between later stages of infection as chronicity is firmly established and maintained. Of all genes expressed above background levels included in the merged analysis, 454 genes (grey, 49.8% of total) are significantly altered at all timepoints.

***T. gondii* stage-specific gene expression correlates with host gene changes.**

Toxoplasma goes through several phases of development and in the intermediate mammalian host, two stages dominate: i) a fast-replicating tachyzoite responsible for dissemination, cell lysis, and acute pathologies and ii) the bradyzoite that replicates slowly, and forms cysts in neurons (Montoya and Liesenfeld 2004). How these classical Toxoplasma signatures change in relation to the host transcriptome over the course of *in vivo* infection has not been explored in depth. The broad significant changes in host genes following infection may represent a triggering of inflammation cascades and neurological remodeling that is independent of infection, or they could be closely tied to the development of the parasite niche in the brain. To determine the relationship between host and parasite genetic changes, Toxoplasma stage-specific genes were selected based on their stage specificity and frequency of expression in RNAseq data sets of Me49 bradyzoites, tachyzoites and late-stage bradyzoites as seen in ToxoDB and in recent publications (Goerner et al. 2020). These genes were incorporated into the NanoString analysis via the use of custom codesets, and changes in expression of these genes were analyzed at each time point. To further elucidate *T. gondii* stage-specific gene expression changes across the course of infection, fold changes of tachyzoite-associated genes and bradyzoite-associated genes compared to naïve controls were analyzed via OneWay

ANOVA for significance. Normalized parasite gene counts for each sample at each time point were used to determine fold change. To verify normal progression of infection, parasite B1 amplification was conducted (**Supplemental Figure 1**). Visualization of parasite-specific gene expression changes correlates with development of chronic and sustained infection (**Fig. 2A-C; Suppl. Fig.1**).

Most tachyzoite associated genes (top 5 genes in heat map) are expressed at or around background levels in the brain and remain so for the duration of infection (**Fig. 2A**). *ROP18, GDA1/CD39,* and *ADF* are constitutively expressed across all developmental stages according to ToxoDB but are never detectable above background here and may indicate limitations in sensitivity compared to the abundance of host genetic material (**Fig. 2A-B**). These are all genes constitutively expressed in varying stages of Me49 strain development, and their expression is not altered at any point during chronic infection (**Fig. 2B**). Therefore, although C57BL/6 mice are susceptible to infection exhibiting increasing parasite burden over time, the stable expression of *ROP18, GDA1/CD39,* and *ADF* in this study suggest that even at 56dpi, there are not classical indicators of parasite reactivation and bradyzoite genes continue to dominate.

The genes *GRA12* (Krishnamurthy and Saeij 2018) and *SRS22A* (Michelin et al. 2009) help with formation of the parasitophorous vacuole (PV) membrane that protects the parasite during both acute and chronic infection, and *GRA12* is one of the genes that orchestrates cyst formation in the transition from tachyzoite to bradyzoite and is seen in the 99th percentile in both tachyzoites and bradyzoites (Guevara et al. 2019). Our data

show *GRA12* increasing by 2.5-fold at 56 days post infection, signifying the presence of non-replicating parasites in the brain while *SRS22A* remains unchanged compared to naïve controls (**Fig. 2B**).

In addition to tachyzoite associated genes, early- and late-stage bradyzoite genes were selected for this analysis based on ToxoDB expression values. *SRS35A*, also known as *SAG4*, is a surface protein expressed above the 95th percentile in both early and late-stage bradyzoites (Zhou and Wang 2017). *SRS44*, also known as *CST1*, is a cyst wall component that is expressed above the 89th percentile in both bradyzoite stages and maintains the integrity of the cyst during chronic infection (Tomita et al. 2013). The bradyzoite-specific antigen *BAG1*, also thought to aid in cyst formation (Zhang et al. 1999b), is expressed at the 91st and 100th percentile in early and late stage bradyzoites respectively. *LDH2*, one of the main controllers of bradyzoite differentiation (Abdelbaset et al. 2017) is expressed between the early and late bradyzoite stages of growth.

All of these genes increase in percentile of expression in early- and/or late-stage bradyzoite stages of growth compared to tachyzoites. In contrast to the lack of tachyzoite genes, kinetics of these selected bradyzoite genes follow a pattern of increasing expression from 14dpi to 56dpi (**Fig. 2A-B**). Fold change analysis of bradyzoite associated genes reveal significant increases of the bradyzoite specific *SRS35A, BAG1* and *LDH2* as infection progresses (**Fig 2A and C**). *SRS35A* shows a 5-fold change compared to naïve controls at 56 days post infection. *SRS44* experiences an increasing trend but does not reach significance. *BAG1* demonstrates between a 5-10-fold increase in expression at 28 and 56 days post infection, supporting the presence of bradyzoites in

the brain at these later chronic stages. *LDH2* shows an approximately 10-fold increase at 28 and 56 days post infection. Expression of *LDH2* at the mid- and late-chronic stage is also significantly higher compared to expression at 14dpi.

Thus, several ToxoDB-identified constitutively expressed tachyzoite genes were unchanged between the early and late chronic stages of infection based on their expression at or below background levels. However, by 28dpi a significant pattern of Toxoplasma gene expression has been established dominated by late-stage bradyzoite specific genes (Goerner et al. 2020, Hong et al. 2017, Garfoot et al. 2019). Interestingly, this pattern remains mostly unchanged 4 weeks later at 56dpi with the exception of *GRA12* that may support renewed cyst formation at this later stage (Watts et al. 2015). Taken together, the kinetics of parasite-specific gene expression in the C57BL/6 mouse indicate an established chronic infection, minimal tachyzoite replication and a predominantly late-stage bradyzoite phenotype.

Kinetics of chronic infection demonstrates classical immune cell activation and increases in IFNγ signaling-related genes.

Regulation of inflammation is especially important in the CNS during chronic infection, and a balanced host immune response is vital for survival. The role of T cells in protection against Toxoplasmic encephalitis has been known for some time however, the accumulation of innate immune cells, resident CNS cells and subsets of all of these are still not fully documented (Landrith et al. 2015, Khan, Hwang and Moretto 2019). In contrast to RNA-seq, the direct counting of transcripts (Geiss et al. 2008) allows cell type profiling analysis of immune cells based on the counts of particular cell-specific

transcripts (Danaher et al. 2017). Results of cell type profiling demonstrate significant changes in abundance of canonical cell types involved in the *T. gondii* immune response (**Fig. 3A**). As would be expected all T cells and specifically CD8+ T cells significantly increase in abundance over naive and 14dpi as infection progresses (Hu et al. 2020) (**Fig. 3A**). In addition, macrophages and resident microglia also increase in abundance and activation. The increase in these innate immune cell types follows the same pattern as T cells, with macrophages demonstrating the largest increase over time. Both macrophages and microglia exhibit significant increases over naïve at all time points and level off after 28dpi.

To examine the overall directional change of specific infection-associated pathways, gene set analysis (GSA) was performed and directed global significance scores were analyzed. As seen in **Figure 3B**, classical inflammatory response pathways follow a trend of steady upregulation across all time points supporting the need for a maintained robust immune response. Our pathway analysis results show an anticipated initial increase in IFN signaling during the early chronic stage of infection that consistently increases over time (**Fig. 3C**). Downstream IFNγ-dependent mechanisms such as *STAT1* signaling and parasite-killing genes *GBP1* and *ZBP2* are vital to prevent parasite reactivation in the brain (Hidano et al. 2016, Kravets et al. 2012, Virreira Winter et al. 2011, Pittman, Cervantes and Knoll 2016). To address the kinetics of *IFNγ, STAT1, GBP1,* and *ZBP2* Log_2 scores of transcript numbers were plotted for each time point (**Fig. 3D**). *IFNγ* expression serves as a reassuring control of previously known infection-induced brain changes, results demonstrate low *IFNγ* at 14dpi consistent with lower numbers of T cells

at this early stage in the brain (**Fig. 3D, left**). This increases as chronicity progresses and reaches peak significance at 56dpi compared to the mid-chronic stage. Despite this conservative *IFNγ* expression, it is highly effective with large increases in IFNγ-dependent signaling including *STAT1*. Corresponding to increased IFNγ-dependent signaling, *STAT1* expression is increased 2-fold in the brain at 14dpi and continues to increase as infection progresses through the mid-chronic stage, levelling off between 28 and 56dpi (**Fig. 3D, second from left**). *GBP2* and *ZBP1* expression are also increased at 14dpi compared to naïve controls, but while *GBP2* remains constant until the late stage of infection, *ZBP2* is significantly increased at each time point (**Fig. 3D, right**). The differences in timing of expression of these genes suggests stage-specific, IFNγ-dependent mechanisms of parasite control. Taken together, these results demonstrate classical activation of immune cells and infection-associated pathways that supports previous research as well as previously unknown kinetics of IFNγ-dependent signaling mechanisms.

Kinetic analysis reveals progressive neuropathological changes and previously unexplored attempts at repair during chronic T. gondii infection.

Changes in neurochemistry in the infected brain have previously been reported including alterations in the excitatory and inhibitory neurotransmitters (David et al. 2016, Brooks et al. 2015, Xiao et al. 2013, Barbosa et al. 2020) that suggest that even in the absence of clinical pathology, there are underlying changes in neuronal structure and connectivity that would be described as pathological. To determine the full extent of genetic changes related to neuropathology, we analyzed a group of genes with known roles in transmitter

function, neural connectivity and function, and neural maintenance and repair via GSA and pathway analyses. GSA results demonstrate upregulation of most of the Neuropathology panel pathways at each time point while a handful of pathways (namely, Vesicle Trafficking, Neural Connectivity, Transmitter Synthesis and Storage, Transmitter Release, and Carbohydrate Metabolism) experience noticeable downregulation (**Fig. 4A**). To confirm worsening of neuropathology via the activation of CNS-resident immune cells and decreases in neuronal function, Log_2 scores of the astrocyte activation gene *GFAP* and the inhibitory neurotransmitter GABA signaling gene *GABRA1* were analyzed (**Fig. 4B**). Astrocytic *GFAP* increases in expression initially during the early chronic stage of infection, remains steady between 14 and 28dpi, and then experiences a significant increase in expression by 56dpi (**Fig. 4B, top**). Over the course of chronic infection, *GABRA1* remains at levels comparable to naïve controls until 56dpi where it demonstrates a significant decrease (**Fig. 4B, bottom**).

As neurons are the primary CNS-resident cell type infected by *T. gondii*, and these cells undergo changes in morphology and function during infection, the pathway of neural connectivity was examined more thoroughly via pathway analysis and corresponding volcano plots. Pathway analysis supports GSA results and shows a steady decrease in neural connectivity across all timepoints (**Fig. 4C**). Volcano plots of the genes driving the neural connectivity score show increases in significantly downregulated genes as infection progresses corresponding with the lower GSA score at each time point (**Fig. 4C**). One gene that drives this downregulation at all time points is *Glrb*, a receptor that functions as a neurotransmitter-gated ion channel (Handford et al. 1996, Ridderbusch et

al. 2019). *Slc9a6,* a gene that encodes the protein NHE6 which plays a role in dendritic spine growth (Park et al. 2006, Gao et al. 2019), becomes highly downregulated at the later time points (**Fig. 4C**). *Slc17a6* which aids in glutamate uptake (Takamori et al. 2001, Serrano-Saiz et al. 2020) drives downregulation of neural connectivity at 14dpi (**Fig. 4C**). In addition to supporting previous findings and in contrast to immune scoring, this data suggests a continuous progression of neuropathology specifically in the areas of neurotransmitter production, function (**Supplemental Table 1**).

GSA and pathway analyses also reveal an increase in pathways associated with myelination (**Fig. 4A and D**). The myelination pathway experiences consistent upregulation as infection progresses through chronicity (**Fig. 4A and D**). It is well known that myelination of neuronal axons is a critical process not only for neuronal signaling, but also for continued supply of required metabolites to neurons for their survival and function and the process of re-myelination has been seen in various instances of CNS injury and disease (Saab and Nave 2017, Wang et al. 2018). Throughout all stages of infection, the increase in the myelination pathway is driven by the genes *Hexb, Tgfb1*, and *Cxcr4* (**Fig. 4D**). These results demonstrate an increase in genes associated with myelination and support increased attempts at repair of neuropathology.

Kinetics of T. gondii infection reveals significant alteration of novel genes.

In addition to changes in expression of canonical *T. gondii* infection-associated genes, differential expression analysis also identified significant changes in several genes previously not associated with this parasitic infection. Of the 25 most significantly upregulated genes from all time points compared to Naïve controls, 4 of these genes were

determined to be novel in the context of *T. gondii* infection, and their Log_2 scores were analyzed further (**Fig. 5A**).

C4A gene expression increases compared to naïve controls beginning at the early stage of chronic infection, and while this expression does not change significantly between 14dpi and 28dpi or 28dpi and 56dpi, expression increases by approximately 1.5 fold overall between the early and late chronic stages (**Fig. 5A**). This gene is primarily known for activation of the complement pathway along with *C3A* and *C5A* (Ji et al. 2019, Liesmaa et al. 2018, Melbourne et al. 2018, Prasad et al. 2018). *CTSS* is a member of the peptidase C1 family that encodes for cathepsin S which is expressed by neurons in the CNS (Ji et al. 2018). Similar to *C4A*, *CTSS* expression experiences >1.5 fold change over the course of infection, but this gene is also significantly increased at each chronic time point (**Fig. 5A**). *IFITM3*, commonly known for its anti-viral functions, expression experiences a similar pattern of upregulation as *CTSS*, and over the course of chronic infection is upregulated >1.5 fold overall (**Fig. 5A**). *PSMB8* expression increases 2-fold overall and follows the trend of a step-wise increase between each time point (**Fig. 5A**). This gene has the greatest fold change in expression compared to naïve controls.

While the majority of novel differentially expressed genes are upregulated over the course of infection, a handful of previously unreported genes are significantly downregulated compared to naïve controls (**Fig. 5B**). One such gene is *ATF2*, activating transcription factor 2, which is required to regulate the transcription of the pro-inflammatory cytokine TNFα (Falvo et al. 2000, Tsytsykova and Goldfeld 2002). *ATF2* decreases significantly from 28dpi to 56dpi after an initial decrease at 14dpi (**Fig. 5B**).

NRG3 belongs to the NRG gene family and is the second most common form of NRG found in the adult brain (Paterson et al. 2017). *NRG3* experiences a similar decrease in expression as *ATF2* over the course of chronicity (**Fig. 5B**). Taken together, the consistent pattern of change in these newly analyzed genes over the course of infection point to additional targets for understanding the complexity of chronic infection.

BALB/c mice exhibit differences in timing and expression of genes, immune cell recruitment, and pathway activation compared to B6 mice suggesting decreased neuropathology and enhanced repair.

Host genetics influence the outcome of Toxoplasma infection even if they do not prevent chronic infection. Thus, C57BL/6 mice are considered susceptible with high cyst burden that levels off around 30 days post infection (Burke et al. 1994) while BALB/c mice, another commonly used mouse strain, are more resistant (**Suppl. Fig.1**) (Mukhopadhyay et al. 2020). While the increased resistance to infection in BALB/c mice has previously been linked to enhanced immune response specifically via MHC gene expression (Brown et al. 1995), less is known regarding how neuropathology signatures differ between resistant BALB/c mice and the more susceptible C57BL/6 model over the course of chronic infection.

To compare neuropathology and neuroinflammatory signatures in BALB/c and C57BL/6 mice during chronic infection, NanoString analysis was conducted on BALB/c mouse brain RNA using the same time points of infection as before. Results of merged BALB/c vs. C57BL/6 analysis demonstrate initial differences in gene expression between naïve mice (**Fig. 6A**) consistent with previous analysis (Yuan et al. 2020, Sellers et al. 2011). In

contrast to B6 mice which generally show a continued increase in gene change over the course of infection, BALB/c mice exhibit the largest change at 14dpi which then returns to patterns similar to naïve at chronic infection. (**Fig. 6A**). Principal component analysis (PCA) shows little variation between biological replicates and no divergent point between BALB/c and B6 instead gene expression in these different hosts at all time points remain separated. Based on PC1 and PC2 clustering of day 28 and d56 post infection on the BALB/c background are almost identical (**Fig. 6B**). When comparing DEGs between naïve C57BL/6 and BALB/c mice, there is an initial difference in gene expression (**Fig. 6C**). While most DEGs (582) are conserved between the 2 strains, the majority of BALB/c genes are downregulated compared to naïve C57BL/6 mice, and there are notably less DEGs that are specific to BALB/c mice (24 BALB/c compared to 230 C57BL/6). At each infection time point, there are between 350-420 genes that remain shared between the 2 mouse strains suggesting conserved gene expression changes relating to neuropathology and neuroinflammation across different mouse species (**Fig. 6D**). However, despite this shared number of altered genes, there is a much higher number of DEGs in C57BL/6 mice (368, 543, and 436 genes respectively) compared to BALB/c mice (94, 31, and 27 genes) at each time point. It is important to note that BALB/c mice also have lower numbers of DEGs overall at each time point compared to C57BL/6 mice (**Supplemental Table 2**). The underlying genetic difference between these two strains of mice is observed in the expression of MHC II (*H2-Ea-ps*) and dominates the genes that are upregulated in BALB/c mice (**Fig. 6D**). It is not apparent in baseline differences as little MHC II expression occurs in a naïve brain. The overall

downregulation of genes following infection of BALB/c mice is dominated by *Mpeg1* and *Pttg1* (**Fig. 6D**). These genes are primarily responsible for innate immune responses and apoptosis via the p53 pathway (Bai et al. 2018, Bernal et al. 2002, McCormack et al. 2020, Ni et al. 2020, Zhang et al. 1999a).

Based on the differences in differential gene expression between BALB/c mice and C57BL/6 mice, cell type profiling and pathway analyses were conducted to determine effects of cell composition and pathway activation on differences in BALB/c vs. C57BL/6 neuropathology signatures. Cell type profiling demonstrates notable differences in cell composition in the brain across chronic infection between these strains (**Fig. 7A**). At each stage BALB/c mice demonstrate drastically different cell composition overall compared to those of C57BL/6 mice at the same infection stage after comparison to control "Tumor Infiltrating Leukocyte" (TIL) expression as well as other cell types. While not all cell types are consistently up- or downregulated in BALB/c mice at each time point, CD4+ and CD8+ T cells show patterns of decreased and increased amounts respectively (**Fig. 7A**) corresponding with previous research demonstrating decreased importance of CD4+ T cells and increased dependence on CD8+ T cell activity in BALB/c chronic infection (Deckert-Schlüter et al. 1994, Parker, Roberts and Alexander 1991, Harris et al. 2010). In addition, there are significantly elevated macrophages at 56dpi in BALB/c mice compared to C57BL/6 mice. Notably, total TILs are predominantly downregulated in BALB/c at 28 and 56dpi suggesting less absolute numbers of immune cells and therefore immune cell recruitment overall while TILs are

relatively comparable at 14dpi between the mouse strains. This is consistent with increased control of parasite replication in BALB/c (**Suppl. Fig.1**).

To compare pathway score profiles between mouse strains, the heatmap of overall pathway scores was analyzed. This summary plot clusters pathways together based on similar expression patterns and arranges samples based on similarity of pathway expression profiles. When evaluating pathway activation associated with neuropathology, BALB/c mice demonstrate downregulation of neuropathological and inflammatory pathways such as “Disease Association,” “Cellular Stress Response,” “Interleukin Signaling,” “Interferon Signaling,” and “MHC II Presentation” when compared to the same C57BL/6 time points (**Fig. 7B**). In addition to decreased neuropathology and inflammatory pathway activation, BALB/c mice also demonstrate upregulation of pathways associated with neurological health and function such as “Transmitter Synthesis and Storage,” “Neural Connectivity,” “Transmitter Release,” “Axon and Dendrite Structure,” and “Transmitter Response and Reuptake” at later chronic time points compared to C57BL/6 mice. While pathway activation patterns are comparable between BALB/c and B6 mice at Naïve and 14dpi, there is a switch in up- and downregulated pathways associated with neuropathology, inflammation, and neurological health at later chronic time points.

To determine if the contrasting pathway activation between BALB/c and C57BL/6 mice are driven by differences in neurological DEGs at each time point, Log_2 scores for specific neurological signaling (*GABRA1* and *GABRG2*) and repair (*MAGEE1* and *LPAR1*) genes were compared between BALB/c and C57BL/6 mice (**Fig. 7C**). *GABRA1*

expression is comparable at both naïve and 14dpi timepoints and significantly increases compared to C57BL/6 mice at both 28 and 56dpi (**Fig. 7C**). In contrast, neuronal signaling *GABRG2* expression is significantly elevated in BALB/c mice at all time points (**Fig. 7C**). Neuronal signaling and repair genes *MAGEE1* and *LPAR1* also follow similar patterns of expression at each time point and are significantly elevated in BALB/c mice at each stage of infection (**Fig. 7C**). Taken together, these results collectively demonstrate differences in timing and expression of genes, immune cell recruitment, and pathway activation in resistant BALB/c mice compared to B6 mice indicating decreased neuropathology and enhanced repair.

Discussion

In this study, we utilized a targeted approach to analysis of gene expression and investigated >1500 genes associated with neurological and immunological processes by direct counting of RNA transcripts without the need for amplification via NanoString technology (Geiss et al., 2008). We determined the changes in these host genes over time in parallel with changes in *T. gondii* developmental-specific genes. While much is known about changes in gene expression at specific stages of infection via commonly used sequencing techniques like RNAseq, there is a gap in knowledge regarding how gene expression fluctuates as infection progresses through chronicity and how these changes relate to development of the parasite (Montoya and Liesenfeld, 2004; Jia et al., 2013; Ngôet al., 2017). In addition, we compared gene expression changes between susceptible and resistant mouse strains with specific focus on differences in neuropathology and neuroinflammatory signatures. Results demonstrate a dramatic shift in both previously

demonstrated and novel gene expression relating to neuropathology and neuroinflammation as chronic infection progresses and reveals possible pathways of inflammation resolution.

The establishment and maintenance of chronic infection involves complex changes as infection progresses from parasite entry and formation of cysts early during infection to long-term control of encysted parasites via immune cell recruitment and cytokine production leading to subtle worsening of neuropathology as infection progresses through the mid- and late chronic stages (Liesenfeld et al., 1996; Denkers, 1999; Lee and Kasper, 2004; Lachenmaier et al., 2011; Feustel et al., 2012; Lilue et al., 2013; Hong et al., 2017; Radke et al., 2018; Graham et al., 2020; Mukhopadhyay et al., 2020). Our chosen timepoints represent each of these stages to capture as much directional change in gene expression as possible. Initial results demonstrate that despite the establishment of chronic infection seen by stabilization of Toxoplasma genes by 28dpi, there continue to be changes in overall gene expression relating to neuropathology, neuroinflammation, and inflammation at varying stages of chronicity. The multitude of signature changes suggests an initial activation of neuropathology and neuroinflammation phenotypes by 14dpi. This switch becomes more pronounced as chronicity progresses even while immune parameters between 4 and 8 weeks post infection steady. 454 DEGs remain shared between time points indicating conserved transcriptomic changes as chronic infection progresses, with fewer specific genes for each time point.

Previous analyses of parasite genes at different developmental stages have established some developmental specific gene signatures of the parasite as it transitions from

disseminating tachyzoite to cyst-forming bradyzoite (Hong et al., 2017; Radke et al., 2018; Garfoot et al., 2019; Goerner et al., 2020; Krishnan et al., 2020; Waldman et al., 2020). Evaluating selected genes whose expression corresponds with either constitutive, tachyzoite, or immature/mature bradyzoite phenotypes using ToxoDB, we identified gene expression during chronic infection that supports the phenotype of maturing cysts and little reactivation to tachyzoite replication even in a susceptible mouse model. The genes were selected based on their percentile of expression in each growth stage of *T. gondii*, for example, *BAG1* is expressed at the 91st and 100th percentile in ME49 early and late-stage bradyzoites but only at the 15th percentile in tachyzoites making it a bradyzoite associated gene. Our results show that the constitutively expressed tachyzoite genes *ROP18*, *GDA1/CD39*, and *ADF* remain lowly expressed throughout the course of chronic infection. The transitional gene *GRA12* is upregulated at 56dpi indicating possible continued cyst formation in line with a general low-level increase in cyst numbers overtime (Sinai et al., 2016). Even though neuropathology scores worsen in the C57BL/6 strain, these data do not suggest that significant parasite reactivation is the cause. Most bradyzoite-specific genes such as *SRS35A*, *BAG1*, and *LDH2* accumulate over time and remain dominant as infection progresses with increased presence of late-stage bradyzoites and support a maturation of cysts in the brain (Watts et al., 2015; Garfoot et al., 2019; Goerner et al., 2020).

Our results confirm previous research demonstrating immune response and canonical T cell activation while also showing accumulation of macrophages and continued proliferation and activation of CNS microglia. While cell type profiling and pathway

analyses used in this study identify the most significantly changed cell types and broad pathway changes, other cell types and more specific pathways can be excluded or overlooked due to low probe counts. In the future, additional genes relating to cell types and pathways of interest such as neurons and astrocytes could be added and analyzed. We confirm classical immune pathway activation that demonstrates possible stabilization over time. Recent work has demonstrated similar increases in these pathways between the acute and chronic stage of infection after infection with *T. gondii* oocysts following GO analysis of RNAseq (Hu et al., 2020). In addition, we provide new in-depth analysis of *IFNγ* expression and downstream IFNγ-signaling genes *STAT1*, *GBP2*, and *ZBP1* in the context of chronic infection in the brain. Specifically, the differences in timing of expression of these genes suggests stage-specific, IFNγ-dependent mechanisms of parasite control.

While our results offer further insight into the kinetics of expression for genes previously associated with chronic *T. gondii* infection, our analysis also reveals novel genes associated with neuropathology and neuroinflammation that have not been explored. Specifically, results demonstrate significant upregulation of the genes *C4A*, *CTSS*, *IFITM3*, and *PSMB8* and downregulation of *ATF2* and *NRG3* across all stages of chronic infection. *C4A* works in conjunction with *C3A* and *C5A* to activate the complement cascade and together, these genes trigger the degranulation of mast cells and basophils and increase vascular permeability in the context of the inflammatory immune response. In addition, *C4A* has been associated with roles in schizophrenia (Liesmaa et al., 2018; Melbourne et al., 2018; Prasad et al., 2018; Ji et al., 2019). While complement activation

has been previously demonstrated in the brain during Toxoplasma infection, the common functions of *C4A* point toward a possible role in increasing vascular permeability gradually during chronic infection for the continued infiltration of peripheral immune cells into the brain (Xiao et al., 2016; Huang et al., 2019). Interestingly, BALB/c mice experience significantly less expression of *C4A* at each infection time point compared to C57BL/ 6 mice which is an indication that there is decreased vascular permeability in these mice compared to B6. *CTSS* encodes for cathepsin S that is expressed by neurons and is required for elastase activity in alveolar macrophages (Ji et al., 2018; Doherty et al., 2019). It has also been demonstrated that *CTSS* participates in both the production of pro-inflammatory cytokines interleukin 6 (IL-6), interleukin 8 (IL-8), tumor necrosis factor-α (TNFα), and interleukin-1β (IL-1β) during ocular inflammation (Klinngam et al., 2018) as well as the degradation of antigenic proteins to peptides during antigen presentation (Hughes et al., 2016; Klinngam et al., 2018). The pattern of *CTSS* expression at each stage of chronic infection suggests a potential role for this gene in pro-inflammatory cytokine production, neuronal function, and continued antigen presentation as part of the immune response to *T. gondii* infection. There are no known functions of *IFITM3* during *T. gondii* infection but is important for anti-viral effector functions via inhibition of viral protein synthesis and shuttling incoming virus particles to lysosomes for degradation (Lee et al., 2018; Appourchaux et al., 2019; Bedford et al., 2019; Kenney et al., 2019; Spence et al., 2019). *IFTIM3* plays a role in viral infections through IFN signaling, indicating possible novel anti-parasitic functions of this gene during *T. gondii* infection. *PSMB8* is involved in the degradation of cytoplasmic antigen processing to

generate MHC I binding proteins via stimulation by IFNγ production, provides instructions to make one subunit of immunoproteasomes responsible for helping in response to infections, and also regulates glioma cell migration proliferation and apoptosis (Agarwal et al., 2010; Basler et al., 2018a; Basler et al., 2018b; Yang et al., 2018). While previous work on *PSMB8* has produced minimal data in relation to Toxoplasma infection (Agarwal et al., 2010), further research specifically relating to chronic infection could elaborate on anti-parasitic functions in the CNS. In addition to regulating TNFα production, *ATF2* is a cAMP or activator protein-dependent transcription factor that regulates the transcription of various genes involved in anti-apoptosis, cell growth, and DNA damage response (Falvo et al., 2000; Tsytsykova and Goldfeld, 2002; Watson et al., 2017; Meijer et al., 2020). While the effect of *T. gondii* infection on the transcription of TNFα has been studied in the past, the specific role of *ATF2* in the context of chronic *T. gondii* infection in the CNS has not been elucidated, and this gene may play a vital role in regulating TNFα production specifically in the brain or by CNS-resident cells (Leng et al., 2009). *NRG3* is well-known for aiding in the development and survival of neurons and oligodendrocytes in the brain in addition to aiding in excitatory and inhibitory synapse formation and controlling glutamate release by neurons (Müller et al., 2018; Wang Y. N. et al., 2018). While it has not been explored previously in *T. gondii* infection, the significant decrease in *NRG3* may be partly responsible for some infection-induced neuropathology such as increases in extracellular glutamate concentration and excess neuronal firing.

Our results demonstrate a progressive worsening of neuropathology and increased attempted repair of this pathology via upregulated angiogenesis genes as infection becomes more chronic in a susceptible mouse model. While most of these directional changes are not as dramatic as those associated with the immune response (**Figure 3**), these changes support previous research demonstrating neuropathology caused by infection (Cabral et al., 2016; David et al., 2016; Ngôet al., 2017), and a small group of pathways such as Cytokines, Activated Microglia, and Angiogenesis experience drastic changes as infection progresses to the late chronic stage. It is important to note that this worsening neuropathology is unlikely to be caused by reactivation of cysts in the brain even at the late stage of infection as seen by the low expression of tachyzoite genes and instead suggests more indirect neurological consequences of infection. However, the limitations in sensitivity of measuring parasite genes in samples dominated by host material means that we cannot rule out low level cyst activation despite a consistent late-stage bradyzoite phenotype over the duration of infection. Analysis results of astrocytic activation marker *GFAP* and neuronal signaling gene *GABRA1* support this idea of progressive worsening neuropathology. While the initial increase in astrocytic *GFAP* is expected as part of the initial response to CNS infection, what isn't expected is the significant increase in expression that takes place in the late stage of infection after chronicity has been well established. *GABRA1*, along with *GABRB3*, is vital for the formation of $GABA_A$ receptors and plays a pivotal role in GABAergic signaling that protects neurons in the brain from over-signaling, which can often lead to diseases such as epilepsy (McKernan et al., 1991; Tozuka et al., 2005). The significant drop in

GABRA1 expression during the mid- and late chronic stage could be a major target for treatment of infection-induced neuropathology and chronic infection in the future. In addition to supporting previous findings, our data also suggests a continuous progression of neuropathology specifically in the areas of transmitter production, function, and response, areas that were previously lacking in the context of chronic infection. However, while our results indicate progressive neuropathology as seen via decreased overall neural connectivity, we also see increases in genes and pathways such as myelination that suggest enhanced attempts at repairing and resolving this neuropathology. Neuroprotective and repair mechanisms in other non-infectious models of CNS injury include remyelination to increase conductivity between previously damaged neurons, synaptic pruning by microglia to limit over-signaling, regeneration of axons, and various others. Recent work by the Harris lab indicates a role for local release of the DAMP IL-33 either by oligodendrocytes or astrocytes that is then required for protection against Toxoplasma (Still et al., 2020). Such innate sensing mechanisms may be needed not just for parasite recognition but also as a trigger to activate neural repair during late infection. The process of myelination has been explored extensively in the context of other models of CNS disease and injury (Gonsette, 2010; Kapitein and Hoogenraad, 2015; Felten et al., 2016; Li et al., 2017; Pałasz et al., 2017; Saab and Nave, 2017; Wang F. et al., 2018; Avila et al., 2020). The myelination pathway in this analysis is driven by several genes that are also associated with immune modulation. Throughout all stages of infection in the susceptible C57BL/6 strain, the increase in the myelination pathway is driven by the genes *Hexb*, *Tgfb1*, and *Cxcr4*. *Hexb* encodes enzymes in lysosomes that break down

toxic substances and act as recycling centers (Mahuran, 1999; Ogawa et al., 2018). *Tgfb1* has been shown to promote remyelination in the adult CNS in addition to its classical proinflammatory role (Hamaguchi et al., 2019; Mota et al., 2020). *Cxcr4* is a known regulator of remyelination in other models of infection and CNS inflammation (Carbajal et al., 2011; Tian et al., 2018; Beigi Boroujeni et al., 2020). The steady increase in myelination genes throughout the kinetics of chronic *T. gondii* infection demonstrates a possible role of myelination in maintaining neuronal signaling and function to prohibit worsening of neuropathology as well as the possibility of remyelination to heal pathology or reorganize neuronal circuits (David et al., 2016). Thus, further experiments need to be conducted to determine if there is an increase in myelin or attempts at remyelination during infection which are now warranted following this data.

In contrast, the use of resistant BALB/c mice in these experiments reveals enhanced repair and resolution during infection allowing for insights into the role of neurological repair mechanisms in the context of resistance to chronic Toxoplasma infection. BALB/c mice exhibit differences in pathway activation of neuropathology and neurological health and function. Specifically, BALB/c mice experience downregulation in neuropathological and inflammatory pathways and upregulation in neurological transmitter function and neuronal structure compared to C57BL/ 6. This indicates that BALB/c mice may have differences in specific neurological genes that aid in maintaining neurological signaling and repairing damage done by infection. The differentially expressed neuronal signaling genes *GABRA1* and *GABRG2* and the repair genes *MAGEE1* and *LPAR1* were analyzed in BALB/c mice to answer this question. *GABRA1* and *GABRG2* are both critical for the

formation of $GABA_A$ receptors that regulate neuronal signaling (McKernan et al., 1991; Tozuka et al., 2005; Li X. et al., 2020), and these receptors are significantly upregulated in BALB/c mice compared to C57BL/6 mice indicating possible enhanced GABAergic signaling in BALB/c mice brains enabling better control of neuropathology caused by infection. *MAGEE1*, also known as melanoma-associated antigen E1 (MAGE Family Member E1) or *DAMAGE*, plays roles in neuronal signaling and functions in tissue growth and repair (Albrecht and Froehner, 2004). *LPAR1* induces downstream signaling cascades that are essential for normal brain development and function of the nervous system and functions as intrinsic axon growth modulators for neurons after injury (Fink et al., 2017; Plastira et al., 2019). Both of these genes are also significantly upregulated in BALB/c mice at all chronic time points suggesting enhanced neuronal signaling, DNA repair, and regulation of regrowth of neurons during infection.

It is known that host background is a factor in resistance to *T. gondii* infection. While increased resistance to infection in BALB/c mice has previously been linked to enhanced immune response, less is known regarding how neuropathology signatures differ between resistant BALB/c mice and the more susceptible C57BL/6 model over the course of chronic infection. Results of merged BALB/c vs. C57BL/6 analysis demonstrate differences in gene expression at each stage of chronic infection. BALB/c mice exhibit their largest change in gene expression at 14dpi which then plateaus by 56dpi while the opposite is true for C57BL/6 mice. This indicates that BALB/c mice may experience pathological changes in the brain early during infection which are then at least partially rescued as indicated by the plateauing of gene expression at the later chronic stages.

While 350-420 neuropathology and neuroinflammation genes are conserved between the mouse species during infection, BALB/c mice exhibit more downregulated DEGs compared to C57BL/6 mice. This indicates a definitive difference in neuropathology signatures between BALB/c and C57BL/6 mice that indicates less neuropathology in the resistant BALB/c strain.

In conclusion, the results of absolute RNA counts of inflammatory and neuropathology genes support previously published whole genome RNAseq data sets while demonstrating novel gene expression relating to neuropathology and neuroinflammation as chronic Toxoplasma infection progresses. It reveals possible pathways of resolution through the use of a targeted transcriptomic approach in a susceptible and resistant mouse model of infection. The use of this technology presents an additional analysis tool in the *T. gondii* scientific field with the possibility for more strategic analysis in the future. These results also open a doorway to a multitude of potential gene candidates that can be explored to elucidate possible therapeutic targets and to further the vital understanding of the kinetics of chronic infection in the brain.

Figures and Tables

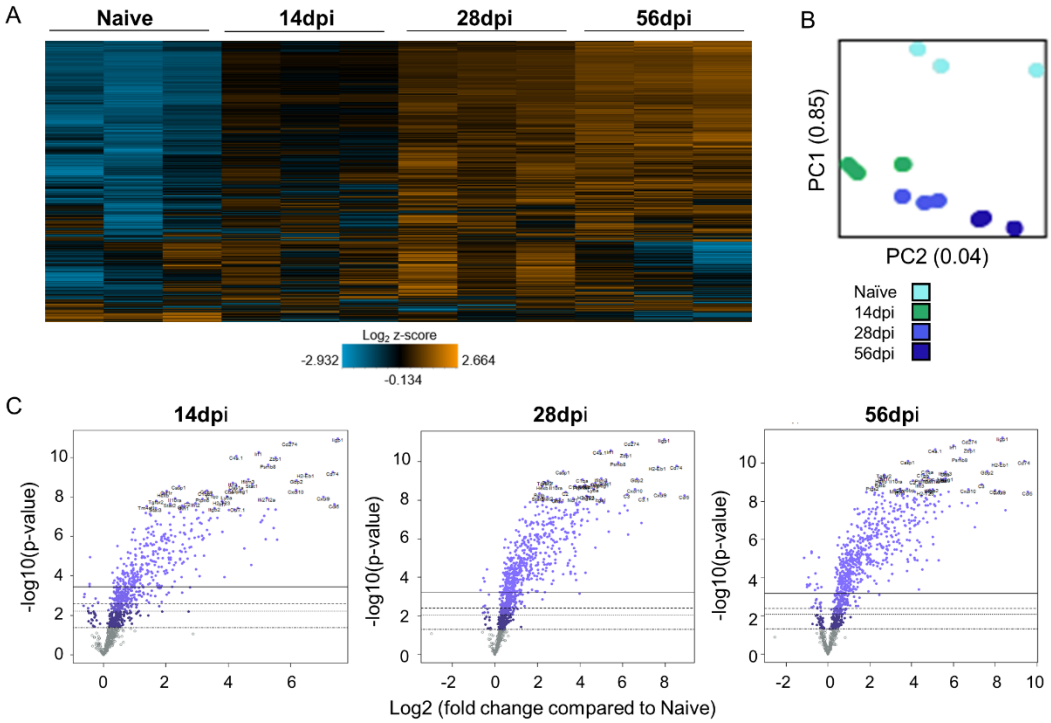

D

14dpi	28dpi	56dpi
IIGP1 (7.50)	*IIGP1* (7.96)	*IIGP1* (8.35)
CD274 (5.97)	*CD274* (6.45)	*CD274* (6.79)
IRF1 (4.98)	*IRF1* (5.46)	*IRF1* (6.00)
C4A.1 (4.26)	*C4A.1* (4.93)	*ZBP1* (6.80)
ZBP1 (5.52)	*ZBP1* (6.17)	*C4A.1* (5.13)
PSMB8 (5.28)	*PSMB8* (5.81)	*PSMB8* (6.32)
CD74 (7.35)	*CD74* (8.54)	*CD74* (9.40)
H2-EB1 (6.49)	*H2-EB1* (7.67)	*CASP1* (3.84)
IFITM3 (4.64)	*CASP1* (3.23)	*H2-EB1* (8.26)
GBP2 (6.19)	*IFITM3* (5.00)	C1QA (4.77)

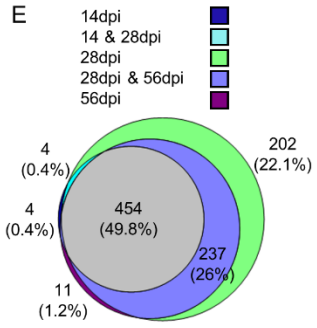

Figure. 1. Chronic *T. gondii* infection stimulates a dramatic shift in gene expression as infection progresses from early to late chronic stages. (A) Heat map of all genes from merged Neuropathology, Neuroinflammation, and InflammationPLUSCustomCodeset panels. Gene expression depicted from low expression (blue) to high expression (orange). Heat map generated from normalized gene expression data using nSolver software. **(B)** PCA plot of biological replicates at all time points. Numbers on axes represent percentage of variation in that component. **(C)** Differential expression analysis results of 14dpi, 28dpi, and 56dpi compared to Naïve control values demonstrates the majority of genes as upregulated. Top 25 genes most significantly upregulated identified based on fold chage (x-axis) vs. p-value (y-axis). 4 adjusted p-value cutoffs in each plot are as follows from bottom (dashed line) to top (solid line): <0.50, <0.10, <0.05, <0.01. **(D)** Table of 10 most significantly upregulated genes at each time point (from C) **(E)** Overlap between differentially expressed genes plotted in B. Numbers and percentages in diagram based on genes significantly upregulated with adjusted p-value cutoff <0.05.

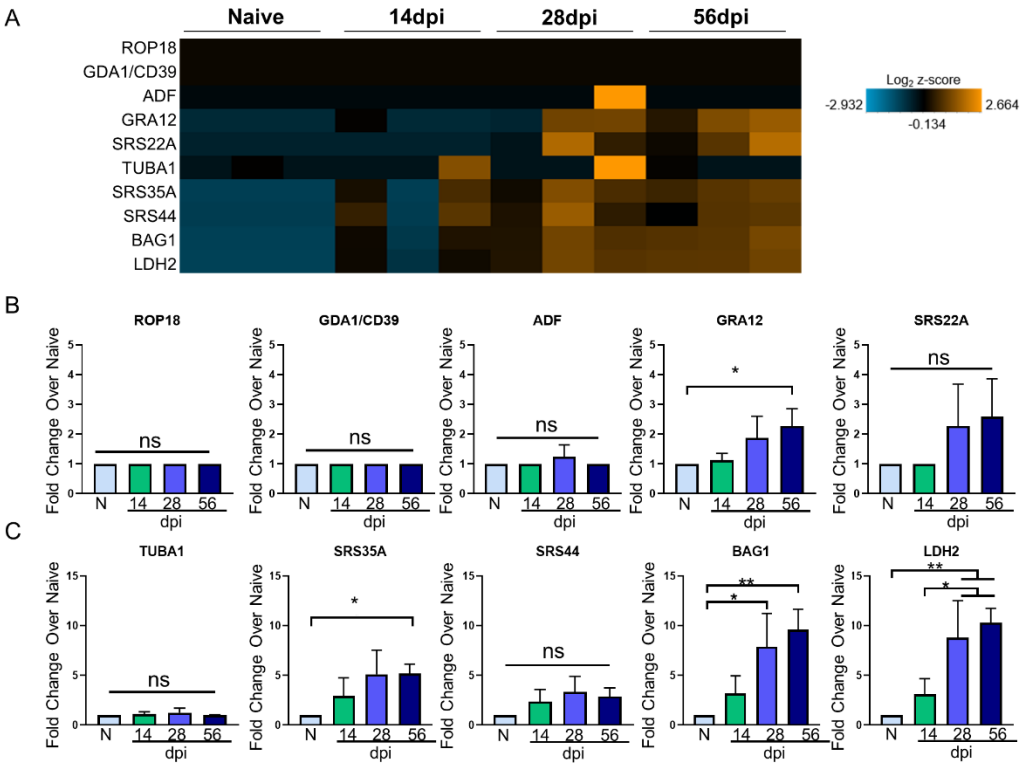
A
Naive
14dpi
28dpi
56dpi
ROP18
GDA1/CD39
ADF
GRA12
SRS22A
TUBA1
SRS35A
SRS44
BAG1
LDH2
Log2 z-score
-2.932
2.664
-0.134
B
ROP18
GDA1/CD39
ADF
GRA12
SRS22A
C
TUBA1
SRS35A
SRS44
BAG1
LDH2
Fold Change Over Naive
dpi
N
14
28
56
ns
*
**

Figure 2. *T. gondii* stage-specific gene expression correlates with host gene changes. **(A)** Heat map of *T. gondii*-specific genes from merged Neuropathology, Neuroinflammation, and InflammationPLUSCustomCodeset panels. Gene expression depicted from low expression (blue) to high expression (orange). Heat map generated from normalized gene expression data using nSolver software and Background Thresholding to account for lower parasite gene counts. **B-C)** Fold change compared to naive of tachyzoite genes **(B)** and bradyzoite genes **(C)** from normalized gene counts. Significance determined by One-Way ANOVA using Multiple Comparisons (* = p-value <0.05, ** = p-value <0.01).

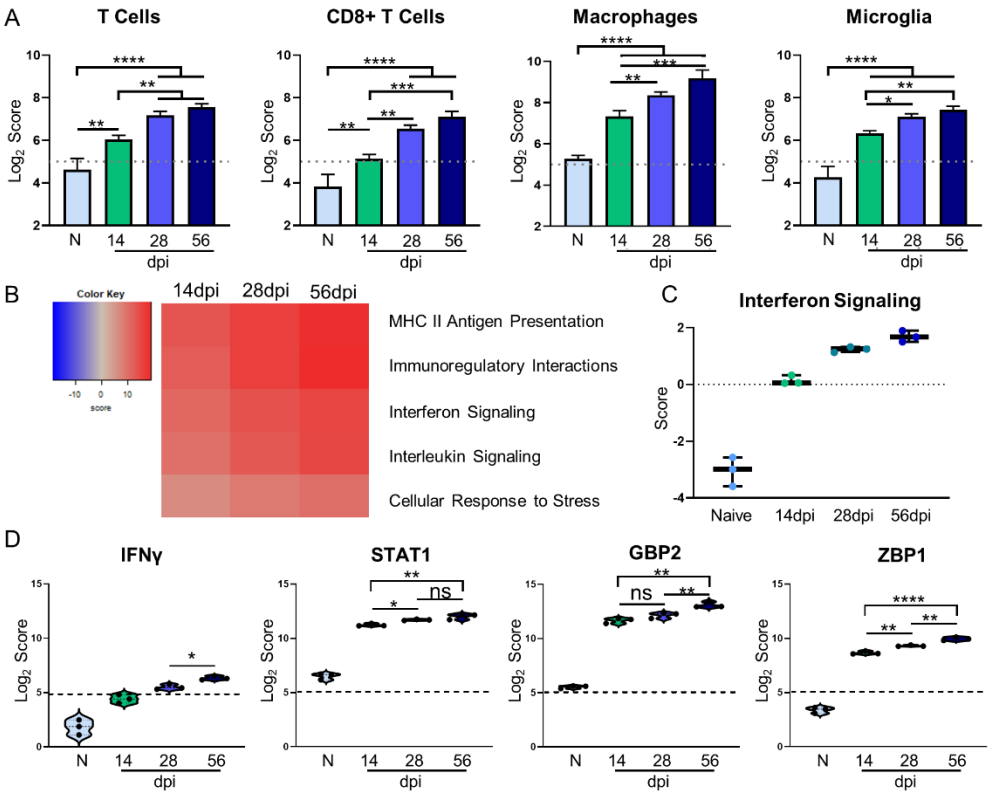
A
T Cells
CD8+ T Cells
Macrophages
Microglia
Log2 Score
N
14
28
56
dpi
B
Color Key
score
14dpi
28dpi
56dpi
MHC II Antigen Presentation
Immunoregulatory Interactions
Interferon Signaling
Interleukin Signaling
Cellular Response to Stress
C
Interferon Signaling
Score
Naive
14dpi
28dpi
56dpi
D
IFNγ
STAT1
GBP2
ZBP1
ns

Figure 3. Kinetics of chronic infection demonstrates classical immune cell activation and increases in IFNγ signaling-related genes. Cell-type profiling, global significance analysis, pathway scoring, and individual gene results of merged Neuropathology, Neuroinflammation, and InflammationPLUSCustomCodeset panels. **(A)** $\log_2$ score plots of infiltrating immune cell types T cells, CD8+ T cells, macrophages, and resident microglia compared to naïve time point control (* = p-value < 0.05, ** = p-value < 0.01, *** = p-value < 0.001, **** = p-value < 0.0001). All cell types checked for expression above background level of 5 (shown by dashed line). **(B)** Heatmap of directed global significance scores compared to naïve controls based on direction of gene set pathway change. Red denotes gene sets whose genes exhibit extensive over-expression with the covariate, blue denotes gene sets with extensive under-expression. **(C)** Pathway analysis results of Interferon Signaling. Pathway checked for expression compared to background score of 0 (shown by dashed line). **(D)** $\log_2$ score plots of specific genes relating to IFNγ signaling, specifically *IFNγ*, *STAT1*, *GBP2*, and *ZBP1* compared to naïve time point control (* = p-value < 0.05, ** = p-value < 0.01, *** = p-value < 0.001, **** = p-value < 0.0001). All genes checked for expression above background level of 5 (shown by dashed line).

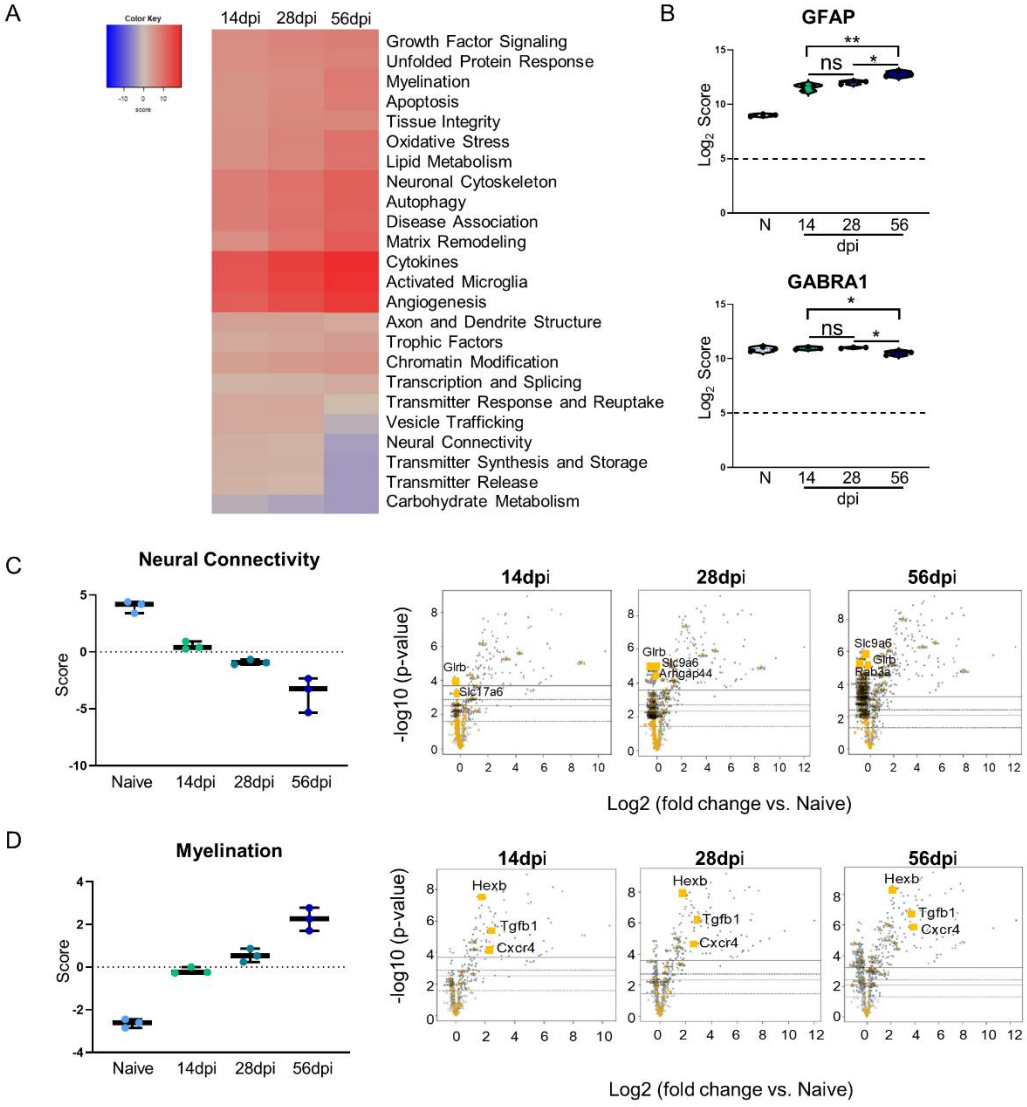
A
Color Key
score
14dpi 28dpi 56dpi
Growth Factor Signaling
Unfolded Protein Response
Myelination
Apoptosis
Tissue Integrity
Oxidative Stress
Lipid Metabolism
Neuronal Cytoskeleton
Autophagy
Disease Association
Matrix Remodeling
Cytokines
Activated Microglia
Angiogenesis
Axon and Dendrite Structure
Trophic Factors
Chromatin Modification
Transcription and Splicing
Transmitter Response and Reuptake
Vesicle Trafficking
Neural Connectivity
Transmitter Synthesis and Storage
Transmitter Release
Carbohydrate Metabolism
B
GFAP
Log2 Score
N 14 28 56
dpi
**
ns
*
GABRA1
C
Neural Connectivity
Score
Naive 14dpi 28dpi 56dpi
14dpi
28dpi
56dpi
-log10 (p-value)
Glrb
Slc17a6
Slc9a6
Arhgap44
Rab3a
Log2 (fold change vs. Naive)
D
Myelination
Hexb
Tgfb1
Cxcr4

Figure 4. Kinetics of chronic infection reveals progressive neuropathological changes and previously unexplored attempts at repair/maintenance during chronic *T. gondii* infection. Global significance analysis, individual gene, and pathway scoring results of Neuropathology Panel. **(A)** Heatmap of directed global significance scores compared to naïve controls based on direction of gene set pathway change. Red denotes gene sets whose genes exhibit extensive over-expression with the covariate, blue denotes gene sets with extensive under-expression. **(B)** $\log_2$ score plots of specific genes relating to neuropathology, specifically *GFAP* and *GABRA1* compared to naïve time point control (* = p-value < 0.05, ** = p-value < 0.01, *** = p-value < 0.001, **** = p-value < 0.0001). All genes checked for expression above background level of 5 (shown by dashed line). **C-D)** Pathway analysis and volcano plot results of neural connectivity **(C)** and myelination **(D)** pathways significantly affected during *T. gondii* infection based on analysis. Volcano plot of directed global significance scores for neural connectivity and myelination gene sets. Genes within the selected gene set are highlighted in orange. Top 3 genes driving directional change identified based on fold chage (x-axis) vs. p-value (y-axis). 4 adjusted p-value cutoffs in each plot are as follows from bottom (dashed line) to top (solid line): <0.50, <0.10, <0.05, <0.01.

A

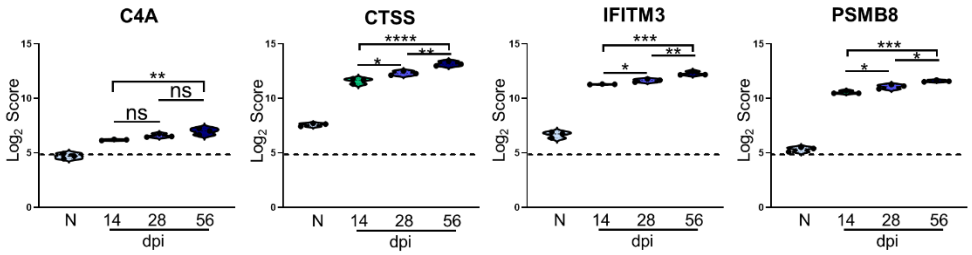
C4A
CTSS
IFITM3
PSMB8
Log2 Score
N
14
28
56
dpi
ns
*
**
***
****

B

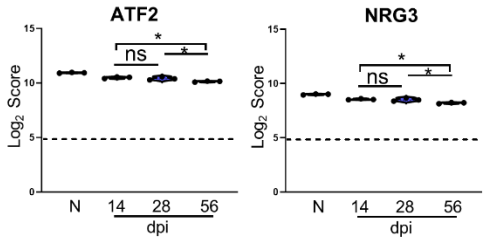
ATF2
NRG3
Log2 Score
N
14
28
56
dpi
ns
*

Figure 5. Kinetics of *T. gondii* infection reveals significant alteration of novel genes. **A-B)** $\log_2$ score plots of specific novel genes from merged Neuropathology, Neuroinflammation, and InflammationPLUSCustomCodeset panels compared to naïve time point control. **(A)** Violin plot results of most highly upregulated non-canonical genes *C4A*, *CTSS*, *IFITM3*, and *PSMB8* as determined by differential expression analysis. **(B)** Results of most highly downregulated non-canonical genes *ATF2* and *NRG3* as determined by differential expression analysis. All genes shown are expressed above background threshold of 5 (shown by dashed line) and are significantly altered during infection based on differential expression analysis statistics (p-value<0.01). All graphs shown as fold change over background. Significance between timepoints determined by One-Way ANOVA using Multiple Comparisons (* = p-value <0.05, ** = p-value <0.01, *** = p-value < 0.001, **** = p-value < 0.0001).

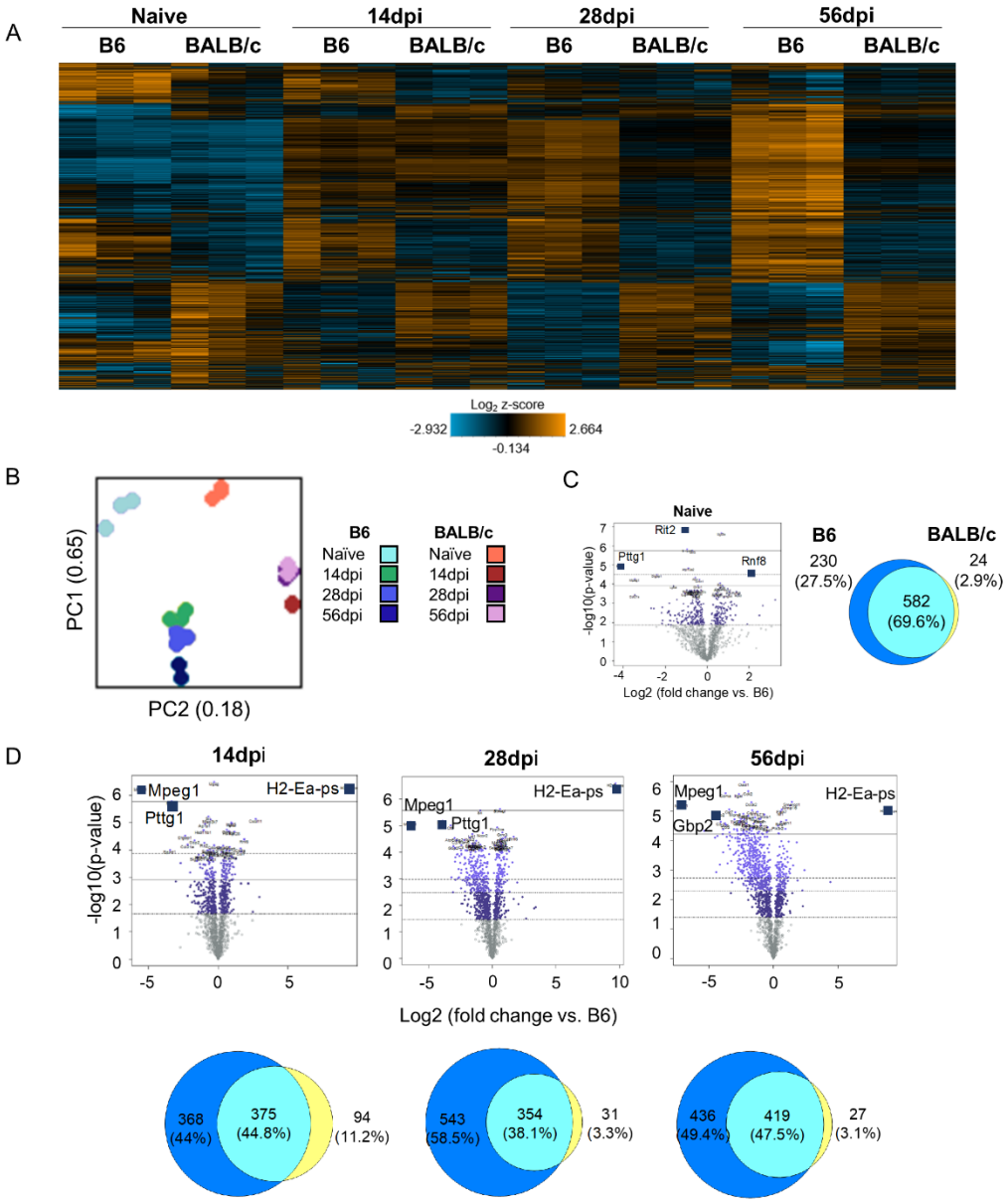
A
Naive
14dpi
28dpi
56dpi
B6
BALB/c
Log2 z-score
-2.932
-0.134
2.664
B
PC1 (0.65)
PC2 (0.18)
B6
BALB/c
Naïve
14dpi
28dpi
56dpi
C
Naive
Rit2
Pttg1
Rnf8
-log10(p-value)
Log2 (fold change vs. B6)
B6
BALB/c
230
(27.5%)
582
(69.6%)
24
(2.9%)
D
14dpi
28dpi
56dpi
Mpeg1
H2-Ea-ps
Pttg1
Gbp2
-log10(p-value)
Log2 (fold change vs. B6)
368
(44%)
375
(44.8%)
94
(11.2%)
543
(58.5%)
354
(38.1%)
31
(3.3%)
436
(49.4%)
419
(47.5%)
27
(3.1%)

Figure 6. BALB/c mice exhibit differences in timing and expression of genes compared to B6 mice during chronic infection. (A) Heat map of all genes from B6vsBALB/c merged Neuropathology, Neuroinflammation, and InflammationPLUSCustomCodeset panels. Gene expression depicted from low expression (blue) to high expression (orange). Heat map generated from normalized gene expression data using Basic nSolver software. **(B)** PCA plot of B6 and BALB/c biological replicates at all time points. Numbers on axes represent percentage of variation in that component. **C-D)** BALB/c differential expression analysis results and overlap between differentially expressed genes of Naïve **(C)** and infection timepoints **(D)** (14dpi, 28dpi, and 56dpi) compared to B6 control values. Top 3 genes identified based on fold chage (x-axis) vs. p-value (y-axis). 4 adjusted p-value cutoffs in each plot are as follows from bottom (dashed line) to top (solid line): <0.50, <0.10, <0.05, <0.01. Numbers and percentages in Venn diagrams based on genes significantly upregulated with adjusted p-value cutoff <0.05.

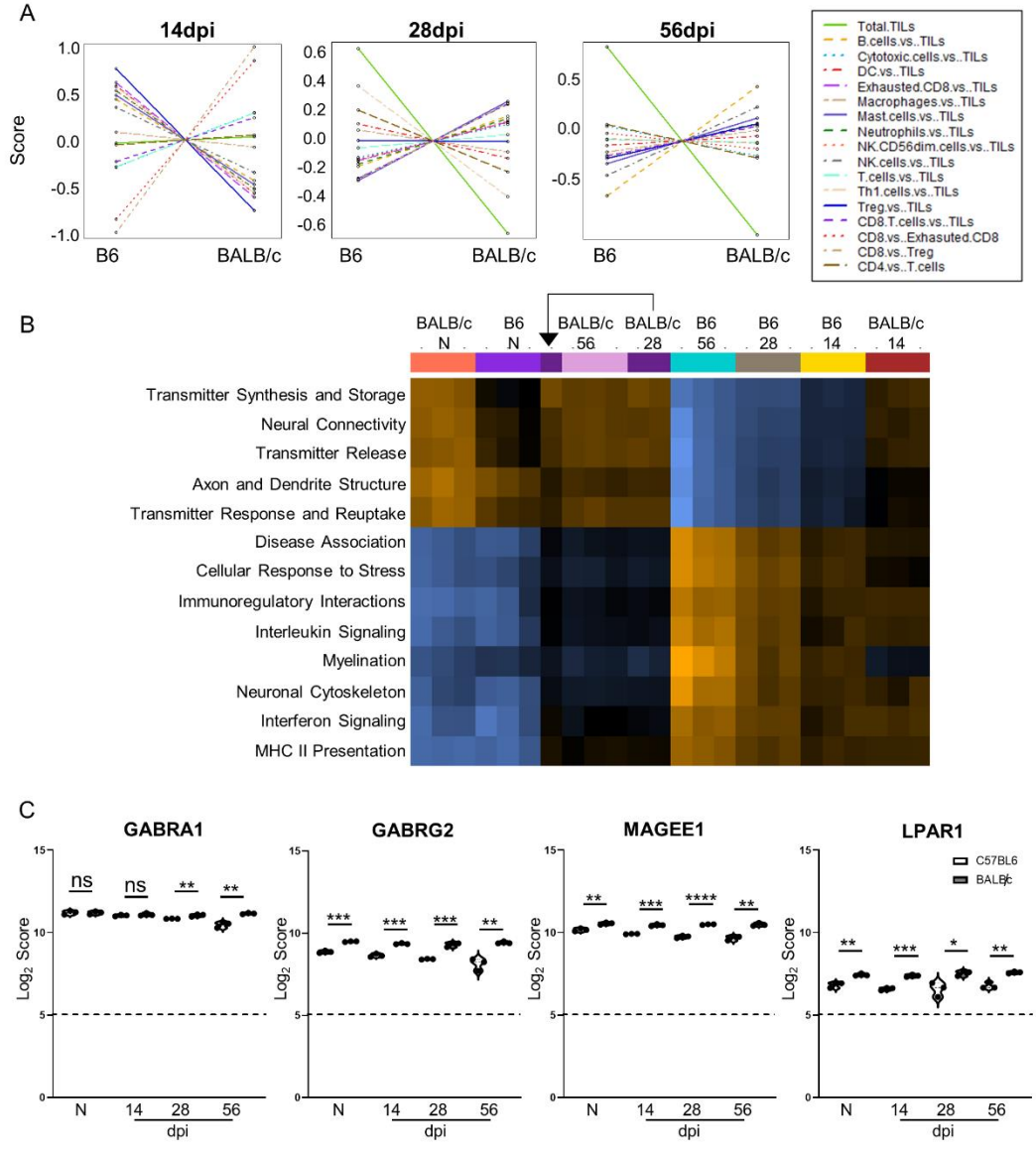
A
14dpi
28dpi
56dpi
Score
B6
BALB/c
Total.TILs
B.cells.vs..TILs
Cytotoxic.cells.vs..TILs
DC.vs..TILs
Exhausted.CD8.vs..TILs
Macrophages.vs..TILs
Mast.cells.vs..TILs
Neutrophils.vs..TILs
NK.CD56dim.cells.vs..TILs
NK.cells.vs..TILs
T.cells.vs..TILs
Th1.cells.vs..TILs
Treg.vs..TILs
CD8.T.cells.vs..TILs
CD8.vs..Exhausted.CD8
CD8.vs..Treg
CD4.vs..T.cells
B
BALB/c N
B6 N
BALB/c 56
BALB/c 28
B6 56
B6 28
B6 14
BALB/c 14
Transmitter Synthesis and Storage
Neural Connectivity
Transmitter Release
Axon and Dendrite Structure
Transmitter Response and Reuptake
Disease Association
Cellular Response to Stress
Immunoregulatory Interactions
Interleukin Signaling
Myelination
Neuronal Cytoskeleton
Interferon Signaling
MHC II Presentation
C
GABRA1
GABRG2
MAGEE1
LPAR1
Log2 Score
ns
dpi
C57BL6
BALB/c

Figure 7. Differences in cell recruitment, pathway activation, and specific regulatory genes demonstrate enhanced control of infection in BALB/c mice. **(A)** Cell type summary plots of recruited cells shown in BALB/c mice vs. B6 mice per time point. **(B)** Pathway score summary plot of BALB/c Vs. B6 mice depicted from downregulation (blue) to upregulation (orange). Summary plot generated by clustering pathways based on similar scores. Samples are arranged in plot according to similarity of pathway score profiles. **(C)** $\log_2$ score plots of specific genes relating to neuronal health and repair, specifically *GABRA1*, *GABRG2*, *MAGEE1*, and *LPAR1* compared to naïve time point control (* = p-value < 0.05, ** = p-value < 0.01, *** = p-value < 0.001, **** = p-value < 0.0001). All genes checked for expression above background level of 5 (shown by dashed line). Gene selection significance determined via differential expression analysis statistics (p-value<0.05). All graphs shown as fold change over background Significance between mouse strains at each time point determined by Unpaired Two-Tailed Student's t-Test (* = p-value <0.05, ** = p-value <0.01, *** = p-value < 0.001, **** = p-value < 0.0001).

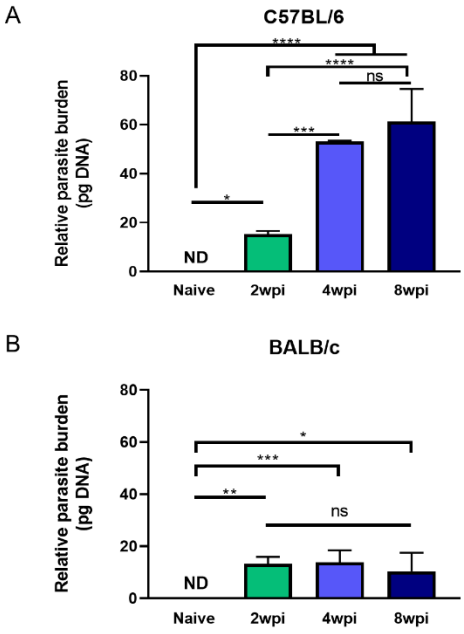
A
C57BL/6
Relative parasite burden (pg DNA)
80
60
40
20
0
ND
Naive
2wpi
4wpi
8wpi
****
****
ns
***
*
B
BALB/c
Relative parasite burden (pg DNA)
80
60
40
20
0
ND
Naive
2wpi
4wpi
8wpi
*
***
**
ns

Supplemental Figure 1. Representative brain parasite burden for susceptible and resistant mouse strains. Quantified parasite burden from whole brain DNA via RT-PCR in susceptible C57BL/6 (n=4/time point) and resistant BALB/c (n=5/time point) mice. **(A)** C57BL/6 brain time point values were collected from multiple separate experiments and analyzed as an overall representation of parasite burden changes over chronic infection. **(B)** Brain samples from BALB/c mice collected for this study were tested and analyzed in parallel for parasite burden along with Nanostring nCounter analysis. Significance between timepoints determined by One-Way ANOVA using Multiple Comparisons (* = p-value <0.05, ** = p-value <0.01, *** = p-value < 0.001, **** = p-value < 0.0001).

Chapter 3: Neutrophils in the brain are sources of neuroprotective molecules and demonstrate functional heterogeneity during chronic *Toxoplasma gondii* infection

Abstract

Infection with the protozoan parasite *Toxoplasma gondii* leads to the formation of lifelong cysts in neurons of the brain that can have devastating consequences in the immunocompromised. However, despite the establishment of a chronic inflammatory state and infection-induced neurological changes, there are limited signs of clinical neuropathology resulting in an asymptomatic infection in the immunocompetent. This suggests the work of neuroprotective mechanisms to prevent clinical manifestations of disease. However, such sources of neuroprotection during infection remain largely unknown. This study identifies a population of neutrophils chronically present in the brain during Toxoplasma infection that express the neuroprotective molecules NRG1, ErbB4, and MSR1. Further phenotyping of this population via flow cytometry and singe-cell RNA sequencing reveals two distinct subsets of neutrophils based on age that display functional heterogeneity. This includes cells transcriptionally prepared to function both as anti-parasitic effector cells and in a more alternative protective manner. Chronic depletion of neutrophils results in increased parasite burden and infection-induced vascular pathology. Lack of neutrophils during chronic infection also deleteriously affects neuronal regeneration and repair mechanisms. In conclusion, this work identifies and demonstrates a functionally diverse chronic neutrophil population that plays a dynamic role in controlling infection outcome in the CNS by balancing classical responses with neuroprotective functions.

Introduction

Ingestion of the protozoan parasite *Toxoplasma gondii* leads to a lifelong infection characterized by the formation of cysts inside neurons of the brain. Prevalence rates vary, however it is estimated that one third of the world's population is infected with Toxoplasma (Montoya and Liesenfeld 2004). While infection is often asymptomatic due to a robust host immune response, an immunocompromised state can result in parasite reactivation in the brain, the onset of Toxoplasmic encephalitis, and death (Wang et al. 2017). Presence of the parasite in the brain leads to the recruitment of both innate and adaptive immune cells which are required to control parasite replication and maintain a balanced tissue environment (McGovern and Wilson 2013, Sasai and Yamamoto 2019, Biswas et al. 2017).

During chronic infection, despite cyst-containing neurons and brain inflammation caused by the recruitment of peripheral immune cells, Toxoplasma causes few clinical symptoms in the immunocompetent host. However, underlying changes in neurochemistry and significant changes in the health of neurons (David et al. 2016, Mendez et al. 2021) suggest a constant need to balance inflammation and protect against neuropathology. Recent work in our lab to determine Toxoplasma-induced changes in immunological and neurological transcripts in the brain (Bergersen et al. 2021) supports these neurological changes but also reveals potential neuroprotective pathways that remain poorly understood.

The concept of neuroprotection and resolution of inflammation has been investigated in models of central nervous system (CNS) injury such as ischemic stroke and spinal cord injury and during experimental cerebral malaria (ECM) infection. In these models, neuronal integrity is maintained via signaling of the endogenous ligand Neuregulin 1 (NRG-1) through its main receptor ErbB4 (Simmons et al. 2016, Liu et al. 2018). Resolution of neuropathology in a model of ischemic stroke is further supported by the clearance of damage signals, debris, and revascularization by macrophage scavenger receptor 1 (MSR1) (Shichita et al. 2017). Transcripts of this scavenger receptor are also upregulated during Toxoplasma infection in a step-wise manner correlating with increasing chronicity (Bergersen et al. 2021). While the expression and function of these neuroprotective molecules contribute to neuroprotection in the above-mentioned diseases, their cellular sources and their functions in protecting against Toxoplasma infection and pathology remain unknown.

In recent years, research has brought recognition that the function of neutrophils is not simply to act as a first responder but can also be critical throughout immune responses including during chronic inflammation. Two recent independent research groups have identified a small population of these cells present in the brain between 2- and 4-weeks post infection (wpi) (Biswas et al. 2017, Schneider et al. 2019). Neutrophils, commonly thought of as one of the earliest host responses to infection, are one of the primary cell types responsible for the recruitment of other innate immune cells, and their presence is vital for control of acute infection (McGovern and Wilson 2013, Debierre-Grockiego et al. 2020, Petri et al. 2000, Bliss et al. 2001). However, this discovery of neutrophils

during chronic infection suggests a more versatile role for these cells. Previous literature focusing on potential alternative roles for neutrophils in non-Toxoplasma models describes two basic classes of these cells based on their differential expression of markers such as CD15 and CD49d among others (Tsuda et al. 2004, Beyrau et al. 2012, Nakayama et al. 2001). While these earlier studies introduce the idea of alternative neutrophil functions, more recent works investigating neutrophils in homeostasis, tissue injury, and non-Toxoplasma models of infection have demonstrated a much broader range of previously undescribed heterogeneity and functions among these cells (Peiseler and Kubes 2019, Xie et al. 2020). Therefore, the presence of neutrophils during chronic T. gondii, may point to an important yet undefined role for these cells in the brain during chronic infection.

In this study, we have discovered the expression of neuroprotective molecules including NRG-1, ErbB4, and MSR1 among others by a persistent population of neutrophils in the brain during *T. gondii* infection. These cells have distinct phenotypic and transcriptomic profiles compared to peripheral neutrophils including CNS-specific signatures that define this population and point to a role in resolution of infection-induced neuropathology. Depletion of this population leads to an increase in vascular pathology and a decrease in neuronal regeneration during infection. The combined data reveal two populations of neutrophils that are capable of acting simultaneously as effector and neuroprotective cells. Such capacity for functional flexibility within these cells presents a paradigm shift in our understanding of neutrophils in the brain during infection and marks them as

playing an important role in protecting against neuropathology caused by chronic Toxoplasma infection.

Materials and Methods

Animals, Parasites, and Mouse Infections/Kinetics Studies

Animals. All research was conducted in accordance with the Animal Welfare Act, and all efforts were made to minimize suffering. All protocols were approved by the Institutional Animal Care and Use Committee (IACUC) of the University of California, Riverside. Female 6-8 weeks old WT C57BL/6J mice were obtained from Jackson Laboratories and were maintained in a pathogen-free environment in accordance with IACUC protocols at the University of California Riverside.

Parasites and infections. The ME49 strain of *T. gondii* was maintained in cyst form by continuous passaging in SW and CBA/J mice. Female 6-8 week old WT C57BL/6J mice were infected with 10 ME49 cysts per mouse in 200µl of sterile 1x PBS solution via intraperitoneal (IP) injection. Naïve controls received 200µl of sterile 1x PBS solution via intraperitoneal (IP) injection.

Mice were infected as described above and sacrificed at the following acute and chronic time points: 1wpi (an acute time point where little cyst formation is seen in the brain), 2wpi (an early chronic time point where cysts are actively forming and immune cells are recruited), 4wpi and 6wpi (2 mid-chronic time points where cysts have been fully formed and a chronic inflammatory state is well-established), and 11wpi (a late chronic time point where increased parasite reactivation can sometimes be seen). At each time point,

half brain and whole spleen were harvested for flow cytometry, and the other half brain and one lobe of liver were harvested for immunohistochemistry or parasite burden, respectively.

Neutrophil Depletion Experiments

After 4 weeks of infection, when chronic infection was well-established, a cohort of infected mice were injected with 500µg/mouse of Ly6G depleting mouse monoclonal antibody in vehicle (sterile 1x PBS) via 200µl intraperitoneal injection every other day for 14 days according to previously published protocols (Biswas et al. 2017). A cohort of infected non-depleted mice received 200µl/mouse of vehicle (sterile 1x PBS) intraperitoneally every other day for 14 days to control for depletion injections.

Cell Processing

Naïve and infected female C57BL/6J mice were sacrificed and perfused intracardially with 20 mL of sterile 1x PBS. Blood, spleens and half brains were harvested, and splenocytes and brain mononuclear cells (BMNCs) were processed according to previously published protocols (Goerner et al. 2020, David et al. 2016). For neutrophil localization studies, whole brain was harvested and dissected into 3 broad regions (cortex, mid-brain region, and cerebellum) using brain morphology to define regions for each mouse. BMNCs were then processed as above.

Flow Cytometry

Processed cells were diluted with FACS buffer (4g BSA, 50mg EDTA, 1L 1xPBS) to 1.0 x10^6 cells/ml (or all cells from respective brain regions) and transferred to FACS tubes for staining. Cells were incubated with 1:10 FC Block (BD) for 10 minutes on ice followed by fluorophore-conjugated or primary unconjugated antibodies for surface staining for 30 minutes protected from light. Cells were washed with FACS buffer solution and incubated in fluorophore-conjugated secondary antibodies as needed for 30 minutes protected from light. Fluorophore-conjugated antibodies used during surface staining are as follows: CD45 PE (Invitrogen), CD11b APCCy7 (Invitrogen), Ly6G PerCPcy5.5 (Clone 1A8, BD), CD62-L APCCy7 (BD), CD3 FITC (BD), CD4 APC (Invitrogen), CD4 APCCy7 (Invitrogen), CD8 PECy7 (Invitrogen), CD11b PerCPCy5.5 (eBioscience), CD11b APC (eBioscience), Ly6G BV510 Clone 1A8 (eBioscience), CXCR4 PECy5.5 (ThermoFisher), and MMP9 AF647 (SantaCruz Biotech). Primary unconjugated antibodies and their corresponding fluorophore-conjugated secondary antibodies are as follows: NRG-1 primary antibody (Invitrogen) with Alexafluor 647-conjugated secondary antibody (ThermoFisher); NRG1 primary (Santa Cruz Biotech) with Alexafluor 568-conjugated secondary (ThermoFisher); MSR1 primary (Invitrogen) with Alexafluor 488-conjugated or Q Dot 655-conjugated secondary (ThermoFisher); VEGF primary (NovusBio) with Alexafluor 680-conjugated secondary (ThermoFisher); and biotinylated CD15 primary (Invitrogen) with PECy7-conjugated Streptavidin (eBioscience). Following surface staining, cells were washed, fixed in 4% PFA, and resuspended in FACS buffer. For intracellular staining, cells were spun at 1500rpm in

0.3% Saponin for 10min to permeabilize cells and then incubated with FITC-conjugated ErbB4 (Santa Cruz Biotech) in Saponin to maintain permeabilization. After incubation, cells were washed and resuspended in FACS buffer. Samples were acquired using either a BD FACS Canto II flow cytometer or NovoCyte Quanteon machine, NovoSampler Q, and NovoExpress Software at the UC Riverside core facility. Analysis was conducted using FlowJo software. For specific panels and gating strategy used, see **Supplemental Table 3** and **Supplemental Figure 2**.

Cell Sorting and Single Cell RNA Sequencing

Cell Sorting. Neutrophils were sorted from brain and spleen based on CD11b/Ly6G positivity. BMNCs and splenocytes were harvested as above at 4wpi. To obtain a large enough number of neutrophils for sequencing, 3 naïve and 3 infected mice were pooled for naïve and infected neutrophil splenocyte samples, and 7 infected mice were pooled for neutrophil BMNC sample. 3 separate infected mice were pooled for an unsorted BMNC control sample. Cells were incubated in fluorescent-conjugated antibodies for CD11b APCCy7 (Invitrogen) and Ly6G PE or PerCPCy5.5 (Clone 1A8; Invitrogen), rinsed, and resuspended at 1.0×10^7 concentration in FACS buffer with 10% FBS to minimize cell death during sorting. Neutrophils were sorted from pooled samples based on gating strategy of Ly6G+CD11b+ cells using a MoFlo Astrios EQ Cell Sorter at 3-4% pressure to maximize cell survival. Sorted cells were re-counted to determine viability, and a minimum of 1.0×10^4 sorted cells were used for single cell sequencing.

10x Sequencing and Analysis. Sorted Ly6G+CD11b+ cells and unsorted BMNC control sample were processed for single cell RNA sequencing according to 10x sample prep protocols for Steps 1-3 (Manual: CG000204 RevD); instructions were followed exactly. Time spent before loading sorted cells onto 10x Chromium controller for Step 1 was <1hr. Processed samples were analyzed after Steps 2 and 3 via Bioanalyzer by the UCR Genomics Core facility for viability and concentration before proceeding to next steps. Upon completion of the 10x protocol, samples were sent to the UC San Diego IGM Genomics Center for sequencing (500 million reads/sample).

Immunohistochemistry

A minimum of 4 biological replicates were used for each group of mice (naïve, infected, and infected neutrophil-depleted). Following perfusion, sagittal half brains were harvested and post-fixed in 4% PFA for at least 24 hours followed by 30% sucrose for 48 hours. Brains were frozen at -80°C in optimal cutting temperature compound (OCT) and sectioned sagittally at 10µm thickness using a cryostat and charged slides.

H&E Staining. Briefly, H&E staining protocol was as follows: fixation of slides in 95% ethanol followed, incubation in hematoxylin followed by eosin stain for 30 seconds each (with fixation step in between), fixation in 95% and 100% ethanol, and final fixation using Citrisolv. Slides were sealed with coverslips using Cytoseal (ThermoFisher) and dried overnight. Imaging was performed using ImageJ software.

Histology Scoring. Slides were blinded and pathological observations in brain tissues (n=4 per group) were scored using the following criteria (lowest possible score = 4, highest possible score = 13):

1. Meningeal Inflammation Score (Scale of 1-3): 1 = little/no inflammation (maximum of 1 layer of cell nuclei present in meninges); 2 = moderate inflammation (evidence of some meningeal thickening and 1-3 layers of cell nuclei present); 3 = severe inflammation (evidence of increased overall meningeal thickening and multiple layers of cell nuclei present).
2. Perivascular Cuffing Score (Scale of 1-3): 1 = no perivascular cuffing present (little/no cell nuclei present inside blood vessels); 2 = perivascular cuffing present (evidence of blood vessel swelling and presence of multiple cell nuclei (1-2 layers of cells) inside blood vessel); 3 = severe perivascular cuffing present (very swollen blood vessels and presence of multiple cells nuclei (2-3 layers of cells) inside blood vessel, also presence of lysed blood vessels with many cell nuclei in these areas).
3. Cyst burden Score (Scale of 1-4): 1 = 0 cysts counted; 2 = <10 cysts counted for whole sample (4 brain slices); 3 = 10 cysts counted for whole sample; 4 = >10 cysts counted for whole sample.
4. Overall Tissue Integrity Score (Scale of 1-3) – based on combined meningeal inflammation and perivascular cuffing severity: 1; = undamaged tissue (little/no meningeal inflammation and no perivascular cuffing present); 2 = moderately damaged tissue (moderate meningeal inflammation and evidence of perivascular

cuffing in tissue); 3 = severely damaged tissue (severe meningeal inflammation and perivascular cuffing present).

Blood Vessel and Cyst Quantification. For quantification of blood vessels and cysts from H&E-stained brain sections, quantification was blinded. Total numbers of blood vessels and cysts were quantified from each whole sample (n=4 per group). Total counts per sample were calculated by adding numbers of blood vessels and cysts counted in each brain section (4 sections/sample) to account for biological variability for each group.

Immunofluorescence. Slides were fixed and permeabilized in 75% acetone/25% ethanol for 10 minutes at room temperature. Slides were blocked with 5% Donkey serum for 30 minutes at room temperature and incubated with primary antibodies at room temperature for 1 hour protected from light. Primary antibodies and dilutions used are listed: Rabbit NeuN (1:200, Abcam); Goat *T. gondii* (1:300, Abcam); Chicken GAP43 (1:200, Novus Biologicals); Rabbit SLPI (1:200, Novus Biologicals); and Rabbit TJP1 (1:200, Novus Biologicals). The PE-conjugated PECAM1 antibody (1:100, eBioscience) was also used. After primary incubation, slides were rinsed three times with 1x PBS for 5 minutes each wash and incubated for 1 hour protected from light at room temperature with the following secondary antibodies (1:1000 dilution, Thermofisher): Donkey anti-Rabbit Alexafluor 488, Donkey anti-Goat Alexafluor 568, Donkey anti-Chicken Alexafluor 647, and Goat anti-Rabbit Alexafluor 488. For specific panels used, see **Supplemental Table 4**. Following secondary incubation, slides were washed 3x in 1x PBS for 5 minutes each wash. Coverslips were mounted on slides using VectaShield Hardset Mounting Medium with DAPI (Vector Labs), and slides were dried overnight in the dark at room

temperature. Imaging was performed using a Leica inverted DMI6000 B microscope at 40x magnification and Las-X software.

GAP43, SLPI, and TJP1 Quantification. Slides were blinded, and a minimum of 10 positive cells were counted per whole sample (counted from a minimum of 5 regions of interest (ROIs) per section x 4 sections/sample = minimum of 20 ROIs per sample). GAP43 positive staining was characterized as either nuclear puncta (Gorup et al. 2015) or cytoplasmic (Sas et al. 2020, Guarnieri et al. 2013) based on previous studies. For TJP1 quantification results, the ratio of TJP1+ vessels: total vessels counted was calculated.

Parasite Burden and B1 Gene Analysis

Parasite burden in brain and peripheral liver was quantified as previously described (Bergersen et al. 2021, Goerner et al. 2020). Briefly, DNA from naïve and 2, 4, 6, and 11-week infected half brains and liver lobes of mice (n=4/group) was extracted and purified using a High Pure PCR Template Prep Kit (Roche). DNA concentration of each sample was determined via NanoDrop, and all DNA was normalized to 12.5 ng/µl before amplification. Parasite burden was measured by amplifying the B1 gene of *T. gondii* by RT-PCR.

Statistical Analyses

All experiments were repeated a minimum of 3 times to confirm accuracy and consistency of results, and all experiments were conducted with a minimum of n=3 to account for biological variability. Statistical significance for all experiments was determined by either 2- tailed unpaired Student's t-test or One-Way ANOVA with

multiple comparisons and a p-value < 0.05 was considered statistically significant. The type of statistical test run for each experimental result is indicated in the corresponding figure legends.

scRNAseq Analysis. Sequencing files were analyzed using the following softwares: FileZilla, HPCC Cluster, Cell Ranger (version 5.0), and Loupe Browser (version 5.0). FastQC and MultiQC were used to evaluate the quality of sequencing reads. Sequencing reads were aligned (fastq) to the mm10 mouse reference genome for analysis, and the expression of transcripts was quantified in each cell. Low quality cells were excluded from analysis using the Normalize function during analysis. Sequencing saturation was confirmed for each sample. After quality control checks, the following cells and average gene reads per cell were obtained: Brain Neutrophils = 3,242 cells, 736 reads/cell; Infected Spleen Neutrophils = 6,804 cells, 782 reads/cell; Naïve Spleen Neutrophils = 4,813 cells, 702 reads/cell; BMNCs = 2,280 cells, 1,014 reads/cell. For differentially expressed genes (DEGs), genes with $p<0.05$ after comparison to control values were considered significantly enriched, and all genes discussed in this study were identified as significantly altered. Selected genes for heatmap analysis were confirmed as significantly altered ($p<0.05$). The top 50 most significantly enriched genes in each identified neutrophil subset were used for Gene Ontology (GO) analyses, and the "Biological Processes" option was selected for the *Mus musculus* host.

Results

Neutrophils in the CNS are sources of neuroprotective molecules during chronic infection.

Our previous work has demonstrated the activation of potential neuroprotective and reparative pathways in the brain during chronic Toxoplasma infection (Bergersen et al. 2021), but the cellular sources of neuroprotection reman widely unknown. To determine sources of previously defined neuroprotective molecules in the CNS during chronic Toxoplasma infection, we performed flow cytometry on BMNCs and peripheral splenocytes at various stages of infection and examined the expression of NRG-1, ErbB4, and MSR1 (**Figure 8**).

In addition to analysis of T cells, microglia and macrophages within the brain and as previously demonstrated by the Dunay lab and colleagues (Biswas et al. 2017), a small but well-defined population of neutrophils was seen in the brain during chronic infection based on their expression of Ly6G and CD11b (**Supplemental Figure 2A**). Neutrophils were classified as fully differentiated and mature based on their expression of CD11b, Ly6G, MHC I, and the lack of the proliferative marker Ki67 (**Supp. Fig. 2B**). To determine the size and duration of this population over the course of infection, neutrophil percentages and absolute cell numbers were quantified from the brain at each time point. Results demonstrated consistency of this population during chronic infection after a slight decrease after 2wpi (**Supplemental Figure 3A**). Previous studies investigating the role of infiltrating inflammatory monocytes in the brain during chronic Toxoplasma infection

have found infection-specific localization to the olfactory tubercle suggesting location-specific functions of these cells (Schneider et al. 2019). To determine if our neutrophil population was recruited to a particular part of the CNS, brains were perfused and the cerebellum, frontal cortex and mid-brain were dissected, anatomical areas that are easily identified and isolated. Although the percentage of neutrophils was higher in the cerebellum, neutrophils showed little localization and instead show broad disbursement throughout the brain (**Supplemental Fig. 3B).** These results demonstrate a persistent broadly disbursed chronic brain neutrophil population.

Strikingly, flow cytometry analysis revealed that these neutrophils were consistent, significant and almost uniformly cellular sources of NRG-1 (>60% of neutrophils). A large percentage were also expressing ErbB4 (20-60% of neutrophils), and MSR1 (>60% of neutrophils) from 2wpi-11wpi (**Fig. 8A-C**). Infiltrating macrophages and resident microglia were also sources of these molecules, NRG-1 (10-30% of macrophages, 40-90% of microglia, **Fig. 8A**), ErbB4 (>60% of macrophages, 10-60% of microglia, **Fig. 8B**), and MSR1 (>40% of macrophages and microglia, **Fig. 8C**) throughout infection. Adaptive T cells did not express ErbB4 nor MSR1 at any time point, however a subpopulation (10-20%) did express NRG-1 which increased over the course of infection (**Fig. 8B**). This data demonstrates that in contrast to other immune cells, neutrophils (>60%) are consistent cellular sources of the neuroprotective molecules NRG-1, ErbB4, and MSR1 in the brain during infection.

Neutrophils were composed of two main subtypes based on their expression of the integrin CD15 (**Fig. 8D-F**). This integrin aids in migration into tissues and has previously

been used to identify broad “classical” (CD15+) and “alternative” (CD15-) categories of neutrophils (Nakayama et al. 2001) with classical neutrophils primed as effector cells for pathogen killing and alternative neutrophils associated with healing, tissue remodeling, and vasculature repair. At 4wpi, more than 80% of neutrophils were NRG-1+ and approximately 60% of these NRG1+ cells expressed CD15, with high expression of NRG-1 correlating with expression of CD15 (**Fig. 8D**). These two neutrophil subtypes were further distinguished by their differential expression of the NRG-1 receptor, ErbB4. Alternative neutrophils that did not express CD15, were more likely to express ErbB4 and therefore be responsive to neuregulin (**Fig. 8E, G**). The expression of MSR1 was more diverse and independent of CD15 expression (**Fig. 8F**). Collectively, these results identify neutrophils as a persistent broadly disbursed cell population in the brain during chronic Toxoplasma infection. These cells are consistent cellular sources of neuroprotective molecules and are composed of 2 main subtypes based on their differential expression of CD15 and ErbB4.

Protein analysis of chronic brain neutrophils reveals a distinct phenotypic profile.

To determine if the expression of NRG-1, ErbB4, and MSR1 by brain neutrophils defined a CNS-specific protective neutrophil phenotype, cells were further analyzed for proteins known to play a role in neutrophil function. Previously identified proteins including MMP9, VEGF, CD62-L, and CXCR4 play a role in alternative/protective neutrophil functions including tissue repair and angiogenesis, but these functions have been observed predominantly in the periphery (Peiseler and Kubes 2019, Biswas et al. 2017). To determine the expression of these molecules previously associated with protective

functions by our brain neutrophils, BMNCs and peripheral splenocytes were incubated with antibodies to Ly6G, CD11b, CD15, NRG-1, ErbB4, MSR1, MMP9, VEGF, CD62-L, and CXCR4, and multi-parameter flow cytometry was conducted. Neutrophils from brain and periphery were identified using previously described techniques (**Supplemental Fig. 2**), and tSNE plots of Ly6G and CD11b expression confirmed positive neutrophil phenotype (**Supplemental Fig. 4**). When neutrophils from the brain were compared to those from the spleen, tSNE plots of all proteins analyzed revealed mostly non-overlapping populations (**Fig. 9A**).

Expression of individual targeted proteins was evaluated to discern phenotypical differences betweenbrain and splenic neutrophils over the course of infection (**Supplemental Fig. 5**). Striking visual differences between brain and splenic neutrophils were seen in expression of ErbB4, MSR1, VEGF, and CD62-L at 4wpi (**Fig. 9B**), with neutrophils from the brain uniformly expressing higher levels of MSR1 and VEGF compared to those from the spleen. In addition, clustering analysis defined brain neutrophil subsets based on the differential expression of ErbB4 and CD62-L which was not observed in the spleen population. Additionally,brain neutrophils demonstrated higher percentages of MSR1+ and VEGF+ cells compared to splenic neutrophils. NRG-1 expression by these cells did not define further subsets but was expressed by all cells at 4- and 11wpi (**Supplemental Fig. 5A**). Contrastingly, splenic neutrophils demonstrated 2 distinct subsets based on NRG-1 expression (**Supplemental Fig. 5B**). Analysis of neutrophils from the blood served as another peripheral population and demonstrated similar results to those of the spleen compared to our brain population (**Supplemental**

Figure 6). This data demonstrates a distinct phenotypic profile ofbrain neutrophils characterized by differential expression of targeted neuroprotective molecules when compared to periphery. As such, this population was defined as unique and will be referred to as "neut^{B} cells" for the duration of this manuscript.

It was thought that the distinctly neuroprotective phenotype observed in neut^{B} cells could be caused by the alteration of one specific subset (CD15+ or CD15-) upon entry into the brain. To test this hypothesis, the above tSNE plots were quantified based on CD15 positivity. Results confirmed neut^{B} expression patterns of ErbB4 and MSR1 based on CD15 positivity as expected (**Fig. 8**). Significant differences were observed between neut^{B} cells and splenic neutrophils independent of CD15 expression in the expression of ErbB4, MSR1, VEGF, and CD62-L (**Fig. 9C**). These results demonstrate that the phenotypic differences in neuroprotective molecule expression observed between neut^{B} cells and peripheral neutrophils encompass the neut^{B} population as a whole, and it is not one specific subset of these cells (CD15+/-) that drives the development of a CNS-specific profile.

In addition to being described as classical and alternative, neutrophils can also be distinguished by age and changes in migratory capability as reviewed by Peiseler and Kubes (Peiseler and Kubes 2019). Thus, it was hypothesized that differences in migration capability and age would be apparent in neut^{B} cells compared to splenic neutrophils as chronic infection progressed. To address this, the expression of CD15 (indicative of the ability to migrate (Nakayama et al. 2001)) and CXCR4 (indicative of aged neutrophils (Casanova-Acebes et al. 2013)) was monitored over the course of chronic infection (**Fig.**

9D). The percent of CD15+ neut^{B} cells increased from 2wpi (20%) to 4wpi (>60%) and dropped back to baseline by 11wpi (20%), but CD15+ splenic neutrophils remained consistent (~30% of whole population) from 4wpi on (**Fig. 9D, left**). Differences were also observed between CXCR4+ neut^{B} and peripheral cells; the percent of CXCR4+ neut^{B} cells increased by 10% from 2- to 4wpi and remained consistent through 11wpi while peripheral CXCR4 expression decreased by 20% from 2- to 4wpi and gradually returned to baseline by 11wpi (**Fig. 9D, right**). The most notable difference in expression of these molecules occurred at 4wpi. These results confirm the hypothesized differences in migration capability and age between neut^{B} and peripheral cells over time. Taken together, these results identify a phenotypically distinct neut^{B} population that differs from the spleen in its expression of alternative-associated proteins and demonstrates changes in migratory capability and age.

Aged resident and non-aged infiltrating subsets of* neut^{B} *cells display functional heterogeneity.

Having previously identified a unique phenotype and proteins associated with different neut^{B} subsets, we performed single cell RNA sequencing (scRNAseq) on sorted neut^{B} and peripheral cells to further assess tissue-dependent differences in the transcriptomic profile of neutrophils during chronic infection. To accomplish this, neutrophils were sorted from pooled brains and spleens of 4wk-infected mice based on positive CD11b and Ly6G expression. Resulting samples were aggregated following sequencing, and transcriptomic profiles of neut^{B} cells vs splenic cells were analyzed (**Figure 10 and Supplemental Figure 7**). To confirm positive neutrophil signatures in all datasets, *Ly6G*

gene enrichment was evaluated in all sequenced samples (**Supplemental Fig. 8**). When comparing all aggregated samples in UMAP format, neut^{B} cells (red cells) clustered predominantly separately from splenic neutrophils (yellow = spleen from infected mouse, orange = spleen from naive mouse) and control BMNC cells (**Supplemental Figure 7**). When all sorted neutrophils were aggregated and analyzed separately, a nearly complete separation of neut^{B} cells (shades of red) from infected (shades of green) and naïve (shades of blue) spleen neutrophils was observed (**Fig. 10A**). This distinct clustering of neut^{B} cells at the transcriptional level supports CNS-dependent transcriptional changes and potential CNS-specific functions of these cells.

scRNAseq analysis of neut^{B} cells alone resulted in 8 distinct clusters. Of these clusters, two (shades of red) were confidently identified as neutrophils based on their enrichment of *Ly6G* and *Itgam* (encodes CD11b) (**Fig. 10B**). To identify remaining cell types, targeted genes for known cell types (T cells, macrophages/microglia, inflammatory monocytes, neurons, astrocytes, and oligodendrocytes) were analyzed (**Supplemental Figure 9**). Heatmap visualization of gene expression identified several cell types: red blood cells (Cluster 5), resident CNS cells (Cluster 1 and 8), T cells (Cluster 7), and unknown/potential apoptotic cells (Cluster 2 and 3) respectively. The two identified neutrophil clusters (Clusters 4 and 6) were identified in our aggregated dataset (**Fig. 10A, blue and black outlines**) and were further classified based on enrichment of the genes *Fut4* (encodes for CD15) and *Cxcr4* based on our flow cytometry results and recent literature (reviewed by Peisler and Kubes (Peiseler and Kubes 2019)). Cluster 4 (**Fig. 10B, blue outline**) was enriched for *Ly6G*, *Fut4*, and *Cxcr4* and termed “Aged Resident

Neutrophils." Cluster 6 (**Fig. 10B, black outline**) was enriched for *Ly6G*, showed intermediate enrichment for *Fut4*, and was not enriched for *Cxcr4*. This cluster was named "Non-aged Infiltrating Neutrophils." These results demonstrate two major subsets of neut^{B} cells namely "Aged" and "Non-aged" defined primarily by *Cxcr4* enrichment.

When compared directly to each other, "Neuroprotective Phenotyping" heatmap analysis demonstrated enrichment for *Vegfa*, *Nrg1*, *Flt1* (encodes for VEGF receptor), and *Msr1* in Aged-resident cells while Non-aged Infiltrating cells showed enrichment for *Sell* (encodes for CD62-L) and *Mmp9* and had increased *ErbB4* compared to the Aged Resident subset (**Fig. 10C**). Heatmap comparison analysis looking at gene enrichment corresponding to classical NETosis and alternative angiogenesis demonstrated enrichment of genes relating to both NETosis and angiogenesis in each subtype indicating functional heterogeneity of these cells (**Fig. 10D**). Aged Resident cells demonstrated enrichment for *Bmf* (NETosis gene) and the angiogenic genes *Pdgfb*, *Vegfa*, *Kdr,* and *Hif1a*, andNon-aged Infiltrating cells were enriched for the NETosis-associated genes *Mapk3* and *Padi4* and the angiogenic genes *Mmp8* and *Mmp9*. Specific indicators of apoptosis were also examined including *Bcl2*, *Casp1*, *Akt1*, and *Akt2* and showed no significant enrichment in either subset. These results show differential enrichment for neuroprotective-associated genes and function-related genes between neut^{B} cells which demonstrates functional heterogeneity.

GO analysis of the top 50 most enriched genes in each neut^{B} subset showed different upregulation of GO terms (**Fig. 10E-F**). Aged Resident cells were most enriched for terms relating to negative regulation and development (**Fig. 10E**). In contrast, Non-aged

Infiltrating cells were enriched for terms associated with classical neutrophils functions (**Fig. 10F**). Taken together, these sequencing results demonstrate a brain-specific transcriptomic profile of neut^{B} cells which can be separated into two major subsets that display neuroprotective characteristics and functional heterogeneity.

Neutrophils during chronic infection are required to control parasite burden.

To determine the requirement of these functionally flexible neut^{B} cells for control of chronic CNS infection, neutrophils were systemically depleted over the course of 2 weeks at starting at 4wpi using a neutralizing Ly6G monoclonal antibody (mAb). Resulting brain and splenic neutrophil numbers, overall brain parasite and cyst burden, and brain pathology were evaluated (**Figure 11**). Neutrophils were again defined as CD11b+Ly6G(Clone 1A8)+ for gating strategy (**Supplemental Fig. 2A**). Flow cytometry analysis demonstrated >90% depletion of neutrophils in brain and spleen (**Supplemental Fig. 10A**). Absolute numbers of neutrophils in both brain and spleen were significantly lower following depletion compared to infected controls indicating successful neutrophil depletion (**Fig. 11A**). Neutrophils in the brain decreased ~4-fold following systemic depletion, and peripheral spleen neutrophils similarly decreased ~5-fold. To confirm that this depletion method was neutrophil-specific and did not affect other infiltrating immune cells, macrophage numbers in brain were also quantified post-depletion and were found to be unaffected (**Supplemental Fig. 10B**).

To test the role of neutrophils in parasite control and pathology prevention during chronic infection, histology and parasite burden quantification was performed on naïve, infected

control, and infected neutrophil-depleted brains. Toxoplasma *B1* gene analysis demonstrated significantly elevated parasite burden (>2-fold increase) in the brain following neutrophil depletion (**Fig. 11B**). This was specific to the brain as peripheral liver parasite burden remained low but unchanged (**Supplemental Fig. 10C**). Histological analysis quantified meningeal inflammation, overall brain pathology, and cyst burden, and no significant difference was observed in inflammation or overall brain pathology (**Fig. 11C**). However, cyst burden was significantly higher in neutrophil-depleted mice compared to infected controls supporting our parasite burden results (**Fig. 11D**). Collectively, these experiments demonstrate significant increases in both parasite and cyst burden in the absence of chronic brain neutrophils.

Lack of neut^{B} cells leads to increased blood brain barrier permeability.

It is known that Toxoplasma employs various mechanisms to enter into the brain environment including transmigration through cells in the blood brain barrier (BBB) during the early stages of infection (Olivera et al. 2021). Supporting this previous finding, Evans Blue (EB) staining of infected brains during acute and chronic stages of infection demonstrated an initial increase in EB disbursement into the brain indicative of increased BBB permeability (**Fig. 12A, left**). This dissipated through 2wpi and was then present again at 4- and 6wpi. Quantification of these results confirmed significant increases in EB staining intensity at 3dpi and at the chronic time points of 4- and 6wpi (**Fig. 12A, right**). The enrichment of pro-angiogenic and vasculature repair-associated genes in neut^{B} cells (**Figure 10**) led us to hypothesize that neut^{B} cells play a role in angiogenesis and vasculature repair. To test this, we sought to determine the effect of neutrophil depletion

on angiogenesis, BBB permeability, and vasculature repair (**Fig. 12B-C**). Blinded quantification of blood vessels from naïve, infected control, and infected neutrophil-depleted brains demonstrated significantly more blood vessels counted in infected control and neutrophil-depleted brains compared to naïve controls (**Fig. 12B**) which suggests damage to followed by repair of the vasculature in the brain as demonstrated in **Fig. 12A**. However, total blood vessels quantified from neutrophil-depleted brains did not differ significantly from infected control brains suggesting that neut^{B} cells do not play a role in angiogenesis. When BBB permeability was investigated via scoring of perivascular cuffing severity following neutrophil depletion, neutrophil-depleted brains demonstrated increased perivascular cuffing severity compared to infected and naïve controls (**Fig. 12C**). These results demonstrate that while a lack of neut^{B} cells does not affect vasculature angiogenesis, it does lead to increased BBB permeability.

Because a lack of neut^{B} cells led to increased BBB permeability which is often detrimental to the host if not controlled, it was hypothesized that neut^{B} cells play a necessary role in vasculature repair attempts and vascular remodeling. To test this, infected control and neutrophil-depleted brains were incubated in antibodies for mature blood vessels (PECAM1+) and newly formed vessels (TJP1+) (Liu et al. 2022, Strauss et al. 2021), and ratios of newly formed blood vessels: total blood vessels were compared. Qualitative differences in staining for TJP1 were observed between blood vessels from infected control and neutrophil-depleted brains (**Fig. 12D**). TJP1+ vessels from neutrophil-depleted brains demonstrated staining constricted to the outer edge of the vessel (**Fig. 12D, top**) while infected control vessels exhibited more diffuse cytoplasmic

staining indicating increased regeneration (**Fig. 12D, bottom**). The overall ratio of TJP1+ vessels: total vessels did not change following neutrophil depletion (**Fig. 12E**), but differences in TJP1 expression observed in **Fig. 12D** indicates a change in vasculature repair capability. Taken together, these results demonstrate increased BBB permeability and differences in vasculature repair-related protein expression in the brain in the absence of neut^{B} cells.

Neuronal regeneration attempts during chronic infection are inhibited in the absence of neutrophils.

Neutrophils have previously been identified as neuroprotective in the CNS by encouraging neuronal regeneration via promoting upregulation of GAP43 by neurons in models of optic nerve and spinal cord injury (SCI) (Sas et al. 2020, Kurimoto et al. 2013). Additionally, neutrophil expression of secretory leukocyte protease inhibitor (SLPI) and neutrophil-dependent neuronal expression of SLPI has been shown to encourage regeneration of neuronal axons in models of SCI and optic nerve injury (Ghasemlou et al. 2010, Hannila et al. 2013). Despite this protective role of neutrophils in the spinal cord and optic nerve (other areas of the CNS), neuroprotective functions of neutrophils in the brain have yet to be demonstrated. To determine whether neut^{B} cells are directly neuroprotective (actively influencing neuronal function) during Toxoplasma infection, we investigated GAP43 and SLPI expression in the brain following depletion of neutrophils (**Figure 13**).

Immunofluorescence imaging demonstrated visual differences in GAP43 staining between infected control and neutrophil depleted brains (**Fig. 13A**). Two different types of GAP43 expression were observed in both control and depleted tissues: 1) GAP43 staining that was restricted to the nucleus indicative of activation of GAP43 signaling but not active regeneration (Gorup et al. 2015) and 2) diffuse GAP43 expression throughout the cell cytoplasm indicative of actively regenerating neuronal cells (Sas et al. 2020, Guarnieri et al. 2013). Infected control brains demonstrated both obvious GAP43+ cytoplasmic and nuclear staining (**Fig. 13A, top panel, pink and white arrows**) while neutrophil-depleted brains demonstrated primarily GAP43+ nuclear staining (**Fig. 13A, bottom panel, white arrows**). When both types of GAP43 staining were blindly quantified, neutrophil-depleted brains showed a trend towards decreased cytoplasmic and increased nuclear-restricted GAP43+ staining, but these trends did not reach significance (**Fig. 13B**). These results demonstrate that neutrophils do not significantly alter neuronal regeneration during infection via the GAP43 signaling pathway.

While neutrophils were not responsible for activation of the GAP43-dependent neuronal regeneration pathway, immunofluorescence imaging of SLPI demonstrated significant differences following depletion of neutrophils (**Fig. 13C-D**). SLPI+ cell bodies and SLPI+ cell projections (shown by white arrows) were identified in both infected control and neutrophil-depleted brains (**Fig. 13C**). Based on morphology, SLPI+ cell bodies and projections were confidently identified as neurons and neuronal axons respectively and were classified as “SLPI+ cells”. When this data was blindly quantified, mice lacking neutrophils showed significantly fewer SLPI+ cells when compared to infected controls

(**Fig. 13D**). These results collectively demonstrate neutrophil-dependent neuronal axon regeneration during chronic Toxoplasma infection.

Discussion

The predominantly asymptomatic infection in immunocompetent hosts caused by Toxoplasma despite continuous inflammation suggests that there are undescribed neuroprotective mechanisms at work to maintain brain homeostasis. This study describes a chronic neutrophil population in the brain capable of protecting against infection and maintaining tissue homeostasis via direct and indirect neuroprotection. We found a persistent neutrophil population present in the brain during chronic infection based on their expression of the canonical neutrophil markers Ly6G and CD11b (**Supplemental Figure 2**). This population remains in the brain for the duration of chronic infection after a brief drop in both percentage and total cell numbers from 2- to 4wpi (**Supplemental Fig. 3A**). This drop is evidence of the development of a long-lasting chronic neutrophil population after initial die-off of acute infiltrating cells during early chronic infection. These cells are also broadly disbursed in the brain (**Supplemental Figure 3B)** disproving our hypothesis that they are regionally-restricted to areas where Toxoplasma cysts are predominantly found.

Our results demonstrate that neutrophils in the brain are consistent cellular sources of neuroprotective molecules including NRG-1, ErbB4, and MSR1 (**Figure 8**). Expression of these previously identified neuroprotective molecules indicates neuroprotective functions of these otherwise innate immune cells. Additionally, lack of NRG-1 and

ErbB4 expression by lymphocytes demonstrates that expression of these molecules is specific to innate immune cells (**Fig. 8A-B**). This innate-dependent expression of neuroprotective molecules could be the result of a shift in the needs of the brain once adaptive lymphocytes take over the main anti-parasitic and infection control functions. Supporting this idea, the expression of ErbB4 by a subset of neutrophils points to NRG-1 expressed in the brain signaling through these cells (**Fig. 8E**). The continuous homogenous NRG-1 and MSR1 expression by neutrophils at all time points and across subtypes in the brain demonstrates the presence of alternative neutrophils during chronic Toxoplasma infection.

Two broad categories of neutrophils that differ in their functions have been identified previously. The first is a "classical" pro-inflammatory subset that is associated with classical macrophage activation, increased granularity, NETosis, and the production of Th1 cytokines IL-12 and TNFα (Nakayama et al. 2001, Beyrau et al. 2012). The second class is considered "alternative" based on anti-inflammatory cytokine expression like IL-10 and IL-4, association with alternative macrophage activation, decreased granularity, and angiogenesis and vascular repair (Tsuda et al. 2004, Beyrau et al. 2012). Expression of the neuroprotective molecules NRG-1, ErbB4, and MSR1 by chronic brain neutrophils paired with neutrophil persistence in the brain throughout chronic infection with little evidence for increased inflammation or pathology led us to hypothesize that these cells have an alternative phenotype in the brain compared to periphery. Our results demonstrated that $neut^{B}$ cells at 4wpi have a distinct phenotypic profile and express neuroprotective/alternative molecules differentially compared to splenic neutrophils (**Fig.**

9A-B). It is possible that the differences observed in the expression of the targeted proteins between brain and spleen neutrophils were due to brain-induced changes in one specific neutrophil subset (CD15+ or CD15-). Our results demonstrate that differential expression of the above molecules by brain neutrophils compared to spleen neutrophils was independent of the expression of CD15 (**Fig. 9C**). This indicates that neutrophils as a whole population differ in the brain compared to the spleen during chronic infection, and this phenotypic difference is not due to one specific neutrophil subset. Finally, CD15 and CXCR4 expression by neutrophils differed between brain and spleen at 4wpi, and the expression of both of these molecules in the brain changed over time (**Fig. 9D**). The gradual decrease in CD15 positivity by brain neutrophils from 4wpi-11wpi combined with the steady maintenance of CXCR4 expression confirms the loss of classical migratory integrin expression by neutrophils once they enter and remain in the brain. These neutrophils then develop an aged resident phenotype and express alternative and neuroprotective molecules in the brain that are not seen in the spleen.

Previous studies have demonstrated marked transcriptional changes in neutrophils driven not only by their age but also by their environment, focusing majorly on the differences between immature cells in the bone marrow and mature cells in terminally differentiated peripheral organs (Xie et al. 2020). Our scRNAseq results confirm this idea of environment-dependent neutrophil transcriptomes and provide a previously unexplored environmental influence on these innate immune cells: the infected brain (**Figure 10**). Our identified $neut^{B}$ cells differed transcriptionally compared to those found in spleen, and these cells were separated into two main subsets: Aged Resident and Non-Aged

Infiltrating cells (**Fig. 10A and B**). These subsets were differentially enriched for genes encoding for previously targeted neuroprotective molecules and displayed functional heterogeneity at the transcriptional level (**Fig. 10C-D**). While these cells displayed functional heterogeneity, GO analysis of each subset demonstrated a predominantly alternative phenotype of Aged Resident cells and a predominantly classical phenotype of Non-aged Infiltrating cells (**Fig. 10E-F**). It is possible that these identified neutrophil populations make up only a portion of the subsets found in the infected brain and that these populations were able to survive the intense processing prior to sequencing as shown by the presence of an "Unknown/Apoptotic" population identified in our analyses (**Fig. 10B and Supplemental Figure 9**). Future studies could more thoroughly investigate this population for additional subsets found in previous research (Tsuda et al. 2004) pending updated protocols to increase neutrophil survival. Additionally, future studies investigating the transcriptional changes in this distinct $neut^{B}$ population over the course of chronic infection could identify additional subsets not found at 4wpi.

Neutrophils and chemokine-dependent neutrophil recruitment are a vital source of protection against acute infection (Bliss et al. 2001, Del Rio et al. 2001), and additional work has demonstrated increased parasite burden following neutrophil depletion during the transition from acute to chronic infection (Biswas et al. 2017). We confirmed these results at the mid-chronic stage of infection, and we also demonstrated increased cyst burden following neutrophil depletion (**Figure 11**). This increased cyst burden suggests that there is latent parasite reactivation occurring in the brain (Dellacasa-Lindberg, Hitziger and Barragan 2007) and indicates a role for neutrophils in directly controlling

infection in the CNS. While chronic neutrophil depletion did not affect total numbers of other infiltrating immune cells (**Supplemental Figure 10**), it is known that neutrophils are pre-formed sources of IL-12 (Cassatella et al. 1995) and that lack of IL-12 leads to a decreased IFNγ response which is detrimental to control of infection (Bliss et al. 2001, Sukhumavasi et al. 2007). Given this information, it is possible that the increase seen in parasite burden and cyst burden in the brain could be indirectly caused by chronic neutrophil depletion due to the lack of IL-12 and subsequent IFNγ production by other immune cells. Future studies could test this via the investigation of intracellular cytokine levels in all BMNCs following neutrophil depletion.

Neutrophils have been previously shown to aid in angiogenesis and wound repair in the periphery. In this study, we have demonstrated vascular damage followed by vascular repair over the course of infection via EB staining and an increase in BBB permeability in the absence of chronic brain neutrophils (**Figure 12A-C**). This increase in BBB permeability could be the result of increased parasite burden seen after neutrophil depletion (**Figure 11**), leading to an increased necessity of immune cell infiltration and potentially damaging inflammatory response to control infection. The increased brain permeability following depletion paired with the expression of proangiogenic genes and proteins by our $neut^{B}$ cells (**Figure 9 and 10**) indicates that neutrophils play a role in CNS vasculature repair during Toxoplasma infection. We tested this by investigating the expression of TJP1 by blood vessels following neutrophil depletion as a marker of newly formed blood vessels and an indicator of vasculature repair (Liu et al. 2022, Strauss et al. 2021). We found no significant difference in the amount of TJP1+ vessels in the brain in

the absence of neutrophils (**Fig. 12E**). However, TJP1+ staining in depleted brains demonstrated restriction to the outer edges of the blood vessel endothelial cells when compared to more diffuse cytoplasmic staining in infected controls (**Fig. 12D**). This difference in TJP1 expression by blood vessels in the absence of neutrophils must be investigated further. TJP1-mediated formation of new blood vessels is not the only mechanism of vascular remodeling, and there are additional mechanisms that remain to be explored. These mechanisms include recent work demonstrating revascularization by neutrophils via MMP-9/VEGF-A signaling (Christoffersson et al. 2012, Gong and Koh 2010) neutrophil-dependent recruitment of proangiogenic T cells (Nadkarni et al. 2016), and neutrophil-produced myeloperoxidase activity that aids in CNS angiogenesis (Azcona et al. 2022).

Our results in this study demonstrate that neutrophils do not affectGAP43-mediated neuronal regeneration attempts during Toxoplasma infection, but instead play a role in upregulating SLPI expression on regenerating neuronal axons (**Figure 13**). This change in SLPI expression by neurons following depletion indicates a direct neuroprotective role of neutrophils in the brain during chronic infection. This role of neutrophils in neuronal regeneration via upregulation of SLPI occurs in a GAP43-indepednent manner. While GAP43 expression showed no significant changes, it is possible that there are other cell types compensating for any decrease in GAP43-dependent signaling induced by a lack of neutrophils. One of the cell types that could play an additional role in this pathway in the brain is astrocytes. Astrocytes have shown reduced reactivity following neutrophil depletion which leads to decreased healing after SCI (Stirling et al. 2009). It also known

that GAP43 expression can be restricted in the mature brain to neurons in areas associated with high plasticity such as the hippocampus and olfactory bulb where infection often does not often occur (De la Monte et al. 1989). There are also multiple other factors associated with neutrophil-dependent neuronal regeneration and protection that could be investigated including the pro-reparative growth factors NGF and IGF-1 and the role of N2 neutrophils specifically in protecting against neuronal injury (Sas et al. 2020, Hou et al. 2019).

In conclusion, this study identifies and characterizes a population of chronic brain neutrophils that aid in protection against Toxoplasma infection through functional heterogeneity. We present here a population of chronic neutrophils maintained in the brain that expresses neuroprotective molecules, possesses distinct phenotypic and transcriptomic profiles compared to peripheral cells, and displays functional heterogeneity. These traits portray a functionally diverse neutrophil group that protects against infection by balancing classical antimicrobial and alternative functions. In addition, depletion of these chronic neutrophils results in increased vascular damage and decreased neuronal regeneration in the brain indicating both indirectly and directly neuroprotective functions of these cells. This study demonstrates a previously unexplored neuroprotective role of neutrophils in models of chronic infection and introduces a potential new therapeutic target for treating chronic CNS disease.

Figures and Tables

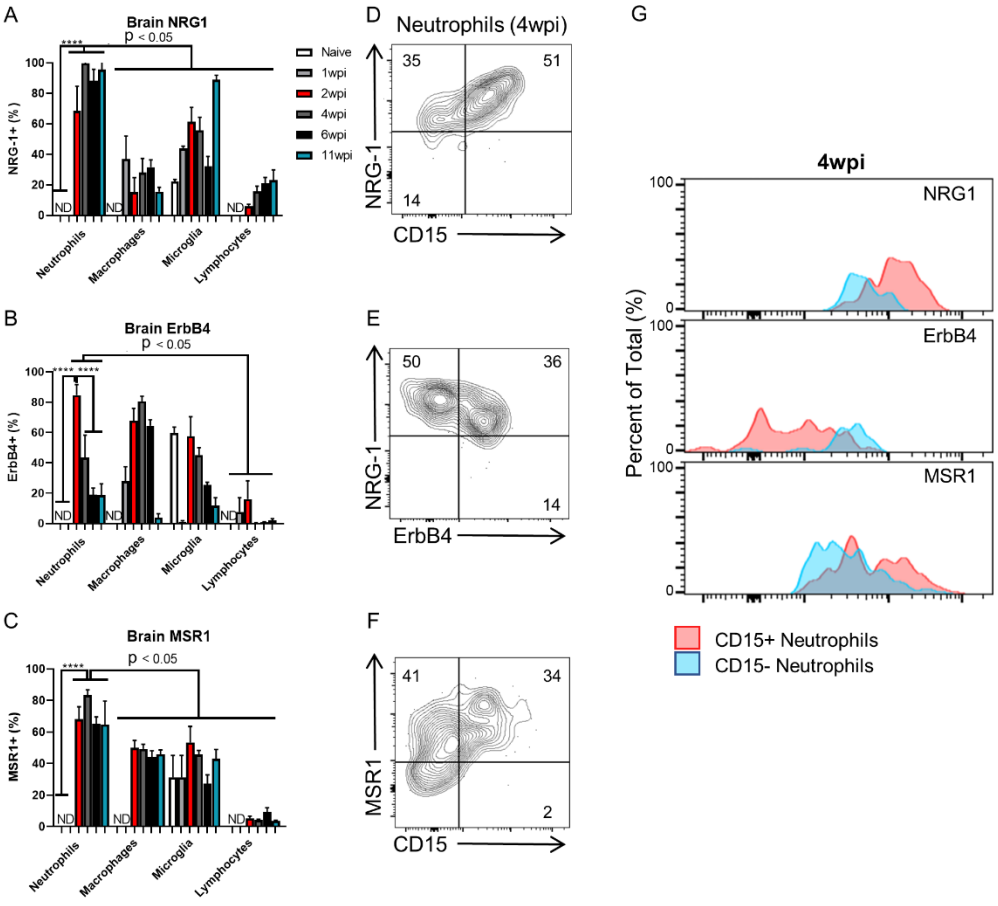

Figure 8. Infiltrating neutrophils in the CNS are sources of neuroprotective molecules during chronic infection. C57BL/6J mice were infected intraperitoneally with 10 *T. gondii* cysts (n=4 per time point) or injected with PBS as a control (n=3) and analyzed for immune cells in the brain and expression of neuroprotective molecules at both acute (1wpi) and chronic (2, 4, 6, and 11wpi) time points via flow cytometry. **A-C)** Time course quantification of expression frequencies (shown by percent of positive cells) of NRG1 **(A)**, ErbB4 **(B)**, and MSR1 **(C)** by brain mononuclear cells (BMNCs). **D-F)** Representative flow plots of NRG-1 **(D)**, ErbB4 **(E)**, and MSR1 **(F)** expression by neutrophils at 4wpi. Neutrophil subsets are identified based on expression of the integrin CD15 and ErbB4. Numbers on flow plots represent the average percentage of expression (n=4). **(G)** Expression overlap of neuroprotective molecules distinguished by CD15+ (pink) and CD15- (blue) neutrophils. For all graphs, ****=$P < 0.0001$ (remaining significance indicated as $p<0.05$); significance determined via One-way ANOVA, and error bars indicate SD. Experiments were repeated 2-3 times to confirm consistency of results.

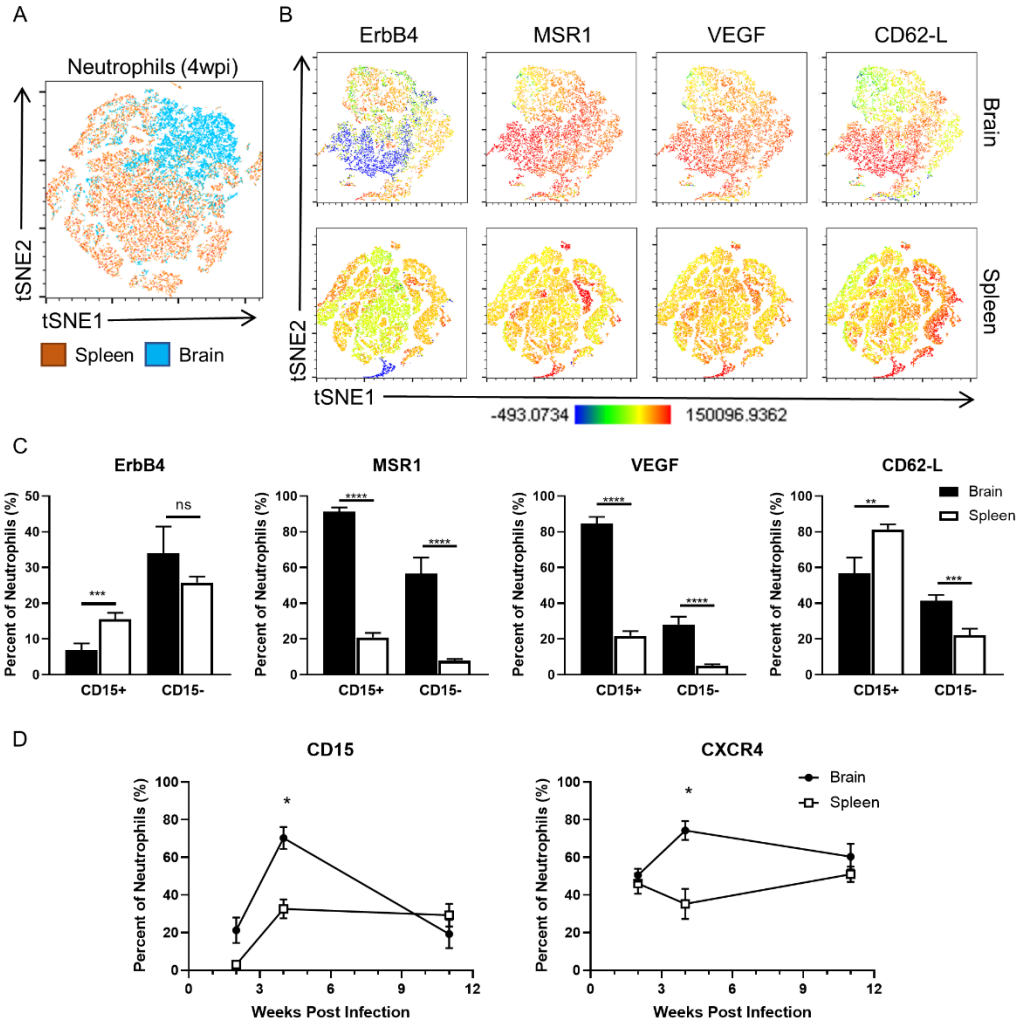
A
Neutrophils (4wpi)
tSNE2
tSNE1
Spleen
Brain
B
ErbB4
MSR1
VEGF
CD62-L
Brain
Spleen
tSNE2
tSNE1
-493.0734
150096.9362
C
ErbB4
MSR1
VEGF
CD62-L
Percent of Neutrophils (%)
CD15+
CD15-
ns
Brain
Spleen
D
CD15
CXCR4
Percent of Neutrophils (%)
Weeks Post Infection
Brain
Spleen

Figure 9. Protein analysis of chronic brain neutrophils reveals a distinct phenotypic profile. C57BL/6J mice were infected intraperitoneally with 10 *T. gondii* cysts (n=4 per time point), and neutrophil phenotypic profiles from brain and spleen were evaluated at different chronic (2, 4, and 11wpi) time points via flow cytometry. Neutrophils from brain and spleen were identified based on expression of CD11b and Ly6G (Supplemental Figure 1). **(A)** tSNE plot of concatenated brain and spleen neutrophils at 4wpi. **(B)** tSNE plots of selected alternative molecules from concatenated brain (top) and spleen (bottom) neutrophils at 4wpi. tSNE plot scale shows populations with low expression (blue) to high expression (red) of molecules. **(C)** Flow cytometry quantification of selected alternative molecules by neutrophils in brain and spleen based on CD15 expression at 4wpi. ** = $p< 0.01$, *** = $p< 0.001$, **** = $p<0.0001$. **(D)** Flow cytometry quantification of CD15 and CXCR4 expression by brain and spleen neutrophils at each time point during infection (2, 4, and 11wpi). * = $p<0.05$. For all graphs, significance determined via unpaired student t-test, and error bars indicate SD.

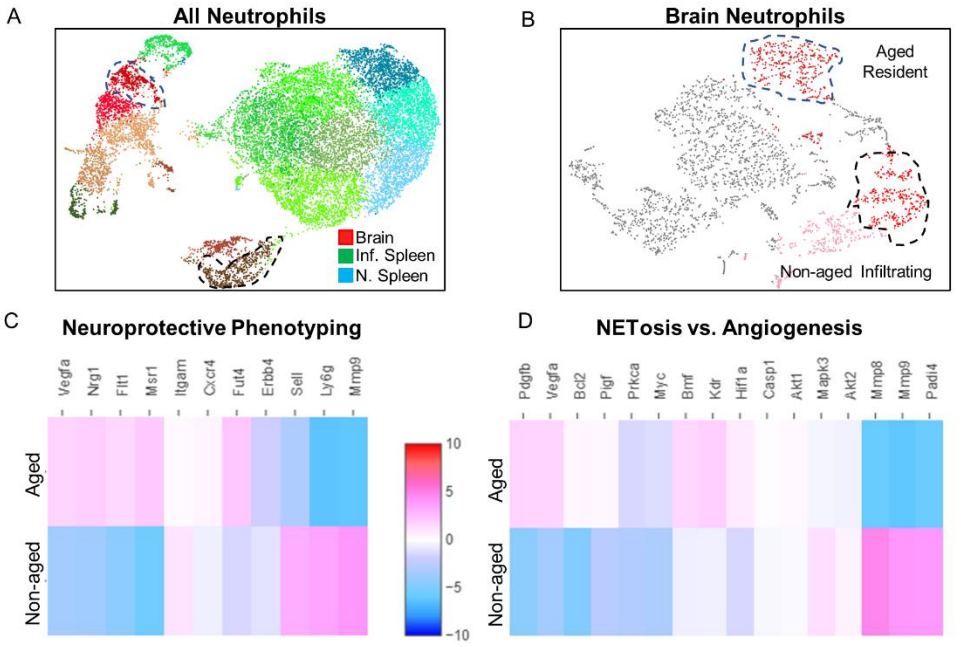

E

Aged Resident Neutrophils

GO Enrichment Term	Fold Enrichment	FDR
Immune complex clearance	>100	1.80E-02
Negative regulation of dendritic cell differentiation	>100	1.76E-02
Neural crest migration – ANS development	>100	3.99E-02
Blood coagulation, fibrin clot formation	>100	4.53E-02

F

Non-aged Infiltrating Neutrophils

GO Enrichment Term	Fold Enrichment	FDR
Neutrophil aggregation	>100	1.26E-02
Neutrophil extravasation	>100	6.05E-04
Neutrophil-mediated killing of gram-negative bacterium	>100	2.46E-02
Chemokine production	>100	2.42E-02

Figure 10. Aged resident and non-aged infiltrating subsets of neut^{B} cells display functional heterogeneity. Neutrophils from chronically infected mice were sorted from brain (n=7) and spleen (n=3) at 4wpi via flow cytometry and prepped for single cell RNA sequencing along with chronically infected BMNC (n=3) and naïve spleen (n=3) controls. Following sequencing, samples were aggregated via Loupe Browser software and also analyzed separately. **(A)** UMAP plot of aggregated sorted neutrophil samples from Brain, Infected Spleen (Inf. Spleen), and Naïve Spleen (N. Spleen). **(B)** UMAP plot of brain neutrophils (red = neutrophil population) identified as "Aged Resident" (blue outline, *Ly6G+*,*Fut4+*,*CXCR4+*) and "Non-aged Infiltrating" (black outline, *Ly6G*^{hi},*Fut4*^{int},*CXCR4-*) neutrophil subsets. Subsets are also identified in aggregated dataset. **C-D)** Heat maps of neuroprotective genes **(C)** and genes relating to classical (NETosis) vs alternative (angiogenesis) **(D)** functions. **E-F)** GO enrichment terms from top 50 most significantly upregulated genes in "Aged" **(E)** and "Non-aged" **(F)** neutrophils.

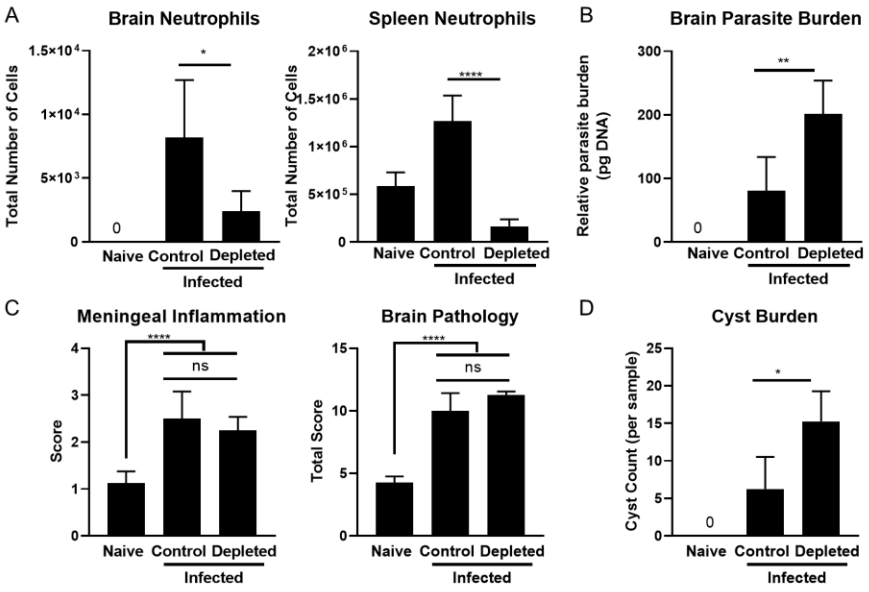
A
Brain Neutrophils
Total Number of Cells
1.5×10^4
1×10^4
5×10^3
0
*
0
Naive Control Depleted
Infected
Spleen Neutrophils
Total Number of Cells
2×10^6
1.5×10^6
1×10^6
5×10^5
0
****
Naive Control Depleted
Infected
B
Brain Parasite Burden
Relative parasite burden (pg DNA)
300
200
100
0
**
0
Naive Control Depleted
Infected
C
Meningeal Inflammation
Score
4
3
2
1
0
****
ns
Naive Control Depleted
Infected
Brain Pathology
Total Score
15
10
5
0
****
ns
Naive Control Depleted
Infected
D
Cyst Burden
Cyst Count (per sample)
25
20
15
10
5
0
*
0
Naive Control Depleted
Infected

Figure 11. Depletion of neutrophils during chronic infection leads to increased parasite and cyst burden. C57BL/6J mice were infected intraperitoneally with 10 *T. gondii* cysts or injected with PBS as a control (n=5 per group), and a cohort of infected mice received neutralizing Ly6G mAb treatment at 4wpi for 2 weeks to deplete neutrophils. **(A)** Total quantified numbers of neutrophils in brain (left) and spleen (right) following Ly6G mAb treatment as determined via flow cytometry. **(B)** Quantified parasite burden from whole brain DNA via RT-PCR using *T. gondii* B1 gene (n=5/time point). **(C)** Histopathological analysis of brains using pre-defined scoring system (see Methods). **(D)** Cyst burden quantified via direct counting from H&E-stained slides. *= $p< 0.05$, **= $p< 0.01$, ****= $p< 0.0001$; significance determined via unpaired student t-test, and error bars indicate SD.

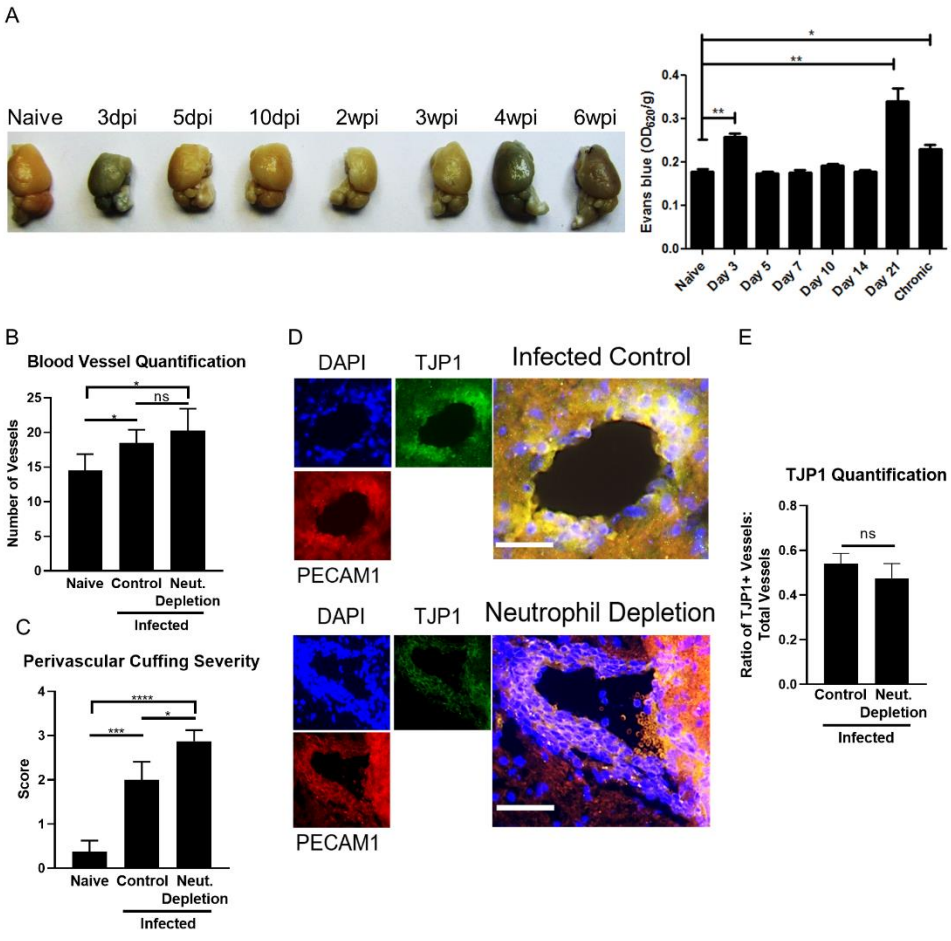
A
Naive
3dpi
5dpi
10dpi
2wpi
3wpi
4wpi
6wpi
Evans blue (OD620/g)
Naive
Day 3
Day 5
Day 7
Day 10
Day 14
Day 21
Chronic
B
Blood Vessel Quantification
Number of Vessels
Naive
Control
Neut. Depletion
Infected
C
Perivascular Cuffing Severity
Score
D
DAPI
TJP1
Infected Control
PECAM1
Neutrophil Depletion
E
TJP1 Quantification
Ratio of TJP1+ Vessels: Total Vessels
ns

Figure 12. Lack of chronic brain neutrophils leads to increased vascular pathology. C57BL/6J mice were infected intraperitoneally with 10 *T. gondii* cysts or injected with PBS as a control (n=5 per group), and a cohort of infected mice received neutralizing Ly6G mAb treatment at 4wpi for 2 weeks to deplete neutrophils. **(A)** Evans Blue staining images (left) and quantification (right) of naïve and infected mouse brain at varying stages of infection. **B-C)** Blinded histological analysis of brains quantifying total blood vessels counted from a minimum of 5 randomized fields of view (FOV) **(B)** and perivascular cuffing severity **(C)** using pre-defined scoring system (see Methods). **D-E)** Immunofluorescence images **(D)** and quantification **(E)** of infected control and neutrophil depleted brains, 40x images. Blue = DAPI, Green = TJP1, Red = PECAM1, Scale bar = 25μm. *=P < 0.05, **=P < 0.01, ****=P < 0.0001; significance determined via 1-way ANOVA and unpaired student t-test, and error bars indicate SD.

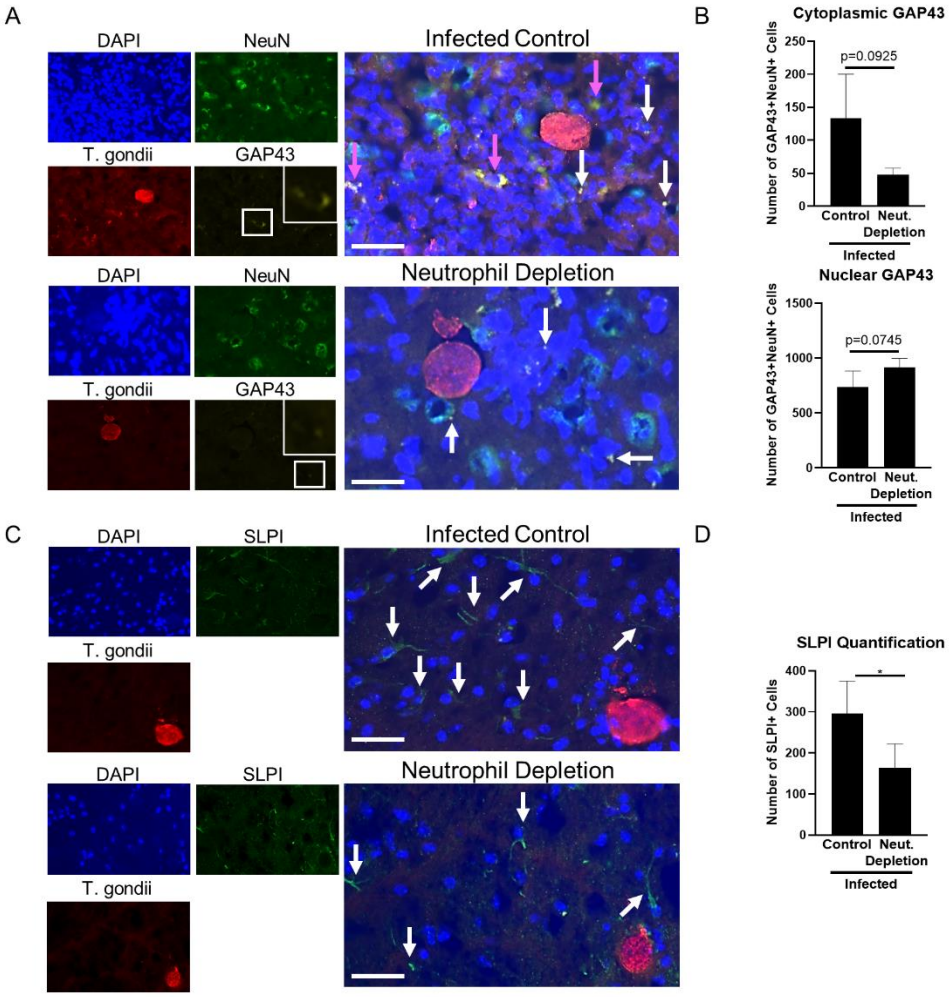
A
DAPI
NeuN
Infected Control
T. gondii
GAP43
DAPI
NeuN
Neutrophil Depletion
T. gondii
GAP43
B
Cytoplasmic GAP43
Number of GAP43+NeuN+ Cells
p=0.0925
Control
Neut. Depletion
Infected
Nuclear GAP43
Number of GAP43+NeuN+ Cells
p=0.0745
Control
Neut. Depletion
Infected
C
DAPI
SLPI
Infected Control
T. gondii
DAPI
SLPI
Neutrophil Depletion
T. gondii
D
SLPI Quantification
Number of SLPI+ Cells
*
Control
Neut. Depletion
Infected

Figure 13. Neuronal regeneration attempts during chronic infection are inhibited in the absence of neutrophils. C57BL/6J mice were infected intraperitoneally with 10 *T. gondii* cysts or injected with PBS as a control (n=5 per group), and a cohort of infected mice received neutralizing Ly6G mAb treatment at 4wpi for 2 weeks to deplete neutrophils. **A-B)** Immunofluorescence images **(A)** and blinded quantification **(B)** of infected control and neutrophil depleted brains. 40x images, Scale bar = 25µm. White arrows indicate positive nuclear GAP43 staining, pink arrows indicate positive cytoplasmic GAP43 staining. **C-D)** Immunofluorescence images **(C)** and blinded quantification **(D)** of infected control and neutrophil depleted brains, 40x images. Scale bar = 25µm. White arrows indicate SLPI+ cells. *=P < 0.05, **=P < 0.01, ****=P < 0.0001; significance determined via 1-way ANOVA and unpaired student t-test, and error bars indicate SD.

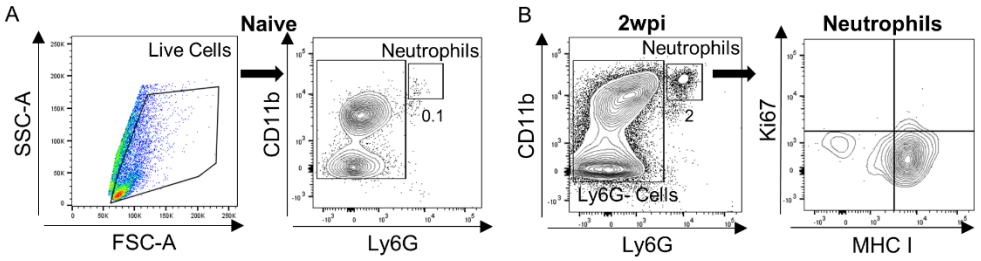
A
Naive
Live Cells
SSC-A
FSC-A
Neutrophils
0.1
CD11b
Ly6G
B
2wpi
Neutrophils
2
CD11b
Ly6G
Ly6G- Cells
Neutrophils
Ki67
MHC I

Supplemental Figure 2. Neutrophil identification and gating strategy. (A) Representative gating strategy and gating of CD11b+Ly6G+ cells from the brain of naïve controls. Neutrophils were defined as CD11b+Ly6G+ after gating on live cells. Numerical values represent average percentages. **(B)** Representative gating of CD11b+Ly6G+ cells from the brain of *T. gondii*-infected mice at the early chronic stage of infection (2wpi). Non-proliferating neutrophils were then defined as Ki67-MHC I+. This gating strategy was also used for identification of neutrophils from peripheral spleen and blood.

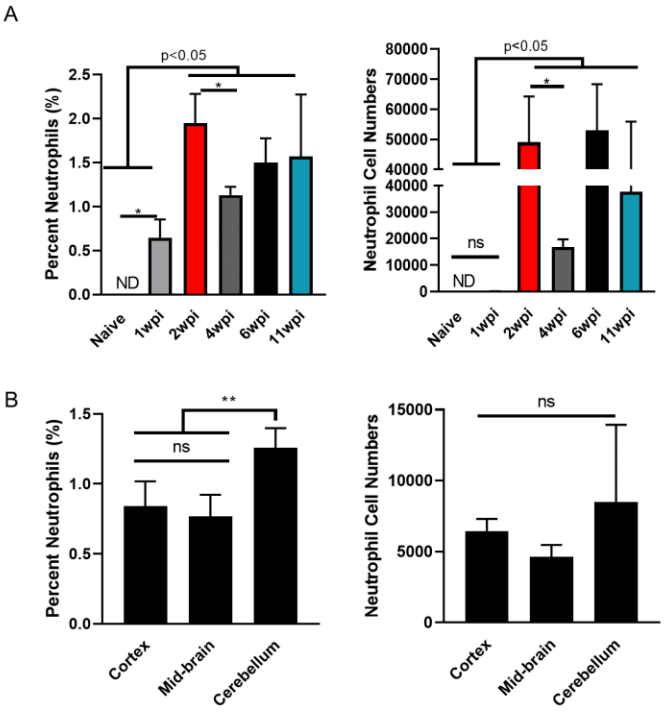
A
p<0.05
*
*
ND
Percent Neutrophils (%)
2.5
2.0
1.5
1.0
0.5
0.0
Naive
1wpi
2wpi
4wpi
6wpi
11wpi
p<0.05
*
ns
ND
Neutrophil Cell Numbers
80000
70000
60000
50000
40000
40000
30000
20000
10000
0
B
**
ns
Percent Neutrophils (%)
1.5
1.0
0.5
0.0
Cortex
Mid-brain
Cerebellum
ns
Neutrophil Cell Numbers
15000
10000
5000
0

Supplemental Figure 3. Protective neutrophils that persist throughout chronic infection are broadly disbursed in the brain. C57BL/6J mice were infected intraperitoneally with 10 *T. gondii* cysts (n=4 per time point) or injected with PBS as a control (n=3) and analyzed for immune cells in the brain at both acute (1wpi) and chronic (2, 4, 6, and 11wpi) time points via flow cytometry. For location studies, mice (n=5) were sacrificed at 4wpi, brains were dissected into 3 distinct regions, and BMNCs were analyzed via flow cytometry to determine neutrophil location in the brain. **(A)** frequencies (left) and numbers (right) of CD11b+Ly6G+ neutrophils in brain at each time point. **(B)** Quantification of neutrophil percentages (left) and numbers (right) in each defined brain region. ** = $P < 0.01$, * = $P < 0.05$, "p-val<0.05" indicates varying degrees of significance between indicated time points; significance determined via 1-way ANOVA, and error bars indicate SD.

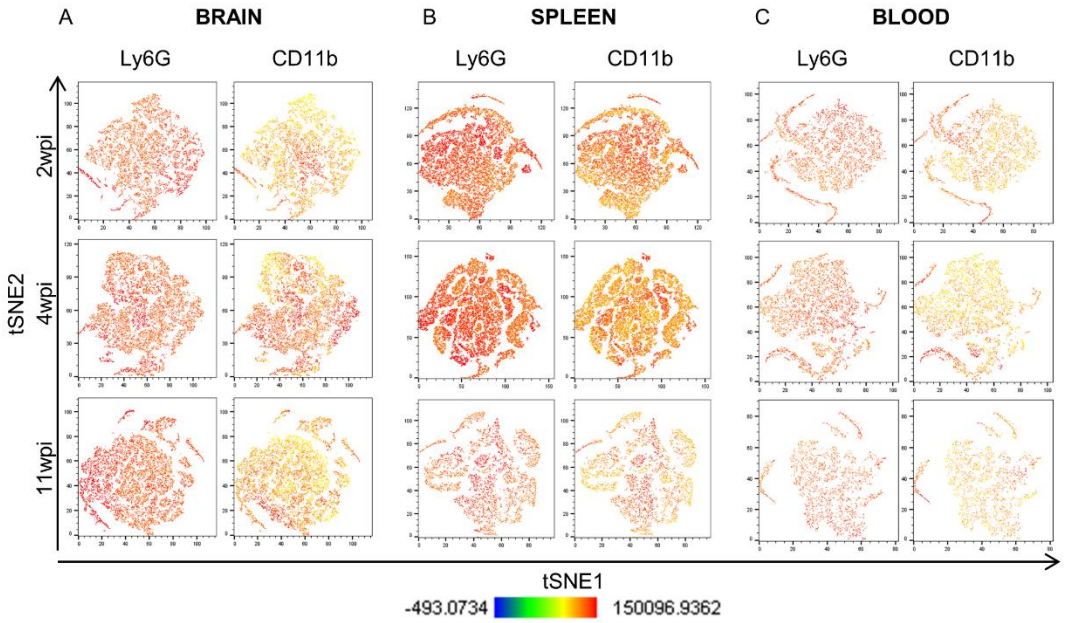
A
BRAIN
B
SPLEEN
C
BLOOD
Ly6G
CD11b
Ly6G
CD11b
Ly6G
CD11b
2wpi
4wpi
11wpi
tSNE2
tSNE1
-493.0734
150096.9362

Supplemental Figure 4. Confirmation of neutrophil phenotype for tSNE analysis. C57BL/6J mice were infected intraperitoneally with 10 *T. gondii* cysts (n=4 per time point) or injected with PBS as a control (n=3), and neutrophil phenotype was confirmed via expression of Ly6G and CD11b in brain, spleen, and blood at different chronic (2, 4, and 11wpi) time points via flow cytometry. Representative tSNE plots of concatenated brain **(A)**, spleen **(B)**, and blood **(C)** neutrophils are shown. tSNE plots scale shows populations with low expression (blue) to high expression (red) of molecules.

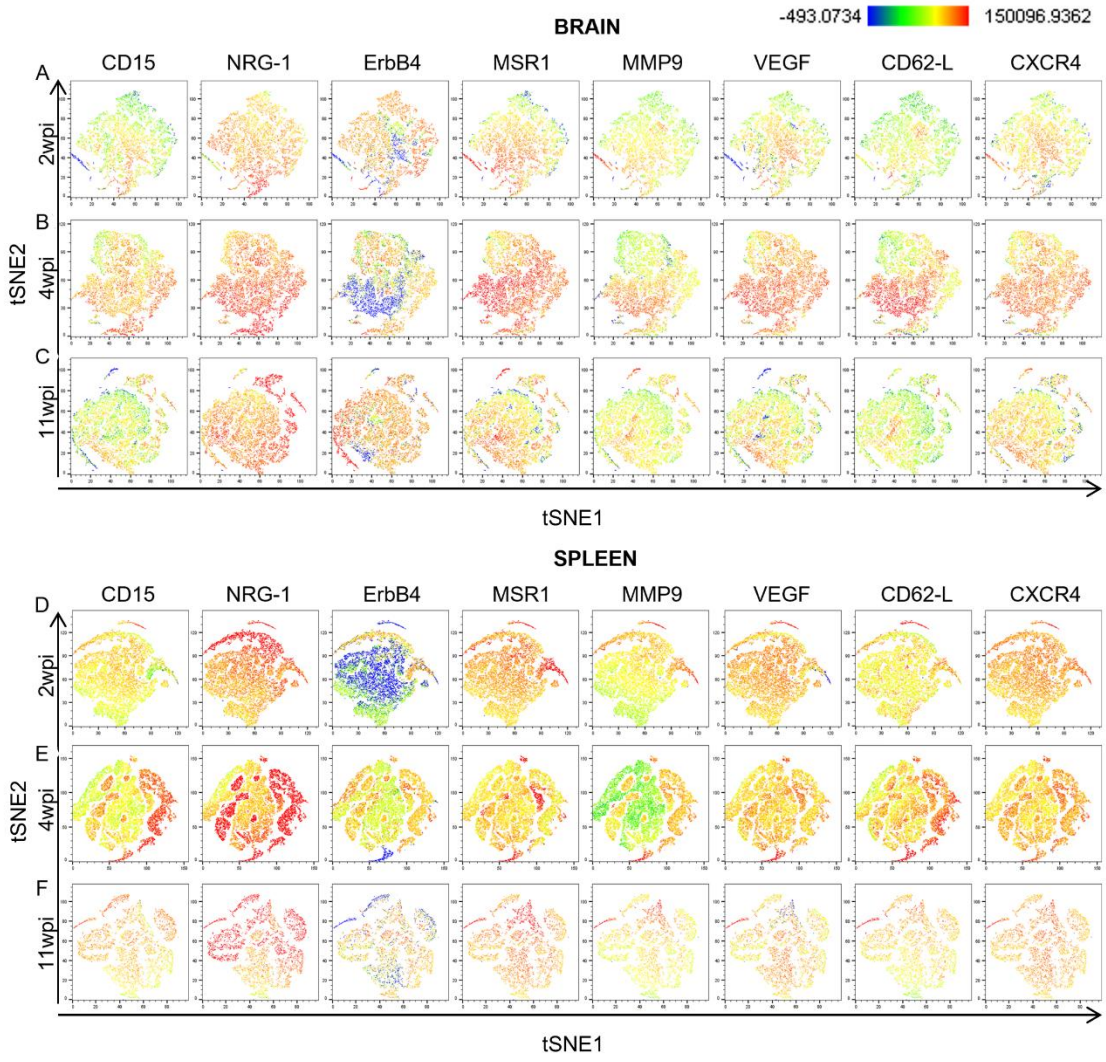
BRAIN
-493.0734
150096.9362
CD15
NRG-1
ErbB4
MSR1
MMP9
VEGF
CD62-L
CXCR4
A
B
C
2wpi
4wpi
11wpi
tSNE2
tSNE1
SPLEEN
D
E
F
2wpi
4wpi
11wpi
tSNE2
tSNE1

Supplemental Figure 5. Chronic brain neutrophils demonstrate a distinct phenotypic profile and express a range of alternative proteins. C57BL/6J mice were infected intraperitoneally with 10 *T. gondii* cysts (n=4 per time point) or injected with PBS as a control (n=3), and neutrophil phenotypic profiles from brain, spleen, and blood were evaluated at different chronic (2, 4, and 11wpi) time points via flow cytometry. Neutrophils from brain, spleen, and blood were identified based on expression of CD11b and Ly6G (Supplemental Figure 1). tSNE plots of concatenated brain **(A-C)**, spleen **(D-F)**, and blood **(G-I)** neutrophils are shown. tSNE plots scale shows populations with low expression (blue) to high expression (red) of molecules.

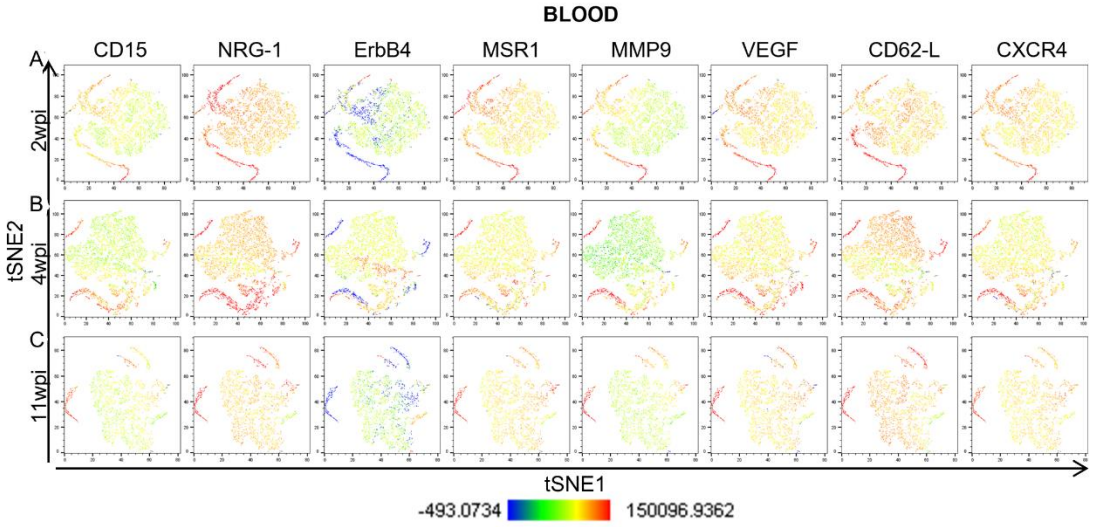
BLOOD
CD15
NRG-1
ErbB4
MSR1
MMP9
VEGF
CD62-L
CXCR4
A
2wpi
B
4wpi
C
11wpi
tSNE2
tSNE1
-493.0734
150096.9362

Supplemental Figure 6. Blood neutrophil phenotype. C57BL/6J mice were infected intraperitoneally with 10 *T. gondii* cysts (n=4 per time point) or injected with PBS as a control (n=3), and neutrophil phenotypic profiles from blood were evaluated at different chronic (2, 4, and 11wpi) time points via flow cytometry. Neutrophils from blood were identified based on expression of CD11b and Ly6G. tSNE plots of concatenated blood samples at 2 **(A)**, 4 **(B)**, and 11wpi **(C)** neutrophils are shown. tSNE plots scale shows populations with low expression (blue) to high expression (red) of molecules.

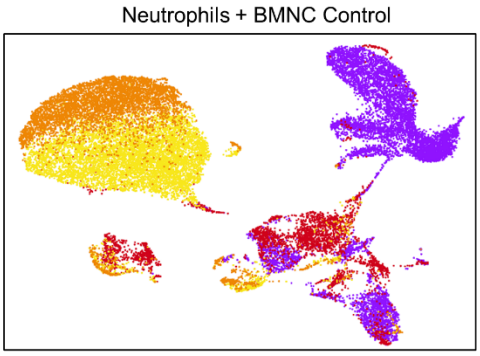
Neutrophils + BMNC Control

Supplemental Figure 7. ScRNAseq of peripheral and brain neutrophils during chronic infection demonstrates distinct clustering of chronic brain neutrophils. Neutrophils from chronically infected mice were sorted from brain (n=7) and spleen (n=3) at 4wpi via flow cytometry and prepped for single cell RNA sequencing along with chronically infected BMNC (n=3) and naïve spleen (n=3) controls. Following sequencing, samples were analyzed separately and aggregated via Loupe Browser software. UMAP plot of all aggregated samples (BMNCs (purple), Brain Neutrophils (red), Infected Spleen Neutrophils (yellow), and Naïve Spleen Neutrophils (orange)).

A

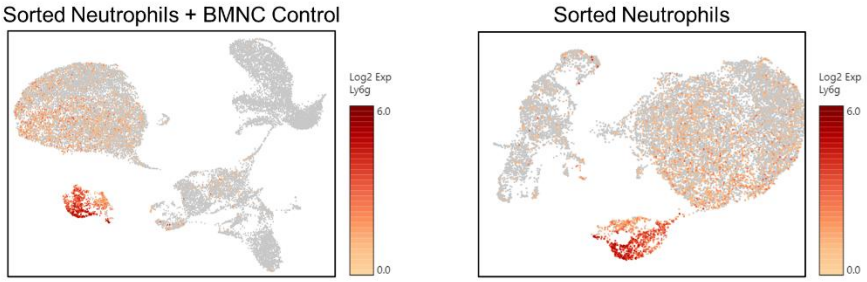
Sorted Neutrophils + BMNC Control
Log2 Exp
Ly6g
6.0
0.0
Sorted Neutrophils
Log2 Exp
Ly6g
6.0
0.0

B

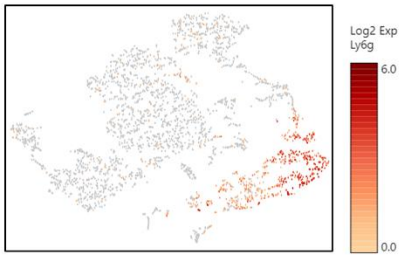
Log2 Exp
Ly6g
6.0
0.0

Supplemental Figure 8. Identification of neutrophil populations from scRNAseq data after sorting BMNCs based on Ly6G+CD11b+ expression. (A) Ly6G log_2 gene expression of respective aggregated UMAPs from scRNAseq to confirm positive neutrophil phenotype. **(B)** UMAP of Ly6G log_2 gene expression of sorted brain neutrophils only.

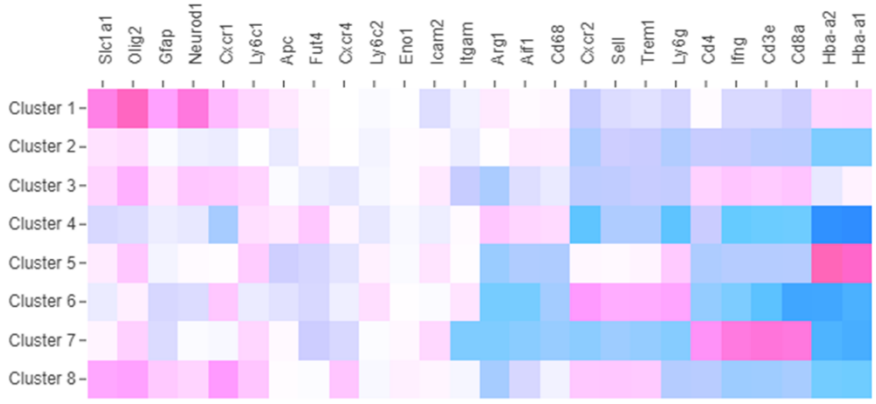
Slc1a1
Olig2
Gfap
Neurod1
Cxcr1
Ly6c1
Apc
Fut4
Cxcr4
Ly6c2
Eno1
Icam2
Itgam
Arg1
Aif1
Cd68
Cxcr2
Sell
Trem1
Ly6g
Cd4
Ifng
Cd3e
Cd8a
Hba-a2
Hba-a1
Cluster 1
Cluster 2
Cluster 3
Cluster 4
Cluster 5
Cluster 6
Cluster 7
Cluster 8

Supplemental Figure 9. Identification of cell types from sorted "Brain Neutrophil" sample. Heat map of canonical markers of various cell types found in the brain during chronic Toxoplasma infection identified via scRNAseq analysis.

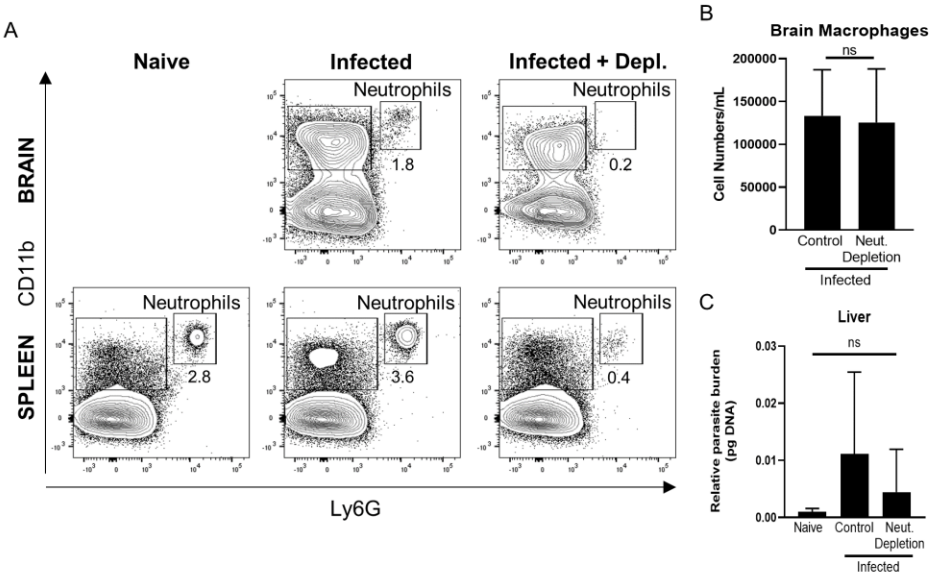
A
Naive
Infected
Infected + Depl.
BRAIN
SPLEEN
CD11b
Ly6G
Neutrophils
1.8
0.2
2.8
3.6
0.4
B
Brain Macrophages
ns
Cell Numbers/mL
200000
150000
100000
50000
0
Control
Neut. Depletion
Infected
C
Liver
ns
Relative parasite burden (pg DNA)
0.03
0.02
0.01
0.00
Naive
Control
Neut. Depletion
Infected

Supplemental Figure 10. Successful and specific depletion of neutrophils after treatment with neutralizing Ly6G antibody. (A) Representative gating of CD11b+Ly6G+ neutrophils from the brain and spleen of naïve controls, infected controls, and infected neutrophil-depleted mice. Neutrophils were defined as CD11b+Ly6G+ after gating on live cells. Numerical values represent average percentages. **(B)** Number of macrophages in brain following Ly6G depletion treatment demonstrates neutrophil-specific depletion.

Supplemental Table 3. Flow cytometry antibody panels.

Name of Panel	Primary Antibody	Secondary Antibody (if applicable)
NRG-1 and ErbB4 Kinetics (BD FACS Canto II)	ErbB4 OR CD3 FITC	N/A
	CD45 PE	N/A
	Ly6G (Clone 1A8) PerCPCy5.5	N/A
	RbαM NRG-1 (SMDF)	DkαRb Alexafluor 647
	CD15 OR Ki67 Biotin OR CD8 PECy7	Streptavidin PECy7 OR N/A
	CD11b OR CD4 APCCy7	N/A
MSR1 Kinetics (BD FACS Canto II)	RbαM MSR1 OR CD3 FITC	DkαRb Alexafluor 488
	CD45 PE	N/A
	Ly6G (Clone 1A8) PerCPCy5.5	N/A
	CD11b APC OR RbαM MSR1	N/A OR DkαRb Alexafluor 647
	CD15 Biotin	Streptavidin PECy7
	CD62-L OR CD4 APCCy7	N/A
Neutrophil Depletion (BD FACS Canto II)	CD3 FITC	N/A
	CD45 PE	N/A
	Ly6G PerCPCy5.5	N/A
	CD4 APC	N/A
	CD8 PECy7	N/A
	CD11b APCCy7	N/A
Alternative Protein Phenotyping (Novocyte)	ErbB4 FITC	N/A
	MαM NRG1 (SMDF)	DkαRb Alexafluor 568
	CD11b PerCPCy5.5	N/A
	MMP9 Alexafluor 647	N/A
	CD15 Biotin	Streptavidin PECy7
	CD62-L APCCy7	N/A
	Ly6G (Clone 1A8) BV510	N/A
	RbαM MSR1	DkαRb Qdot655
	GtαM VEGF	DkαGt Alexafluor 680
	CXCR4 PECy5.5	N/A

Supplemental Table 4. Immunofluorescence antibody panels.

Name of Panel	Primary Antibody	Secondary Antibody (if applicable)
Brain Vasculature Panel	RBαM TJP1	GtαRb Alexafluor 488
	PECAM1 PE	N/A
Brain GAP43 Panel	RbαM NeuN	DkαRb Alexafluor 488
	GtαToxoplasma	DkαGt Alexafluor 568
	ChkαM GAP43	DkαChk Alexafluor 647
Brain SLPI Panel	RbαM SLPI	DkαRb Alexafluor 488
	GtαToxoplasma	DkαGt Alexafluor 568

Chapter 4: Human neutrophil-like cells demonstrate antimicrobial responses to the chronic cyst form of *Toxoplasma gondii*

Abstract

Infection with the protozoan parasite *Toxoplasma gondii* results in a lifelong infection that is estimated to infect approximately 2.5 billion people worldwide. Infection with this parasite is characterized by the formation of chronic cysts inside neurons of the brain of its host. There are two main stages of infection: 1) an acute stage characterized by rapidly disseminating parasites throughout the body and 2) a chronic stage identified by the entry of parasites into the brain and formation of chronic cysts. Both stages require a dynamic immune response comprised of both innate and adaptive immune cells. Neutrophils are one of the primary responders to acute *T. gondii* infection, and they are vital for control of this stage of infection in both murine and human models.

While extensive research has been done to investigate the role of both murine and human neutrophils in response to the acute-stage parasite, little is known about the role of these cells in controlling the chronic cyst form of *T. gondii*. Using an immortal human neutrophil-like cell (HNLC) line, this study demonstrates the presence of two cell subsets following exposure to Toxoplasma cysts via immunofluorescence studies. Functional studies of these cells indicate cyst-specific immune responses such as cytokine signaling. Additional analysis of HNLC exposure to cysts via time lapse imaging and flow cytometry reveals uptake of cyst material by cells over time. Collectively, this study identifies a novel response of HNLCs to the chronic cyst stage of *T. gondii*, and this

suggests a previously unknown role of human neutrophils in the control of chronic Toxoplasma infection.

Introduction

Infection with *Toxoplasma gondii* is estimated to affect approximately 1 in 3 people around the world (Dunay et al. 2018), and infection in the immunocompromised can have devastating results due to an impaired immune response (Ngô et al. 2017). Under normal conditions, *T. gondii* stimulates a robust immune response upon entry into the host, and the stage of infection heavily dictates which immune responses are employed. Response to the acute stage is characterized by early recruitment of innate immune cells like neutrophils to sites of peripheral infection and early production of pro-inflammatory cytokines like IL-12 and chemokines like CCL2 (Sukhumavasi et al. 2007, Bliss et al. 1999). Without these cells, acute infection is unable to be controlled and often leads to fatal pathology (Bliss et al. 2001). In addition to early production of vital cytokines and chemokines that recruit other cell types to control infection, neutrophils are also able to directly kill the parasite through mechanisms like direct phagocytosis (Konishi and Nakao 1992), reactive oxygen species (ROS) production (Alves et al. 2013), and the process of NETosis where neutrophils produce neutrophil extracellular traps (NETs) to ensnare and kill free-floating pathogens (Brinkmann et al. 2004, Abi Abdallah et al. 2012). Based on these previous works, neutrophils have been deemed an essential part of the innate immune response to acute *T. gondii* infection.

While neutrophils are a well-known first line of defense against the acute stage of Toxoplasma infection, recent work by Dunay and colleagues has discovered a small but defined population of neutrophils in the brain during chronic infection (Biswas et al. 2017). During this chronic stage, the parasite enters the brain of its host, where it transitions from rapid dissemination to a slow replicating form and forms lifelong cysts inside neurons (Cabral et al. 2016). While these dormant cysts are much less recognized by infiltrating immune cells, murine studies have investigated infection control mechanisms employed by immune cells in the CNS as reviewed by Blanchard et. al (Blanchard, Dunay and Schlüter 2015).

Extensive work has been done in murine models of Toxoplasmosis, but much less is known about the immune responses of human immune cells, specifically neutrophils, during chronic Toxoplasma infection. Due to the broad range of acute symptoms and the asymptomatic nature of chronic infection, many *in vivo* human studies are restricted to those of antibody detection to determine infection stage (Anuradha and Preethi 2014, Villard et al. 2016) and post-mortem studies where *T. gondii* has been detected (Hofman et al. 1993, Diaconu et al. 2016). Previous work has been conducted investigating the human immune response to infection as reviewed by Fisch et. al (Fisch et al. 2019), but research investigating specific immune cell functions in human infection must often be conducted *in vitro*.

Previous work investigating the neutrophil-specific response to *T. gondii* demonstrates parasite-dependent release of ROS (Ashander et al. 2019, Kikuchi-Ueda, Ubagai and Ono 2013), and destruction of acute tachyzoites by both murine and human neutrophils via

NETosis (Abi Abdallah et al. 2012). Furthermore, more recent work utilizing primary human neutrophils has shown that Toxoplasma infection leads to NET-dependent amplification of innate and adaptive immune responses which can be seen upon re-exposure to tachyzoites in co-culture (Miranda et al. 2021). While this work shows neutrophil response to the acute stage of *T. gondii*, the discovered presence of neutrophils in the brain during chronic Toxoplasma infection suggests a previously undescribed role of these cells. However, whether these cells are capable of responding to the chronic cyst form of the parasite remains unknown.

In this study, we demonstrate uptake of cyst material by an immortal human neutrophil-like cell (HNLC) line following exposure. Additional studies identify cyst-specific responses of HNLCs including cytokine production. Overall, we have discovered a novel response of human neutrophils to the chronic cyst stage of *T. gondii* demonstrating a previously unknown role of human neutrophils in the control of chronic Toxoplasma infection.

Materials and Methods

Human Neutrophil Cell (HNLC) Culturing

HL-60 cells were graciously provided by the Mercer lab at California State Polytechnic University, Pomona and cultured according to their protocol. Briefly, cells were cultured in defined HL-60 media (10% FBS, 1% Pen-Strep, 1% Glutamax, and incomplete RPMI to volume) at 37°C with 5% CO_2. Cells were split regularly and kept at between 0.2-1.5 million/ml during culturing. To differentiate cells into neutrophil-like cells, HL-60 cells

were spun down at 100xg for 10min at room temperature, counted using an automated cell counter, and plated at a concentration of 0.2 million/ml in neutrophil differentiation media (HL-60 media from above with 1.3% DMSO and 100ng/ml of G-CSF). Cells were left alone for 6-7 days, and successful differentiation was confirmed via neutrophil morphology.

Stimulation Experiments

In vitro HNLCs. For *in vitro* stimulations of HNLCs, Toxoplasma tachyzoites of the Me49 (B7) strain were maintained in culture and purified from HFFs. In addition, Me49 cysts were maintained in mice and purified from a chronically infected CBA mouse strain. Tachyzoite maintenance, cyst maintenance, tachyzoite purification, and cyst purification techniques were completed according to previously published protocols (Goerner et al. 2020, Bergersen et al. 2021). Parasite antigen from both Me49 tachyzoites and cysts was harvested according to previously published protocols (Nance et al. 2012). For infections, HNLCs plated at 0.2 million cells/ml in 200µl of neutrophil differentiation media were infected with Me49 tachyzoites at an MOI of 5 (n=4), Me49 cysts at a concentration of 100 cysts/well (n=4) or stimulated with tachyzoite or cyst antigen at a concentration of 25µg/mL (n=4 per condition). Uninfected/unstimulated cells (n=4) and cells stimulated with LPS (125 ng/mL for cytokine studies) or PMA (100µg/ml for NET studies) (n=4) were used as controls. Upon infection/stimulation, cells were incubated for 6 hours (for cytokine production) or 4 hours (for NET production and imaging studies) at 37°C with 5% CO_2. Cells were spun down at 100xg for 10min at room temperature,

supernatant was collected for cytokine analysis or NET production analysis, and coverslips were prepared for immunofluorescence.

Brain mononuclear cells. Brain mononuclear cells (BMNCs) from 4 week-infected mice were harvested according to previously published protocols (David et al. 2016). For re-stimulation of BMNCs for NET production studies, processed BMNCs were plated at a concentration of 0.2 million cells/mL in 200µl of complete RPMI media. These cells were infected with Me49 tachyzoites or cysts or stimulated with tachyzoite or cyst antigen exactly as explained in the *in vitro* experiments. Unstimulated BMNCs and BMNCs stimulated with PMA (100µg/ml) were used as controls (n = 4/group). As an additional control, brain homogenate from a naïve mouse was purified using the same protocol for cyst purification and was added to cells (n =4).

Immunofluorescence Studies

After collection of supernatants, coverslips were washed once with 1x PBS to remove any residual media. Coverslips were fixed in 4% PFA for 15min, washed once with 1x PBS for 5 min, permeabilized in 0.5% Triton X 100 for 15min, and blocked in 5% Donkey Serum for 30min. Coverslips were incubated in primary antibodies to CD11b (ThermoFisher), CD15 (ThermoFisher), and *T. gondii* (Abcam) for 1 hour at room temperature in 1% Donkey Serum/0.5% Tween20/1x PBS. Coverslips were washed and incubated in Alexafluor secondary fluorescent antibodies (488, 568, and 647, ThermoFisher) for 1 hour at room temperature in 1% Donkey Serum/0.5% Tween20/1x PBS. Slips were washed again and mounted on microscope slides using Vectashield with

DAPI. Cells were imaged on a Leica inverted DMI6000 B microscope using 40x magnification with Leica LASX software. For quantification of CD15+ cells, total numbers of CD15+ cells (minimum of 50) were counted from a minimum of 7 regions of interest (ROIs) from each exposure condition.

HNLC Time Lapse Experiments

HNLCs were cultured and differentiated as above. Me49 cysts were purified as above and stained with CMFDA Green Cell Tracker dye for 30 minutes protected from light at room temperature. 20µm diameter YG-fluorescent beads were coated in cyst antigen (25µg/mL) and used as a control. A total of 100 cysts or beads were plated in a glass-bottom 24-well plate in neutrophil differentiation media, and plate was placed in the appropriate holder of a Keyence BZ-X710 microscope with Tokai-Hit Climate Control attachment (37ºC, 5% CO_2) to maximize cell survival and biological response. Designated areas of cysts or beads were identified for imaging based on positive fluorescent staining, and HNLCs were added to one well at a time at a concentration of 2.0 x 10^5 cells/mL. Cells were allowed to settle for 5 minutes, and wells were imaged one at a time for 4hrs, with images being taken every 60seconds. Cysts and beads were visualized using the fluorescent GFP channel, and cells were visualized using Bright Field imaging. Live imaging was performed at 40x magnification for all wells.

Kinetics Flow Cytometry Experiments

Me49 cysts were purified and stained using CMFDA Green Cell Tracker dye (ThermoFisher) as stated above. Differentiated HNLCs were transferred from culture

plate to 5ml polysterene round-bottom FACS tubes at a concentration of 1.0 x 10^4 cells/tube in 300µl neutrophil differentiation media and stained using Deep Red Cell Tracker dye (ThermoFisher) for 30 minutes protected from light at 37ºC. Cysts were added to each tube, and tubes were incubated at 37°C with 5% CO_2 protected from light for the following time durations (n = 3 per time point): 1min, 5min, 10min, 30min, 60min. After completion of incubation, tubes were removed, vortexed briefly, and samples were acquired using a BD FACS Canto II flow cytometer. Stained cysts were acquired in the FITC channel, and stained cells were acquired in the APC channel. Cysts alone and cells alone were used as controls. Analysis was conducted using FlowJo software.

LEGENDplex Cytokine Assay

LEGENDplex cytokine assay for mouse inflammation panel of 13 Th1-associated cytokines (BioLegend) was performed on undiluted cell supernatants according to LEGENDplex kit instructions for V-bottom plate (Manual for Cat. No. 740446). Following completion of assay, samples were acquired on a BD FACS Canto II flow cytometer, and analysis was conducted using BioLegend software available on the BioLegend website.

PicoGreen Assay

For quantification of extracellular DNA indicative of NETosis, preparation of cells for PicoGreen assay (ThermoFisher) protocol was performed according to previously published protocols (Abi Abdallah et al. 2012). PicoGreen assay kit instructions (Manual

Reference: MP 07581) were modified for 96-well plate format and followed exactly. For incubation, supernatant was incubated for 5 minutes protected from light and immediately read on a fluorimeter at an excitation of 450nm and emission of 520nm.

Statistical Analyses

All experiments were repeated a minimum of 3 times to confirm accuracy and consistency of results, and all experiments were conducted with a minimum of n = 3. Statistical significance for all experiments was determined by either 2- tailed, unpaired Student's t-test or One-Way ANOVA with multiple comparisons, and a p-value < 0.05 was considered statistically significant. The type of statistical test run for each experimental result is indicated in the corresponding figure legends.

Results

Two different types of human neutrophil-like cells (HNLCs) are present following exposure to T. gondii cysts.

Previous work investigating the function of neutrophils has demonstrated differentiation into distinct subsets depending on location, age, and host immune status (Tsuda et al. 2004, Xie et al. 2020). These subsets are then able to perform specific "classical" antimicrobial vs. "alternative" regulatory functions that are dependent on subset type and the surrounding environment. One method of "classical" neutrophil identification is demonstrated through the expression of the integrin CD15 (Nakayama et al. 2001).

We hypothesized that HNLC differentiation into subsets would be observed in response to different stages of the parasite, specifically *T. gondii* cysts. To test this, HNLCs were cultured and differentiated from HL-60 cells and were exposed to purified cysts or tachyzoites (**Figure 14**). Immunofluorescence analysis demonstrated the presence of a CD15+ (green cytoplasm) and a CD15- (non-green cytoplasm) cell subset following cyst exposure (**Fig. 14A, bottom panels**). These subsets were also observed following 4hr exposure to media and tachyzoite controls (**Fig. 14A, top and middle panels**). Quantification of CD15+ cell numbers demonstrated an increase in CD15+ cells following infection compared to media controls, but there was no significance between the number of CD15+ cells after exposure to the different parasite stages (**Fig. 14B**). These results demonstrate the differentiation of HNLCs into 2 subsets (CD15+ and CD15-) following infection that is independent of infection stage.

Functional analyses of HNLCs demonstrates cyst-induced responses.

Inflammatory and antimicrobial responses of neutrophils to *T. gondii* have been investigated in the past (Abi Abdallah et al. 2012, Nance et al. 2012), but activity of neutrophils in response to the chronic cyst form of the parasite remains unknown. To determine difference in cytokine production by HNLCs in response to the chronic form of Toxoplasma, cells were stimulated with *T. gondii* cysts, cyst antigen (CAg), tachyzoites, and tachyzoite antigen (TAg) for six hours. LEGENDplex cytokine analysis was performed on cell supernatants to test for production of thirteen Th1-associated cytokines. Results demonstrated a significant increase in the production of canonical IL-6 in response to both cysts and CAg (**Fig. 15A, left**). HNLCs also demonstrated an

approximate 3-fold increase in the amount of secreted IL-1α following exposure to CAg compared to all other experimental and control conditions (**Fig. 15A, middle**). Notably, IL-1α production was specific to cyst antigen exposure but was not significantly induced by exposure to whole cysts. Previous work has discovered a population of IFNγ-expressing murine neutrophils in the brain during chronic infection (Biswas et al. 2017). Our studies of HNLCs showed significantly increased IFNγ secretion in response to both cysts (>2-fold increase) and CAg (>4-fold increase) (**Fig. 15A, right**). Investigation of the canonically-associated IL-12 and GM-CSF yielded no significant increases following exposure to cysts or CAg (**Suppl. Figure 11**). These results reveal previously undemonstrated inflammatory responses of HNLCs following exposure to the chronic form of Toxoplasma.

To determine the activation and employment of NETosis by HNLCs in response to cysts, cells were subjected to the same experimental conditions as above for four hours according to previously published protocols (Abi Abdallah et al. 2012). Extracellular DNA presence in the cell supernatant was quantified as an indicator of NET production. Exposure to PMA and TAg led to a robust NET response and increased extracellular DNA as expected (**Fig. 15B**). While stimulation with chronic-stage *T. gondii* cysts resulted in a trend towards increased extracellular DNA, this was significantly lower than the naïve brain homogenate (NBH) control condition and was not deemed biologically relevant (**Fig. 15B**). This demonstrates no production of NETs by HNLCs in response to cysts.

As the above results were obtained from cells that had not been exposed to CNS environmental conditions typically experienced during chronic infection, extracellular DNA was also quantified from purified brain mononuclear cells (BMNCs) of chronically infected mice following restimulation to determine NET production *in vivo*. As neutrophils should be the only BMNC that produce extracellular DNA, any increase in BMNC extracellular DNA after 4hr exposure was designated as indicative of neutrophil NET production. While extracellular DNA was significantly increased following exposure to purified cysts, this increase did not differ significantly from that of exposure to purified naïve brain homogenate (NBH) (**Fig. 15C**). Taken together, these results demonstrate inflammatory cytokine secretion but not NET production by HNLCs in response to the chronic cyst form of *T. gondii*.

HNLCs demonstrate uptake of cyst material following exposure.

Our imaging studies revealed not only the presence of CD15+ HNLCs following cyst exposure but also a notable loss of cyst numbers and small cyst size (**Figure 14**). Based on these results, we hypothesized that HNLCs are capable of degrading and ingesting cyst material as a method of infection control. To test this, we performed live time lapse imaging and an acute cyst exposure experiment followed by flow cytometry to visualize and quantify any uptake of cyst material.

Cyst exposure for 60 minutes demonstrated attachment of non-fluorescent HNLCs to fluorescent cysts for the duration of the experiment as shown by live time-lapse imaging (**Supplemental Video. 1, left arrow**). HNLCs could also be seen migrating towards,

interacting with, and engulfing or taking up fluorescent cysts (**Supplemental Video. 1, right arrow**). This indicated that these cells are capable of interacting with and degrading the dormant chronic form of *T. gondii*. Use of cyst antigen-coated fluorescent beads as a control condition yielded no attachment of neutrophils or uptake of fluorescent material (**Supplemental Video 2**). To confirm uptake and investigate degradation of cyst material over the course of exposure, a 180-minute time course was performed. Uptake of fluorescent cyst material by HNLCs was seen by the appearance of previously non-fluorescent cells after 60 minutes of exposure (**Fig. 16A, middle left**) compared to 5 minutes post-exposure (**Fig. 16A, left**). This cell-acquired fluorescence gradually started diminishing by 120 minutes post-exposure (**Fig. 16A, middle right**), and fluorescent cells were no longer present at 180 minutes (**Fig. 16A, right**). These results confirm cyst-dependent HNLC attachment and uptake of cyst material by cells within 60 minutes of initial exposure.

To pinpoint when HNLCs begin their uptake of cyst material, cells and cysts were fluorescently labelled with Cell Tracker Dye, an acute 60-minute time course experiment was performed, and cells expressing both cell- (APC+) and cyst-associated (FITC+) fluorescence were quantified as a measure of ingested cyst material. Flow plots demonstrate a 1.5-fold increase in the percentage of double positive (FITC+APC+) cells as early as 10 minutes post-exposure that persists through 60 minutes (**Fig. 16B**). “Cyst Control” and “Cell Control” samples showed no percentage of double positive cells as expected (**Suppl. Fig. 12**). The percentage of double positive HNLCs increased significantly by 10 minutes post-exposure compared to control samples, and similar

results were seen at 60 minutes after addition of cysts (**Fig. 16C**). When the mean fluorescence intensity (MFI) of FITC (cyst material) was quantified in the double positive cells, there was no significant increase observed at any time point (**Fig. 16D**). This indicates an increase in the amount of cells ingesting cyst material but not in the amount of cyst material present in each cell. Taken together these results demonstrate that HNLCs begin responding within 10 minutes following exposure to chronic-stage *T. gondii* cysts, and peak cyst uptake occurs within 60 minutes of exposure followed by gradual degradation and clearance of ingested cyst material.

Discussion

While neutrophil responses to acute Toxoplasma infection have been characterized in depth, very little research has been done to understand the role of these cells during chronic infection. Additionally, most research characterizing neutrophil responses has been done predominantly in murine models, but there is a gap in knowledge regarding human neutrophil responses to infection due to limited resources. This raises important questions about host-dependent differences in the immune response to chronic infection and which defense mechanisms are conserved across species. This study presents a novel response of human neutrophil-like cells to the chronic cyst stage of *T. gondii* and demonstrates a previously unknown role of human neutrophils in the control of chronic Toxoplasma infection.

Following exposure to chronic *T. gondii* cysts, differentiation of HNLCs into two main subsets (CD15+ and CD15-) was observed, but similar differentiation was seen following

exposure to acute-stage tachyzoites (**Figure 14**). Although there was no significant change in the amount of CD15+ and CD15- cells present following exposure to the acute or chronic form of the parasite, increased differentiated cells were seen in both conditions compared to media controls. These results suggest that differentiation of human neutrophils into subsets may be dependent on infection itself or activation of infection-induced signaling pathways as opposed to different stages of the parasite. While CD15 is one of the integrins used to identify different neutrophil subsets, there are a multitude of additional markers that have been used in the past to identify neutrophil subsets and resulting functions (Tsuda et al. 2004, Biswas et al. 2017, Xie et al. 2020). It is also possible that other neutrophil-expressed molecules besides CD15 could be differentially affected following exposure to different stages of the parasite. To further investigate this idea, future studies could be conducted examining the expression of multiple neutrophil subset markers in response to different stages of the parasite via flow cytometry or other quantifiable multi-parameter techniques.

Functional analyses investigating HNLC responses to chronic cysts demonstrated production of inflammatory cytokines associated with canonical neutrophil functions but also previously undemonstrated Toxoplasma-induced cytokine production (**Figure 15A**). IL-6 production by HNLCs was observed in response to both chronic cysts and CAg indicating canonical cytokine production induced by the chronic stage of the parasite. IL-6 production by neutrophils is a vital response acute Toxoplasma infection, and IL-6 production has been previously demonstrated by human neutrophils after exposure to *T. gondii* parasites (Bliss et al. 2001, Ashander et al. 2019, Kikuchi-Ueda et al. 2013,

Mirpuri and Yarovinsky 2012). However, IL-6 production by HNLCs following exposure to the chronic cysts suggests a previously undemonstrated pro-inflammatory response of neutrophils to chronic infection. Surprisingly, IL-1α production was observed following exposure to chronic CAg. Production of this pro-inflammatory cytokine has not previously been reported by neutrophils at all in the context of Toxoplasma infection, but early work demonstrated that IL-1α production by host cells is involved in the recruitment of neutrophils via IL-8 signaling (Denney, Eckmann and Reed 1999). IL-1α secretion in response to CAg and not whole cysts suggests neutrophil production of this cytokine may be dependent on something inside of cysts like specific enzymes or genes involved in latent cyst reactivation (Yang et al. 2022, Guevara, Fox and Bzik 2021). Future studies could be conducted investigating the role of these factors on neutrophil production of IL-1α. The secretion of IFNγ by HNLCs following exposure to both cysts and CAg suggests a direct role of neutrophils in control of chronic infection. Dunay and colleagues previously identified a population of IFNγ-expressing neutrophils in the brain during chronic murine infection (Biswas et al. 2017), but human neutrophil production of IFNγ has not been previously reported. IFNγ production is absolutely necessary to control chronic infection, and a lack of T cell-expressed IFNγ leads to fatal pathology (Nishiyama et al. 2020). While expression of this essential cytokine by neutrophils suggests a direct role in control of chronic infection, the dominant and well-characterized role of T cell production of IFNγ may affect the impact of IFNγ production by neutrophils *in vivo*. It is also possible that the IFNγ production seen is a result of residual T cells present after cyst purification from infected brain. Future kinetics and co-culture

studies could investigate the timing of IFNγ production by neutrophils and T cells to determine the complex interplay between infection control functions of neutrophils and other cell types during infection.

Functional studies investigating NET production demonstrated a trend toward significance in the amount of extracellular DNA present in HNLC supernatant following cyst exposure (**Fig. 15B**) and significantly increased extracellular DNA in re-stimulated BMNC supernatant (**Fig. 15C**). However, our naïve brain homogenate control condition also yielded increased extracellular DNA in both experiments, and this was significantly greater than cyst exposure in HNLCs (**Fig. 15B**). As such, it is possible that the increase in extracellular DNA observed following cyst exposure was due to the presence of excess DNA present following cyst purification and not from NET production. From these results, it can be concluded that HNLCs do not produce NETs in response to chronic *T. gondii* cysts. However, increased extracellular DNA was also seen following exposure to CAg in both experiments, and this could indicate NET production in response to latent parasite reactivation. Future studies investigating this possibility could be conducted to determine the specificity of NET production to cyst-resident bradyzoites and other cyst components released during latent reactivation.

While our results demonstrated both expected and unexpected cytokine expression by HNLCs following exposure to chronic *T. gondii* cysts, these cytokines did not explain the phenomenon of fewer and smaller cysts observed in our imaging studies (**Figure 14**). This led us to hypothesize that HNLCs are somehow capable of ingesting and degrading cysts over time which we tested via the use of live time lapse imaging and flow

cytometry. Results demonstrated striking visual activity of HNLCs including attachment to fluorescent cysts as early as 5 minutes post-exposure and migration of HNLCs to cysts followed by what appeared to be uptake of cyst material within 60 minutes of exposure (**Supplemental Video 1**). Both of these activities were characterized by visual changes in acquired fluorescence of previously non-fluorescent cells which occurred within 60 minutes of exposure, but this gradually decreased after 60 minutes (**Fig. 16A**). Flow cytometry quantification confirmed an increase in cells that had taken up fluorescently labelled cyst material over 60 minutes, and this occurred as early as 10 minutes post-exposure (**Fig. 16B-C**).

The uptake of cyst material by cells confirms our hypothesis that HNLCs are capable of ingesting and degrading cyst material following exposure, and this demonstrates a previously unknown role of neutrophils in antimicrobial activity against the chronic cyst form of *T. gondii*. However, the mechanism of this process remains to be elucidated. Neutrophil uptake and direct killing of pathogens, including Toxoplasma tachyzoites, has been demonstrated previously and includes direct phagocytosis and degradation of small pathogens via activation of autophagy pathways (Wu et al. 2020, Andresen et al. 2022, Alcott et al. 2022). However, phagocytosis by neutrophils is often limited to small pathogens due to the inherently small size of neutrophils. To compensate for this, neutrophils are capable of employing additional mechanisms for larger pathogens such as trogocytosis. This process enables neutrophils to trogocytose or “nibble” away at larger pathogens which leads to degradation and pathogen killing, and this process has been studied in *Trichomonas vaginalis* infection as well as in various models of cancer

(Mercer et al. 2018, Ustyanovska Avtenyuk et al. 2021, Valgardsdottir et al. 2017). Based on these studies and given the broad range of Toxoplasma cyst sizes that range from 10-100µm, it is possible that HNLCs ingest and degrade cyst material through the process of trogocytosis, but this has been previously undescribed in *T. gondii* infection. Future studies investigating the possibility of trogocytosis as a mechanism of cyst antimicrobial activity could be conducted through the use of live imaging and trogocytosis assays as previously described (Mercer et al. 2018).

In conclusion, this study demonstrates Toxoplasma cyst-specific antimicrobial responses of HNLCs. Imaging studies identify differentiation of HNLCs into subsets following cyst exposure, and functional studies of these cells demonstrate cyst-dependent cytokine production. These cells also ingest and degrade cyst material via an unknown mechanism. Collectively, this study identifies a novel response of HNLCs to the chronic cyst stage of *T. gondii*, and this suggests a previously unknown role of human neutrophils in the control of chronic Toxoplasma infection.

Figures and Tables

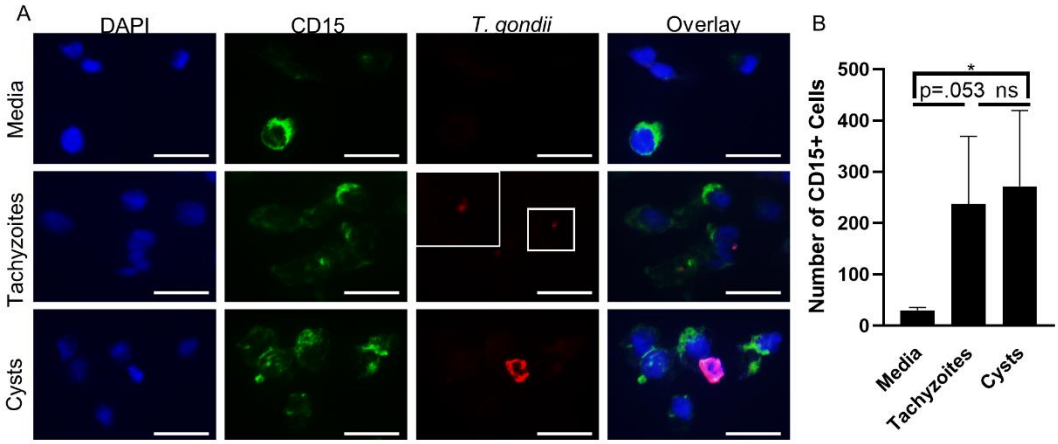

Figure 14. Two different types of human neutrophil-like cells (HNLCs) are present following exposure to *T. gondii* cysts. HNLCs were differentiated from HL-60 cells, cultured *in vitro*, and were exposed to either *T. gondii* tachyzoites or chronic-stage cysts for 4 hours. Coverslips were stained with immunofluorescent antibodies, and cells were imaged at 40x magnification. **(A)** Immunofluorescence staining of neutrophil response to tachyzoites and cysts (blue = DAPI, green = CD15, red = *T. gondii*, scale bar = 25µm). **(B)** Quantification of CD15+ cells (green) from 5 randomized FOV per sample (n=3/group).

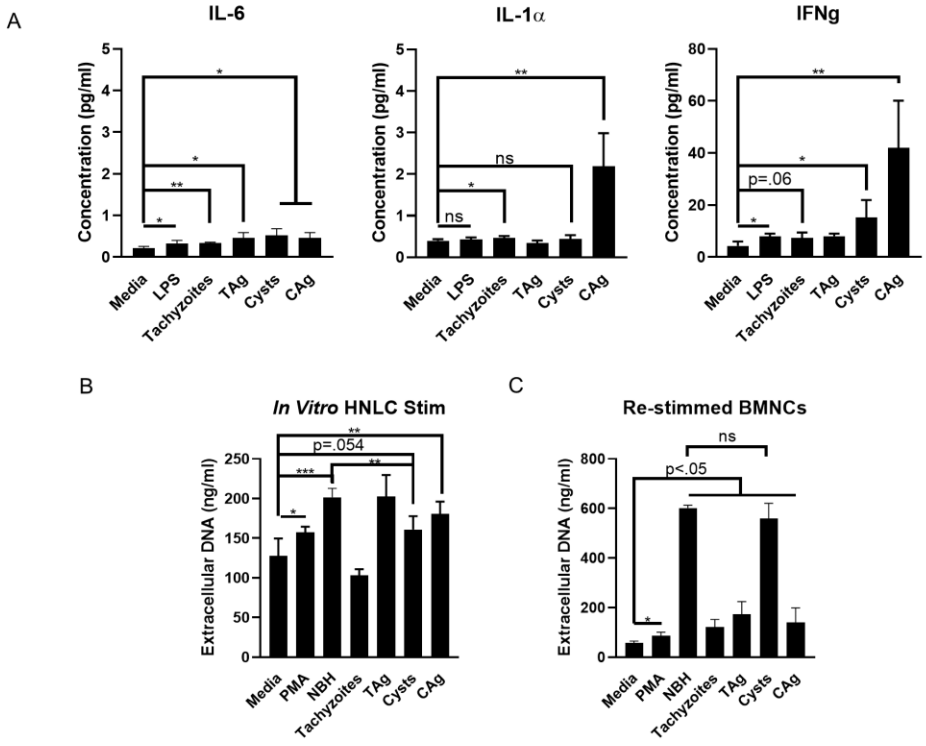
A
IL-6
IL-1α
IFNg
Concentration (pg/ml)
Media
LPS
Tachyzoites
TAg
Cysts
CAg
ns
p=.06
B
In Vitro HNLC Stim
Extracellular DNA (ng/ml)
p=.054
PMA
NBH
C
Re-stimmed BMNCs
p<.05

Figure 15. Functional analyses of HNLCs demonstrates cyst-induced responses. HNLCs were differentiated from HL-60 cells, cultured *in vitro*, and were stimulated with media alone, LPS or PMA, *T. gondii* Me49 tachyzoites, tachyzoite antigen, *T. gondii* Me49 cysts, or cyst antigen for 6 hours. Following stimulation, cell supernatants were tested for cytokine and chemokine production via LEGENDplex assay and NET production via extracellular DNA quantification using a PicoGreen assay. **(A)** Quantification of cytokine production by HNLCs via LEGENDplax assay. **B-C)** Quantification of HNLC **(B)** and re-stimulated brain mononuclear cell **(C)** extracellular DNA concentration via PicoGreen assay. For all significance measures, unpaired Student T-test was performed and p-values are as follows: * = $p<0.05$, ** = $p<0.01$, *** = $p<0.001$, **** = $p<0.0001$.

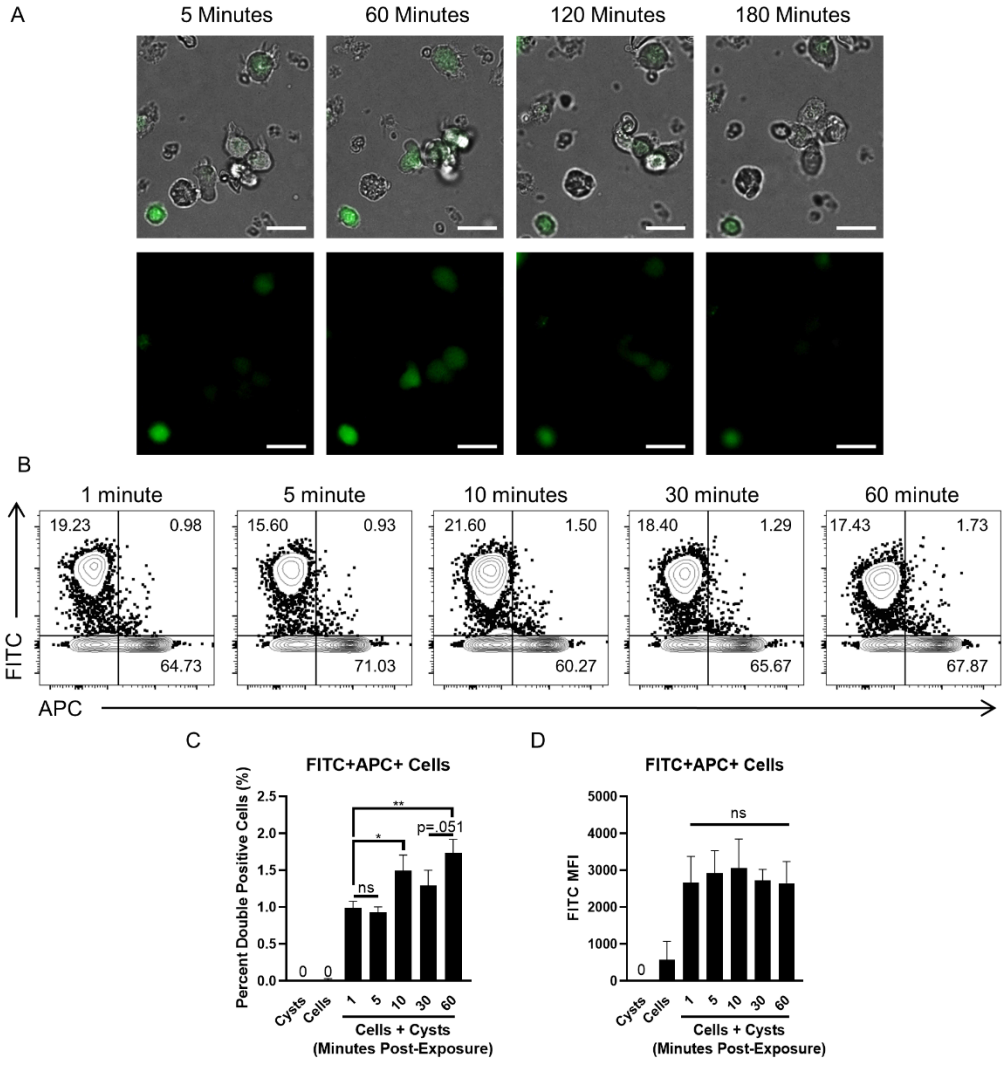
A
5 Minutes
60 Minutes
120 Minutes
180 Minutes
B
1 minute
5 minute
10 minutes
30 minute
60 minute
19.23
0.98
64.73
15.60
0.93
71.03
21.60
1.50
60.27
18.40
1.29
65.67
17.43
1.73
67.87
FITC
APC
C
FITC+APC+ Cells
Percent Double Positive Cells (%)
p=.051
ns
Cysts
Cells
Cells + Cysts
(Minutes Post-Exposure)
D
FITC+APC+ Cells
FITC MFI
ns
Cysts
Cells
Cells + Cysts
(Minutes Post-Exposure)

Figure 16. HNLCs demonstrate uptake of cyst material following exposure. (A) Differentiated HNLCs were exposed to *T. gondii* chronic-stage cysts for 3 hours, and cell-cyst interactions were observed via live time-lapse imaging (40x magnification). Figure shows time-lapse images of brightfield cells overlayed with fluorescent cysts (green) at 5min, 60min, 120min, and 180min post-cyst exposure. Scale bar = 15µm. **B-D)** A separate set of cells was exposed to cysts for 60 minutes, and uptake of fluorescent cyst material was measured via flow cytometry. Representative flow plots **(B)** of fluorescently labelled cells (APC+) and cysts (FITC+) after 1min, 5min, 10min, 30min, and 60min of cyst exposure. Numbers on flow plots represent the average percentage of expression (n=3). Graphs show percent **(C)** and MFI **(D)** of double positive cells (indicative of cyst material uptake by cells) over 60min time course. Significance determined via One-way ANOVA, * = $p<0.05$, ** = $p<0.01$.

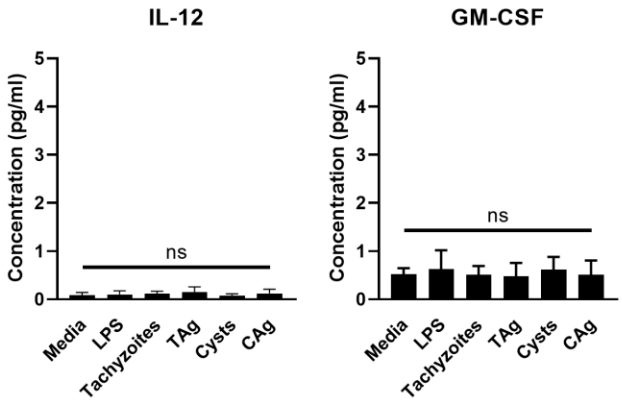
IL-12
GM-CSF
Concentration (pg/ml)
0
1
2
3
4
5
ns
Media
LPS
Tachyzoites
TAg
Cysts
CAg

Supplemental Figure 11. Canonical IL-12 and GM-CSF production by HNLCs is not induced by cysts. Neutrophils were differentiated from HL-60 cells, cultured *in vitro*, and were stimulated with media alone, LPS or PMA, *T. gondii* Me49 tachyzoites, tachyzoite antigen, *T. gondii* Me49 cysts, or cyst antigen for 6 hours. Following stimulation, cell supernatants were tested for cytokine and chemokine production via LEGENDplex assay. For all significance measures, unpaired Student T-test was performed and p-values are as follows: * = $p<0.05$, ** = $p<0.01$, *** = $p<0.001$, **** = $p<0.0001$.

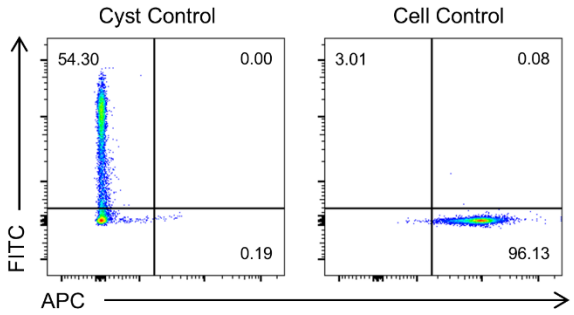
Cyst Control
Cell Control
54.30
0.00
0.19
3.01
0.08
96.13
FITC
APC

Supplemental Figure 12. Flow cytometry results of cyst and cell control samples. Representative flow plots of fluorescently labelled cyst (FITC+) and cell (APC+) control samples. Numbers on flow plots represent the average percentage of expression (n=3).

Chapter 5: Conclusion

Summary

While infection with the parasite *Toxoplasma gondii* can often result in serious disease manifestations in the immunocompromised, there are host defense mechanisms employed in the immunocompetent during chronic infection to maintain brain homeostasis and prevent clinical disease. However, these neuroprotective mechanisms remain widely unknown. This dissertation demonstrates previously unexplored neuroprotective responses to chronic infection including upregulated neuroprotective gene expression and previously undemonstrated neuroprotective cellular properties. The major conclusions that can be drawn from this research can be seen are as follows:

1. This work provides elaboration on previously identified transcriptional changes seen during infection and also offer insights into repair attempts during chronic *T. gondii* infection by utilizing a targeted approach to gene expression analysis in the brain during infection. Importantly, results reveal possible pathways of resolution in a susceptible and resistant mouse model of infection. The use of this targeted approach offers an additional analysis tool in the *T. gondii* scientific field with the possibility for more strategic analysis in the future. These results also open a doorway to a multitude of potential neuroprotective gene candidates that can be explored to elucidate possible therapeutic targets and to further the vital understanding of the kinetics of chronic infection in the brain.
2. This work identifies and explores a functionally diverse chronic neutrophil population that plays a dynamic role in controlling infection outcome in the CNS

by balancing classical responses with neuroprotective functions. These cells express neuroprotective molecules including NRG-1, ErbB4, and MSR1, and they demonstrate distinct phenotypic and transcriptomic profiles compared to peripheral neutrophils including CNS-specific protective signatures. This demonstrates a previously unexplored neuroprotective role of neutrophils in models of chronic infection and introduces a potential new therapeutic target for treating chronic CNS disease.

3. This work reveals a novel response of human neutrophil-like cells (HNLCs) to the chronic cyst stage of *T. gondii*, and this suggests a previously unknown role of human neutrophils in the control of chronic Toxoplasma infection. These human cells demonstrate uptake of cyst material and display cyst-specific functions including cytokine production that aids in control of parasite reactivation. This demonstrates previously unknown functions of neutrophils that specifically target the chronic cyst form of *T. gondii*, and this helps bridge the gap in Toxoplasma knowledge of conserved immune mechanisms between human and murine models of infection.

Discussion and Potential Future Directions

While this dissertation provides novel insights into host- and cell-specific neuroprotective mechanisms at play during chronic *T. gondii* infection, there are still many aspects of these discoveries that remain to be further investigated. The upregulation of genes relating to resolution of infection in the brain throughout chronic infection demonstrates that attempts at neuroprotection are indeed consistently maintained. It also shows that the

baseline immune status of the host plays a pivotal role in whether these neuroprotective attempts are ultimately successful. This collective research study brushes the surface of these baseline differences in resistant and susceptible hosts, but there is a plethora of research options introduced here that could dig deeper into the molecular mechanisms of host-dependent neuroprotection during infection. By investigating some of the key transcriptomic differences found here in both susceptible and resistant hosts, future studies could pinpoint the key players in neuroprotection in the CNS via depletion and functional studies. Discovery of these key players at the functional level could lead to future therapeutic methods of inducing stronger neuroprotective responses not only during Toxoplasma infection but in other models of CNS damage.

The discovery of a functionally diverse neutrophil population capable of inducing neuroprotection in the brain via upregulation of SLPI production by neurons shown in this work opens a previously closed door in the fields of immunology and neuroscience. This work demonstrates a direct impact of neutrophils on regeneration of neurons via the SLPI pathway during infection, however the details of this process remain unknown. Future studies could investigate the mechanistic pathway activated by neutrophils in the brain to encourage SLPI-dependent neuroprotection. Additionally, it is unknown how the expression of neuroprotective molecules including NRG-1, ErbB4, and MSR1 by neutrophils aids in neuroprotective functions of these cells. Blocking of these neuroprotective molecules specifically in neutrophils in future work could elucidate the roles of these molecules in neutrophil-mediated neuroprotection and what specific neuroprotective pathways they affect.

Finally, the cyst-specific responses of human neutrophil-like cells (HNLCs) demonstrated here introduces previously unknown chronic functions of innate neutrophils and a previously unknown role of these cells in controlling parasite replication in the human brain. This combined with the murine neutrophil data in this dissertation helps bridge the gap in knowledge about what immune cell functions are conserved across hosts during chronic Toxoplasma infection, but this is only the beginning. Much more work must be done in this field to: a) determine if the cyst-specific responses of HNLCs seen here translate to *in vivo* models of infection and b) how the chronic parasite control functions of these cells contribute to what is currently known about chronic infection. The work shown here also suggests that human neutrophils may have more versatile roles in other models of chronic CNS disease.

Taken together, the data in this dissertation answer a very important question in the context of chronic brain disease: what mechanisms are employed by the host to maintain brain integrity in instances of damage, and how do these mechanisms balance out necessary immune responses? This work also brings together multiple disciplines of immunology, microbiology, parasitology, and neuroscience by investigating neuroprotective functions employed by the immune response in the brain during chronic *Toxoplasma gondii* infection. The complex interplay between these different components reveals a truly collaborative effort of host defenses that can be applied not only to *T. gondii* infection, but also to any model of chronic infection or disease.

References

Abdelbaset, A. E., B. A. Fox, M. H. Karram, M. R. Abd Ellah, D. J. Bzik & M. Igarashi (2017) Lactate dehydrogenase in Toxoplasma gondii controls virulence, bradyzoite differentiation, and chronic infection. *PloS one,* 12**,** e0173745-e0173745.

Abi Abdallah, D. S., C. Lin, C. J. Ball, M. R. King, G. E. Duhamel & E. Y. Denkers (2012) Toxoplasma gondii triggers release of human and mouse neutrophil extracellular traps. *Infect Immun,* 80**,** 768-77.

Alcott, A. M., L. M. Werner, C. M. Baiocco, M. Belcher Dufrisne, L. Columbus & A. K. Criss (2022) Variable Expression of Opa Proteins by Neisseria gonorrhoeae Influences Bacterial Association and Phagocytic Killing by Human Neutrophils. *J Bacteriol,* 204**,** e0003522.

Alizadeh, A., K. T. Santhosh, H. Kataria, A. S. Gounni & S. Karimi-Abdolrezaee (2018) Neuregulin-1 elicits a regulatory immune response following traumatic spinal cord injury. *Journal of Neuroinflammation,* 15**,** 53.

Alves, C. M., D. A. Silva, A. E. Azzolini, C. M. Marzocchi-Machado, Y. M. Lucisano-Valim, M. C. Roque-Barreira & J. R. Mineo (2013) Galectin-3 is essential for reactive oxygen species production by peritoneal neutrophils from mice infected with a virulent strain of Toxoplasma gondii. *Parasitology,* 140**,** 210-9.

Andresen, S., K. Fantone, D. Chapla, B. Rada, K. W. Moremen, M. Pierce & C. M. Szymanski (2022) Human Intelectin-1 Promotes Cellular Attachment and Neutrophil Killing of Streptococcus pneumoniae in a Serotype-Dependent Manner. *Infect Immun***,** e0068221.

Anuradha, B. & C. Preethi (2014) Seroprevalence of Toxoplasma IgG Antibodies in HIV Positive Patients in and Around Khammam, Telangana State. *J Clin Diagn Res,* 8**,** Dl01-2.

Ashander, L. M., S. Lie, Y. Ma, E. Rochet, J. M. Washington, J. M. Furtado, B. Appukuttan & J. R. Smith (2019) Neutrophil Activities in Human Ocular Toxoplasmosis: An In Vitro Study With Human Cells. *Invest Ophthalmol Vis Sci,* 60**,** 4652-4660.

Azcona, J. A., S. Tang, E. Berry, F. F. Zhang, R. Garvey, J. R. Falck, M. L. Schwartzman, T. Yi, T. M. Jeitner & A. M. Guo (2022) Neutrophil-derived Myeloperoxidase and Hypochlorous Acid Critically Contribute to 20-HETE Increases that Drive Post-Ischemic Angiogenesis. *J Pharmacol Exp Ther*.

Bai, F., R. M. McCormack, S. Hower, G. V. Plano, M. G. Lichtenheld & G. P. Munson (2018) Perforin-2 Breaches the Envelope of Phagocytosed Bacteria Allowing Antimicrobial Effectors Access to Intracellular Targets. *J Immunol,* 201**,** 2710-2720.

Baldursson, S. & P. Karanis (2011) Waterborne transmission of protozoan parasites: review of worldwide outbreaks - an update 2004-2010. *Water Res,* 45**,** 6603-14.

Ballesteros, I., A. Rubio-Ponce, M. Genua, E. Lusito, I. Kwok, G. Fernández-Calvo, T. E. Khoyratty, E. van Grinsven, S. González-Hernández, J. Nicolás-Ávila, T. Vicanolo, A. Maccataio, A. Benguría, J. L. Li, J. M. Adrover, A. Aroca-Crevillen, J. A. Quintana, S. Martín-Salamanca, F. Mayo, S. Ascher, G. Barbiera, O. Soehnlein, M. Gunzer, F. Ginhoux, F. Sánchez-Cabo, E. Nistal-Villán, C. Schulz, A. Dopazo, C. Reinhardt, I. A. Udalova, L. G. Ng, R. Ostuni & A. Hidalgo (2020) Co-option of Neutrophil Fates by Tissue Environments. *Cell,* 183**,** 1282-1297.e18.

Barbosa, J. L., S. R. Béla, M. F. Ricci, M. L. M. Noviello, C. T. Cartelle, B. V. Pinheiro, R. W. A. Vitor & R. M. E. Arantes (2020) Spontaneous T. gondii neuronal encystment induces structural neuritic network impairment associated with changes of tyrosine hydroxilase expression. *Neurosci Lett,* 718**,** 134721.

Berdoy, M., J. P. Webster & D. W. Macdonald (2000) Fatal attraction in rats infected with Toxoplasma gondii. *Proc Biol Sci,* 267**,** 1591-4.

Bergersen, K. V., A. Barnes, D. Worth, C. David & E. H. Wilson (2021) Targeted Transcriptomic Analysis of C57BL/6 and BALB/c Mice During Progressive Chronic Toxoplasma gondii Infection Reveals Changes in Host and Parasite Gene Expression Relating to Neuropathology and Resolution. *Front Cell Infect Microbiol,* 11**,** 645778.

Bernal, J. A., R. Luna, A. Espina, I. Lázaro, F. Ramos-Morales, F. Romero, C. Arias, A. Silva, M. Tortolero & J. A. Pintor-Toro (2002) Human securin interacts with p53 and modulates p53-mediated transcriptional activity and apoptosis. *Nat Genet,* 32**,** 306-11.

Beyrau, M., J. Bodkin & S. Nourshargh. 2012. *Neutrophil heterogeneity in health and disease: A revitalized avenue in inflammation and immunity*.

Binet, F., G. Cagnone, S. Crespo-Garcia, M. Hata, M. Neault, A. Dejda, A. M. Wilson, M. Buscarlet, G. T. Mawambo, J. P. Howard, R. Diaz-Marin, C. Parinot, V. Guber, F. Pilon, R. Juneau, R. Laflamme, C. Sawchyn, K. Boulay, S. Leclerc, A. Abu-Thuraia, J. F. Côté, G. Andelfinger, F. A. Rezende, F. Sennlaub, J. S. Joyal, F. A. Mallette & P. Sapieha (2020) Neutrophil extracellular traps target senescent vasculature for tissue remodeling in retinopathy. *Science,* 369.

Biswas, A., T. French, H. P. Düsedau, N. Mueller, M. Riek-Burchardt, A. Dudeck, U. Bank, T. Schüler & I. R. Dunay (2017) Behavior of Neutrophil Granulocytes during Toxoplasma gondii Infection in the Central Nervous System. *Frontiers in Cellular and Infection Microbiology,* 7**,** 259.

Blackwell, J. M., C. W. Roberts & J. Alexander (1993) Influence of genes within the MHC on mortality and brain cyst development in mice infected with Toxoplasma gondii: kinetics of immune regulation in BALB H-2 congenic mice. *Parasite Immunology,* 15**,** 317-324.

Blanchard, N., I. R. Dunay & D. Schlüter (2015) Persistence of Toxoplasma gondii in the central nervous system: a fine-tuned balance between the parasite, the brain and the immune system. *Parasite Immunol,* 37**,** 150-8.

Bliss, S. K., L. C. Gavrilescu, A. Alcaraz & E. Y. Denkers (2001) Neutrophil depletion during Toxoplasma gondii infection leads to impaired immunity and lethal systemic pathology. *Infection and immunity,* 69**,** 4898-4905.

Bliss, S. K., A. J. Marshall, Y. Zhang & E. Y. Denkers (1999) Human polymorphonuclear leukocytes produce IL-12, TNF-alpha, and the chemokines macrophage-inflammatory protein-1 alpha and -1 beta in response to Toxoplasma gondii antigens. *J Immunol,* 162**,** 7369-75.

Bogdan, C., J. Paik, Y. Vodovotz & C. Nathan (1992) Contrasting mechanisms for suppression of macrophage cytokine release by transforming growth factor-beta and interleukin-10. *Journal of Biological Chemistry,* 267**,** 23301-23308.

Boillat, M., P. M. Hammoudi, S. K. Dogga, S. Pagès, M. Goubran, I. Rodriguez & D. Soldati-Favre (2020) Neuroinflammation-Associated Aspecific Manipulation of Mouse Predator Fear by Toxoplasma gondii. *Cell Rep,* 30**,** 320-334.e6.

Bottari, N. B., K. P. Reichert, M. Fracasso, A. Dutra, C. E. Assmann, H. Ulrich, M. R. C. Schetinger, V. M. Morsch & A. S. Da Silva (2020) Neuroprotective role of resveratrol mediated by purinergic signalling in cerebral cortex of mice infected by Toxoplasma gondii. *Parasitol Res,* 119**,** 2897-2905.

Brien, C. A., S. J. Batista, K. M. Still & T. Harris (2018) IL-10 and ICOS differentially regulate T cell responses in the brain during chronic Toxoplasma gondii infection. *bioRxiv*.

Brinkmann, V., U. Reichard, C. Goosmann, B. Fauler, Y. Uhlemann, D. S. Weiss, Y. Weinrauch & A. Zychlinsky (2004) Neutrophil extracellular traps kill bacteria. *Science,* 303**,** 1532-5.

Brooks, J. M., G. L. Carrillo, J. Su, D. S. Lindsay, M. A. Fox & I. J. Blader (2015) Toxoplasma gondii Infections Alter GABAergic Synapses and Signaling in the Central Nervous System. *mBio,* 6**,** e01428-15.

Brown, C. R., C. A. Hunter, R. G. Estes, E. Beckmann, J. Forman, C. David, J. S. Remington & R. McLeod (1995) Definitive identification of a gene that confers resistance against Toxoplasma cyst burden and encephalitis. *Immunology,* 85**,** 419-28.

Buonsenso, D., D. Pata, A. Turriziani Colonna, M. Iademarco, M. De Santis, L. Masini, G. Conti, F. Molle, A. Baldascino, A. Acampora, R. Luciano, F. Gallini & P. Valentini (2022) Spyramicine and Trimethoprim-Sulfamethoxazole Combination to Prevent Mother-To-Fetus Transmission of Toxoplasma gondii Infection in Pregnant Women: A 28-Years Single-center Experience. *Pediatr Infect Dis J,* 41**,** e223-e227.

Burke, J. M., C. W. Roberts, C. A. Hunter, M. Murray & J. Alexander (1994) Temporal differences in the expression of mRNA for IL-10 and IFN-gamma in the brains and spleens of C57BL/10 mice infected with Toxoplasma gondii. *Parasite Immunol,* 16**,** 305-14.

Cabral, C. M., S. Tuladhar, H. K. Dietrich, E. Nguyen, W. R. MacDonald, T. Trivedi, A. Devineni & A. A. Koshy (2016) Neurons are the Primary Target Cell for the Brain-Tropic Intracellular Parasite Toxoplasma gondii. *PLoS pathogens,* 12**,** e1005447-e1005447.

Cahill, M. E., C. Remmers, K. A. Jones, Z. Xie, R. A. Sweet & P. Penzes (2013) Neuregulin1 signaling promotes dendritic spine growth through kalirin. *Journal of neurochemistry,* 126**,** 625-635.

Casanova-Acebes, M., C. Pitaval, L. A. Weiss, C. Nombela-Arrieta, R. Chèvre, A. G. N, Y. Kunisaki, D. Zhang, N. van Rooijen, L. E. Silberstein, C. Weber, T. Nagasawa, P. S. Frenette, A. Castrillo & A. Hidalgo (2013) Rhythmic modulation of the hematopoietic niche through neutrophil clearance. *Cell,* 153**,** 1025-35.

Cassatella, M. A., L. Meda, S. Gasperini, A. D'Andrea, X. Ma & G. Trinchieri (1995) Interleukin-12 production by human polymorphonuclear leukocytes. *European Journal of Immunology,* 25**,** 1-5.

Christoffersson, G., E. Vågesjö, J. Vandooren, M. Lidén, S. Massena, R. B. Reinert, M. Brissova, A. C. Powers, G. Opdenakker & M. Phillipson (2012) VEGF-A recruits a proangiogenic MMP-9-delivering neutrophil subset that induces angiogenesis in transplanted hypoxic tissue. *Blood,* 120**,** 4653-62.

Da Cunha, S., E. Ferreira, I. Ramos, R. Martins, L. De Freitas, J. L. Borges, R. Côrte-Real, A. Mota, A. Meliço-Silvestre & A. L. Furtado (1994) Cerebral toxoplasmosis after renal transplantation. Case report and review. *Acta Med Port,* 7 Suppl 1**,** S61-6.

Daffos, F., F. Forestier, M. Capella-Pavlovsky, P. Thulliez, C. Aufrant, D. Valenti & W. L. Cox (1988) Prenatal management of 746 pregnancies at risk for congenital toxoplasmosis. *N Engl J Med,* 318**,** 271-5.

Danaher, P., S. Warren, L. Dennis, L. D'Amico, A. White, M. L. Disis, M. A. Geller, K. Odunsi, J. Beechem & S. P. Fling (2017) Gene expression markers of Tumor Infiltrating Leukocytes. *J Immunother Cancer,* 5**,** 18.

David, C. N., E. S. Frias, J. I. Szu, P. A. Vieira, J. A. Hubbard, J. Lovelace, M. Michael, D. Worth, K. E. McGovern, I. M. Ethell, B. G. Stanley, E. Korzus, T. A. Fiacco, D. K. Binder & E. H. Wilson (2016) GLT-1-Dependent Disruption of CNS Glutamate Homeostasis and Neuronal Function by the Protozoan Parasite Toxoplasma gondii. *PLOS Pathogens,* 12**,** e1005643.

De la Monte, S. M., H. J. Federoff, S. C. Ng, E. Grabczyk & M. C. Fishman (1989) GAP-43 gene expression during development: persistence in a distinctive set of neurons in the mature central nervous system. *Brain Res Dev Brain Res,* 46**,** 161-8.

Debierre-Grockiego, F., N. Moiré, M. Torres Arias & I. Dimier-Poisson (2020) Recent Advances in the Roles of Neutrophils in Toxoplasmosis. *Trends Parasitol,* 36**,** 956-958.

Deckert-Schlüter, M., D. Schlüter, D. Schmidt, G. Schwendemann, O. D. Wiestler & H. Hof (1994) Toxoplasma encephalitis in congenic B10 and BALB mice: impact of genetic factors on the immune response. *Infect Immun,* 62**,** 221-8.

Del Rio, L., S. Bennouna, J. Salinas & E. Y. Denkers (2001) CXCR2 Deficiency Confers Impaired Neutrophil Recruitment and Increased Susceptibility During Toxoplasma gondii Infection. *The Journal of Immunology,* 167**,** 6503.

Dellacasa-Lindberg, I., N. Hitziger & A. Barragan (2007) Localized recrudescence of Toxoplasma infections in the central nervous system of immunocompromised mice assessed by in vivo bioluminescence imaging. *Microbes and Infection,* 9**,** 1291-1298.

Denkers, E. Y. (1999) T lymphocyte-dependent effector mechanisms of immunity to Toxoplasma gondii. *Microbes Infect,* 1**,** 699-708.

Denney, C. F., L. Eckmann & S. L. Reed (1999) Chemokine secretion of human cells in response to Toxoplasma gondii infection. *Infect Immun,* 67**,** 1547-52.

Desmonts, G. & J. Couvreur (1974) Toxoplasmosis in pregnancy and its transmission to the fetus. *Bull N Y Acad Med,* 50**,** 146-59.

Di Cristina, M., D. Marocco, R. Galizi, C. Proietti, R. Spaccapelo & A. Crisanti (2008) Temporal and spatial distribution of Toxoplasma gondii differentiation into Bradyzoites and tissue cyst formation in vivo. *Infect Immun,* 76**,** 3491-501.

Diaconu, I. A., L. M. Stratan, L. Nichita, V. Aramă, V. R. Moroti Constantinescu, A. I. Diaconu & D. A. Ion (2016) Diagnosing HIV-associated cerebral diseases - the importance of Neuropathology in understanding HIV. *Rom J Morphol Embryol,* 57**,** 745-750.

Du, J., R. An, L. Chen, Y. Shen, Y. Chen, L. Cheng, Z. Jiang, A. Zhang, L. Yu, D. Chu, Y. Shen, Q. Luo, H. Chen, L. Wan, M. Li, X. Xu & J. Shen (2014) Toxoplasma gondii virulence factor ROP18 inhibits the host NF-κB pathway by promoting p65 degradation. *The Journal of biological chemistry,* 289**,** 12578-12592.

Dubey, J. P. 1988. *Toxoplasmosis of animals and man / authors, J.P. Dubey, C.P. Beattie*. Boca Raton, Fla: CRC Press.

Dunay, I. R., K. Gajurel, R. Dhakal, O. Liesenfeld & J. G. Montoya (2018) Treatment of Toxoplasmosis: Historical Perspective, Animal Models, and Current Clinical Practice. *Clinical microbiology reviews,* 31**,** e00057-17.

Dupont, C. D., D. A. Christian & C. A. Hunter (2012) Immune response and immunopathology during toxoplasmosis. *Seminars in immunopathology,* 34**,** 793-813.

Eyles, D. E. & N. Coleman (1953) Synergistic effect of sulfadiazine and daraprim against experimental toxoplasmosis in the mouse. *Antibiot Chemother (Northfield),* 3**,** 483-90.

Falls, D. L. (2003) Neuregulins: functions, forms, and signaling strategies. *Experimental Cell Research,* 284**,** 14-30.

Falvo, J. V., A. M. Uglialoro, B. M. Brinkman, M. Merika, B. S. Parekh, E. Y. Tsai, H. C. King, A. D. Morielli, E. G. Peralta, T. Maniatis, D. Thanos & A. E. Goldfeld (2000) Stimulus-specific assembly of enhancer complexes on the tumor necrosis factor alpha gene promoter. *Mol Cell Biol,* 20**,** 2239-47.

Feustel, S. M., M. Meissner & O. Liesenfeld (2012) Toxoplasma gondii and the blood-brain barrier. *Virulence,* 3**,** 182-92.

Fisch, D., B. Clough & E. M. Frickel (2019) Human immunity to Toxoplasma gondii. *PLoS Pathog,* 15**,** e1008097.

Gao, A. Y. L., A. Ilie, P. K. Y. Chang, J. Orlowski & R. A. McKinney (2019) A Christianson syndrome-linked deletion mutation (Δ287ES288) in SLC9A6 impairs hippocampal neuronal plasticity. *Neurobiol Dis,* 130**,** 104490.

Garfoot, A. L., G. M. Wilson, J. J. Coon & L. J. Knoll (2019) Proteomic and transcriptomic analyses of early and late-chronic Toxoplasma gondii infection shows novel and stage specific transcripts. *BMC Genomics,* 20**,** 859.

Gazzinelli, R., Y. Xu, S. Hieny, A. Cheever & A. Sher (1992) Simultaneous depletion of CD4+ and CD8+ T lymphocytes is required to reactivate chronic infection with Toxoplasma gondii. *The Journal of Immunology,* 149**,** 175.

Gazzinelli, R. T., I. Eltoum, T. A. Wynn & A. Sher (1993a) Acute cerebral toxoplasmosis is induced by in vivo neutralization of TNF-alpha and correlates with the down-regulated expression of inducible nitric oxide synthase and other markers of macrophage activation. *The Journal of Immunology,* 151**,** 3672.

Gazzinelli, R. T., S. Hieny, T. A. Wynn, S. Wolf & A. Sher (1993b) Interleukin 12 is required for the T-lymphocyte-independent induction of interferon gamma by an intracellular parasite and induces resistance in T-cell-deficient hosts. *Proceedings of the National Academy of Sciences,* 90**,** 6115.

Gazzinelli, R. T., M. Wysocka, S. Hayashi, E. Y. Denkers, S. Hieny, P. Caspar, G. Trinchieri & A. Sher (1994) Parasite-induced IL-12 stimulates early IFN-gamma synthesis and resistance during acute infection with Toxoplasma gondii. *J Immunol,* 153**,** 2533-43.

Ge, Y., J. Chen, X. Qiu, J. Zhang, L. Cui, Y. Qi, X. Liu, J. Qiu, Z. Shi, Z. Lun, J. Shen & Y. Wang (2014) Natural killer cell intrinsic toll-like receptor MyD88 signaling contributes to IL-12-dependent IFN-γ production by mice during infection with Toxoplasma gondii. *Int J Parasitol,* 44**,** 475-84.

Geiss, G. K., R. E. Bumgarner, B. Birditt, T. Dahl, N. Dowidar, D. L. Dunaway, H. P. Fell, S. Ferree, R. D. George, T. Grogan, J. J. James, M. Maysuria, J. D. Mitton, P. Oliveri, J. L. Osborn, T. Peng, A. L. Ratcliffe, P. J. Webster, E. H. Davidson, L. Hood & K. Dimitrov (2008) Direct multiplexed measurement of gene expression with color-coded probe pairs. *Nature Biotechnology,* 26**,** 317-325.

Ghasemlou, N., D. Bouhy, J. Yang, R. López-Vales, M. Haber, T. Thuraisingam, G. He, D. Radzioch, A. Ding & S. David (2010) Beneficial effects of secretory leukocyte protease inhibitor after spinal cord injury. *Brain : a journal of neurology,* 133**,** 126-138.

Goerner, A. L., E. A. Vizcarra, D. D. Hong, K. V. Bergersen, C. A. Alvarez, M. A. Talavera, E. H. Wilson & M. W. White (2020) An ex vivo model of Toxoplasma recrudescence. *bioRxiv***,** 2020.05.18.101931.

Gong, Y. & D. R. Koh (2010) Neutrophils promote inflammatory angiogenesis via release of preformed VEGF in an in vivo corneal model. *Cell Tissue Res,* 339**,** 437-48.

Gorup, D., I. Bohaček, T. Miličević, R. Pochet, D. Mitrečić, J. Križ & S. Gajović (2015) Increased expression and colocalization of GAP43 and CASP3 after brain ischemic lesion in mouse. *Neuroscience Letters,* 597**,** 176-182.

Graham, A. K., C. Fong, A. Naqvi & J. Q. Lu (2020) Toxoplasmosis of the central nervous system: Manifestations vary with immune responses. *J Neurol Sci***,** 117223.

Guarnieri, S., C. Morabito, C. Paolini, S. Boncompagni, R. Pilla, G. Fanò-Illic & M. A. Mariggiò (2013) Growth associated protein 43 is expressed in skeletal muscle fibers and is localized in proximity of mitochondria and calcium release units. *PLoS One,* 8**,** e53267.

Guevara, R. B., B. A. Fox & D. J. Bzik (2021) A Family of Toxoplasma gondii Genes Related to GRA12 Regulate Cyst Burdens and Cyst Reactivation. *mSphere,* 6.

Guevara, R. B., B. A. Fox, A. Falla & D. J. Bzik (2019) Toxoplasma gondii Intravacuolar-Network-Associated Dense Granule Proteins Regulate Maturation of the Cyst Matrix and Cyst Wall. *mSphere,* 4.

Hall, A. O. H., D. P. Beiting, C. Tato, B. John, G. Oldenhove, C. G. Lombana, G. H. Pritchard, J. S. Silver, N. Bouladoux, J. S. Stumhofer, T. H. Harris, J. Grainger, E. D. T. Wojno, S. Wagage, D. S. Roos, P. Scott, L. A. Turka, S. Cherry, S. L. Reiner, D. Cua, Y. Belkaid, M. M. Elloso & C. A. Hunter (2012) The cytokines interleukin 27 and interferon-γ promote distinct Treg cell populations required to limit infection-induced pathology. *Immunity,* 37**,** 511-523.

Handford, C. A., J. W. Lynch, E. Baker, G. C. Webb, J. H. Ford, G. R. Sutherland & P. R. Schofield (1996) The human glycine receptor beta subunit: primary structure, functional characterisation and chromosomal localisation of the human and murine genes. *Brain Res Mol Brain Res,* 35**,** 211-9.

Hannila, S. S., M. M. Siddiq, J. B. Carmel, J. Hou, N. Chaudhry, P. M. Bradley, M. Hilaire, E. L. Richman, R. P. Hart & M. T. Filbin (2013) Secretory leukocyte protease inhibitor reverses inhibition by CNS myelin, promotes regeneration in the optic nerve, and suppresses expression of the transforming growth factor-β signaling protein Smad2. *J Neurosci,* 33**,** 5138-51.

Harris, T. H., E. H. Wilson, E. D. Tait, M. Buckley, S. Shapira, J. Caamano, D. Artis & C. A. Hunter (2010) NF-kappaB1 contributes to T cell-mediated control of Toxoplasma gondii in the CNS. *J Neuroimmunol,* 222**,** 19-28.

Hidano, S., L. M. Randall, L. Dawson, H. K. Dietrich, C. Konradt, P. J. Klover, B. John, T. H. Harris, Q. Fang, B. Turek, T. Kobayashi, L. Hennighausen, D. P. Beiting, A. A. Koshy & C. A. Hunter (2016) STAT1 Signaling in Astrocytes Is Essential for Control of Infection in the Central Nervous System. *mBio,* 7**,** e01881-16.

Hofman, P., J. F. Michiels, M. C. Saint-Paul, A. Galibert, P. Marty, J. Durant, J. G. Fuzibet, J. Mouroux, Y. Le Fichoux & R. Loubiere (1993) [Toxoplasmosis in AIDS patients. Pathoclinical study of 78 cases]. *Ann Pathol,* 13**,** 233-40.

Hong, D.-P., J. B. Radke & M. W. White (2017) Opposing Transcriptional Mechanisms Regulate Toxoplasma Development. *mSphere,* 2**,** e00347-16.

Hou, Y., D. Yang, R. Xiang, H. Wang, X. Wang, H. Zhang, P. Wang, Z. Zhang, X. Che, Y. Liu, Y. Gao, X. Yu, X. Gao, W. Zhang, J. Yang & C. Wu (2019) N2 neutrophils may participate in spontaneous recovery after transient cerebral ischemia by inhibiting ischemic neuron injury in rats. *International Immunopharmacology,* 77**,** 105970.

Hu, R. S., J. J. He, H. M. Elsheikha, Y. Zou, M. Ehsan, Q. N. Ma, X. Q. Zhu & W. Cong (2020) Transcriptomic Profiling of Mouse Brain During Acute and Chronic Infections by Toxoplasma gondii Oocysts. *Front Microbiol,* 11**,** 570903.

Hunter, C. A. & L. D. Sibley (2012) Modulation of innate immunity by Toxoplasma gondii virulence effectors. *Nature reviews. Microbiology,* 10**,** 766-778.

Hwang, Y. S., J.-H. Shin, J.-P. Yang, B.-K. Jung, S. H. Lee & E.-H. Shin (2018) Characteristics of Infection Immunity Regulated by Toxoplasma gondii to Maintain Chronic Infection in the Brain. *Frontiers in Immunology,* 9**,** 158.

Ji, C., M. Tang, J. Harrison, A. Paciorkowski & G. V. W. Johnson (2018) Nuclear transglutaminase 2 directly regulates expression of cathepsin S in rat cortical neurons. *Eur J Neurosci,* 48**,** 3043-3051.

Ji, R. N., L. L. Zhang, M. F. Zhao, H. F. He, W. Bai, R. X. Duan & C. G. Kou (2019) Decreased serum complement component 4 levels in patients with schizophrenia. *Psychiatr Genet,* 29**,** 127-129.

Jia, B., H. Lu, Q. Liu, J. Yin, N. Jiang & Q. Chen (2013) Genome-wide comparative analysis revealed significant transcriptome changes in mice after Toxoplasma gondii infection. *Parasites & vectors,* 6**,** 161-161.

Johnson, J., Y. Suzuki, D. Mack, E. Mui, R. Estes, C. David, E. Skamene, J. Forman & R. McLeod (2002) Genetic analysis of influences on survival following Toxoplasma gondii infection. *International journal for parasitology,* 32**,** 179-85.

Khan, I. A., S. Hwang & M. Moretto (2019) Toxoplasma gondii: CD8 T Cells Cry for CD4 Help. *Front Cell Infect Microbiol,* 9**,** 136.

Kikuchi-Ueda, T., T. Ubagai & Y. Ono (2013) Priming effects of tumor necrosis factor-α on production of reactive oxygen species during Toxoplasma gondii stimulation and receptor gene expression in differentiated HL-60 cells. *J Infect Chemother,* 19**,** 1053-64.

Konishi, E. & M. Nakao (1992) Naturally occurring immunoglobulin M antibodies: enhancement of phagocytic and microbicidal activities of human neutrophils against Toxoplasma gondii. *Parasitology,* 104 (Pt 3)**,** 427-32.

Kostic, M., N. Zivkovic, A. Cvetanovic, I. Stojanovic & M. Colic (2017) IL-17 signalling in astrocytes promotes glutamate excitotoxicity: Indications for the link between inflammatory and neurodegenerative events in multiple sclerosis. *Multiple Sclerosis and Related Disorders,* 11**,** 12-17.

Kravets, E., D. Degrandi, S. Weidtkamp-Peters, B. Ries, C. Konermann, S. Felekyan, J. M. Dargazanli, G. J. Praefcke, C. A. Seidel, L. Schmitt, S. H. Smits & K. Pfeffer (2012) The GTPase activity of murine guanylate-binding protein 2 (mGBP2) controls the intracellular localization and recruitment to the parasitophorous vacuole of Toxoplasma gondii. *J Biol Chem,* 287**,** 27452-66.

Krishnamurthy, S. & J. P. J. Saeij (2018) Toxoplasma Does Not Secrete the GRA16 and GRA24 Effectors Beyond the Parasitophorous Vacuole Membrane of Tissue Cysts. *Frontiers in cellular and infection microbiology,* 8**,** 366-366.

Kurimoto, T., Y. Yin, G. Habboub, H.-Y. Gilbert, Y. Li, S. Nakao, A. Hafezi-Moghadam & L. I. Benowitz (2013) Neutrophils express oncomodulin and promote optic nerve regeneration. *The Journal of neuroscience : the official journal of the Society for Neuroscience,* 33**,** 14816-14824.

Lachenmaier, S. M., M. A. Deli, M. Meissner & O. Liesenfeld (2011) Intracellular transport of Toxoplasma gondii through the blood-brain barrier. *J Neuroimmunol,* 232**,** 119-30.

Landrith, T. A., T. H. Harris & E. H. Wilson (2015) Characteristics and critical function of CD8+ T cells in the Toxoplasma-infected brain. *Semin Immunopathol,* 37**,** 261-70.

Lee, Y. H. & L. H. Kasper (2004) Immune responses of different mouse strains after challenge with equivalent lethal doses of Toxoplasma gondii. *Parasite,* 11**,** 89-97.

Li, B., R.-S. Woo, L. Mei & R. Malinow (2007) The Neuregulin-1 Receptor ErbB4 Controls Glutamatergic Synapse Maturation and Plasticity. *Neuron,* 54**,** 583-597.

Li, S., B. He, C. Yang, J. Yang, L. Wang, X. Duan, X. Deng, J. Zhao & R. Fang (2020) Comparative transcriptome analysis of normal and CD44-deleted mouse brain under chronic infection with Toxoplasma gondii. *Acta Trop,* 210**,** 105589.

Liesenfeld, O., J. Kosek, J. S. Remington & Y. Suzuki (1996) Association of CD4+ T cell-dependent, interferon-gamma-mediated necrosis of the small intestine with genetic susceptibility of mice to peroral infection with Toxoplasma gondii. *J Exp Med,* 184**,** 597-607.

Liesmaa, I., R. Paakkanen, A. Järvinen, V. Valtonen & M. L. Lokki (2018) Clinical features of patients with homozygous complement C4A or C4B deficiency. *PLoS One,* 13**,** e0199305.

Lilue, J., U. B. Müller, T. Steinfeldt & J. C. Howard (2013) Reciprocal virulence and resistance polymorphism in the relationship between Toxoplasma gondii and the house mouse. *Elife,* 2**,** e01298.

Lima, T. S. & M. B. Lodoen (2019) Mechanisms of Human Innate Immune Evasion by Toxoplasma gondii. *Front Cell Infect Microbiol,* 9**,** 103.

Liu, D. L., Z. Hong, J. Y. Li, Y. X. Yang, C. Chen & J. R. Du (2021) Phthalide derivative CD21 attenuates tissue plasminogen activator-induced hemorrhagic transformation in ischemic stroke by enhancing macrophage scavenger receptor 1-mediated DAMP (peroxiredoxin 1) clearance. *J Neuroinflammation,* 18**,** 143.

Liu, M., W. Solomon, J. C. Cespedes, N. O. Wilson, B. Ford & J. K. Stiles (2018) Neuregulin-1 attenuates experimental cerebral malaria (ECM) pathogenesis by regulating ErbB4/AKT/STAT3 signaling. *Journal of Neuroinflammation,* 15**,** 104.

Liu, Q., Z. D. Wang, S. Y. Huang & X. Q. Zhu (2015) Diagnosis of toxoplasmosis and typing of Toxoplasma gondii. *Parasit Vectors,* 8**,** 292.

Liu, X. Q., X. R. Shao, Y. Liu, Z. X. Dong, S. H. Chan, Y. Y. Shi, S. N. Chen, L. Qi, L. Zhong, Y. Yu, T. Lv, P. F. Yang, L. Y. Li, X. B. Wang, X. D. Zhang, X. Li, W. Zhao, L. Sehgal & M. Li (2022) Tight junction protein 1 promotes vasculature remodeling via regulating USP2/TWIST1 in bladder cancer. *Oncogene,* 41**,** 502-514.

Lu, N., C. Liu, J. Wang, Y. Ding & Q. Ai. 2015. Toxoplasmosis complicating lung cancer: a case report. In *Int Med Case Rep J*, 37-40.

Lüder, C. G., T. Lang, B. Beuerle & U. Gross (1998) Down-regulation of MHC class II molecules and inability to up-regulate class I molecules in murine macrophages after infection with Toxoplasma gondii. *Clinical and experimental immunology,* 112**,** 308-316.

Lüder, C. G. K. & F. Seeber (2001) Toxoplasma gondii and MHC-restricted antigen presentation: on degradation, transport and modulation. *International Journal for Parasitology,* 31**,** 1355-1369.

Machala, L., P. Kodym, M. Malý, M. Geleneky, O. Beran & D. Jilich (2015) [Toxoplasmosis in immunocompromised patients]. *Epidemiol Mikrobiol Imunol,* 64**,** 59-65.

Massena, S., G. Christoffersson, E. Vågesjö, C. Seignez, K. Gustafsson, F. Binet, C. Herrera Hidalgo, A. Giraud, J. Lomei, S. Weström, M. Shibuya, L. Claesson-Welsh, P. Gerwins, M. Welsh, J. Kreuger & M. Phillipson (2015) Identification and characterization of VEGF-A-responsive neutrophils expressing CD49d, VEGFR1, and CXCR4 in mice and humans. *Blood,* 126**,** 2016-26.

McCormack, R., R. Hunte, E. R. Podack, G. V. Plano & N. Shembade (2020) An Essential Role for Perforin-2 in Type I IFN Signaling. *J Immunol,* 204**,** 2242-2256.

McGovern, K. E. & E. H. Wilson (2013) Role of Chemokines and Trafficking of Immune Cells in Parasitic Infections. *Current immunology reviews,* 9**,** 157-168.

Meireles, L. R., C. C. Ekman, H. F. Andrade, Jr. & E. J. Luna (2015) HUMAN TOXOPLASMOSIS OUTBREAKS AND THE AGENT INFECTING FORM. FINDINGS FROM A SYSTEMATIC REVIEW. *Rev Inst Med Trop Sao Paulo,* 57**,** 369-76.

Melbourne, J. K., C. Rosen, B. Feiner & R. P. Sharma (2018) C4A mRNA expression in PBMCs predicts the presence and severity of delusions in schizophrenia and bipolar disorder with psychosis. *Schizophr Res,* 197**,** 321-327.

Mendez, O. A., E. Flores Machado, J. Lu & A. A. Koshy (2021) Injection with Toxoplasma gondii protein affects neuron health and survival. *Elife,* 10.

Mendez, O. A. & A. A. Koshy (2017) Toxoplasma gondii: Entry, association, and physiological influence on the central nervous system. *PLoS pathogens,* 13**,** e1006351-e1006351.

Mercer, F., S. H. Ng, T. M. Brown, G. Boatman & P. J. Johnson (2018) Neutrophils kill the parasite Trichomonas vaginalis using trogocytosis. *PLoS biology,* 16**,** e2003885.

Merritt, E. F., H. J. Johnson, Z. S. Wong, A. S. Buntzman, A. C. Conklin, C. M. Cabral, C. E. Romanoski, J. P. Boyle & A. A. Koshy (2020) Transcriptional Profiling Suggests T Cells Cluster around Neurons Injected with Toxoplasma gondii Proteins. *mSphere,* 5.

Michelin, A., A. Bittame, Y. Bordat, L. Travier, C. Mercier, J.-F. Dubremetz & M. Lebrun (2009) GRA12, a Toxoplasma dense granule protein associated with the intravacuolar membranous nanotubular network. *International Journal for Parasitology,* 39**,** 299-306.

Miranda, F. J. B., B. C. Rocha, M. C. A. Pereira, L. M. N. Pereira, E. H. M. de Souza, A. P. Marino, P. A. C. Costa, D. V. Vasconcelos-Santos, L. R. V. Antonelli & R. T. Gazzinelli (2021) Toxoplasma gondii-Induced Neutrophil Extracellular Traps Amplify the Innate and Adaptive Response. *mBio,* 12**,** e0130721.

Mirpuri, J. & F. Yarovinsky (2012) IL-6 signaling SOCS critical for IL-12 host response to Toxoplasma gondii. *Future Microbiol,* 7**,** 13-6.

Montoya, J. G. & O. Liesenfeld (2004) Toxoplasmosis. *The Lancet,* 363**,** 1965-1976.

Mukhopadhyay, D., D. Arranz-Solís & J. P. J. Saeij (2020) Influence of the Host and Parasite Strain on the Immune Response During Toxoplasma Infection. *Front Cell Infect Microbiol,* 10**,** 580425.

Nadkarni, S., J. Smith, A. N. Sferruzzi-Perri, A. Ledwozyw, M. Kishore, R. Haas, C. Mauro, D. J. Williams, S. H. Farsky, F. M. Marelli-Berg & M. Perretti (2016) Neutrophils induce proangiogenic T cells with a regulatory phenotype in pregnancy. *Proc Natl Acad Sci U S A,* 113**,** E8415-e8424.

Naegelen, I., N. Beaume, S. Plançon, V. Schenten, E. J. Tschirhart & S. Bréchard (2015) Regulation of Neutrophil Degranulation and Cytokine Secretion: A Novel Model Approach Based on Linear Fitting. *Journal of immunology research,* 2015**,** 817038-817038.

Nakayama, F., S. Nishihara, H. Iwasaki, T. Kudo, R. Okubo, M. Kaneko, M. Nakamura, M. Karube, K. Sasaki & H. Narimatsu (2001) CD15 expression in mature granulocytes is determined by alpha 1,3-fucosyltransferase IX, but in promyelocytes and monocytes by alpha 1,3-fucosyltransferase IV. *J Biol Chem,* 276**,** 16100-6.

Nance, J. P., K. M. Vannella, D. Worth, C. David, D. Carter, S. Noor, C. Hubeau, L. Fitz, T. E. Lane, T. A. Wynn & E. H. Wilson (2012) Chitinase dependent control of protozoan cyst burden in the brain. *PLoS pathogens,* 8**,** e1002990-e1002990.

Neyer, L. E., G. Grunig, M. Fort, J. S. Remington, D. Rennick & C. A. Hunter (1997) Role of interleukin-10 in regulation of T-cell-dependent and T-cell-independent mechanisms of resistance to Toxoplasma gondii. *Infection and immunity,* 65**,** 1675-1682.

Ngô, H. M., Y. Zhou, H. Lorenzi, K. Wang, T.-K. Kim, Y. Zhou, K. El Bissati, E. Mui, L. Fraczek, S. V. Rajagopala, C. W. Roberts, F. L. Henriquez, A. Montpetit, J. M. Blackwell, S. E. Jamieson, K. Wheeler, I. J. Begeman, C. Naranjo-Galvis, N. Alliey-Rodriguez, R. G. Davis, L. Soroceanu, C. Cobbs, D. A. Steindler, K. Boyer, A. G. Noble, C. N. Swisher, P. T. Heydemann, P. Rabiah, S. Withers, P. Soteropoulos, L. Hood & R. McLeod (2017) Toxoplasma Modulates Signature Pathways of Human Epilepsy, Neurodegeneration & Cancer. *Scientific Reports,* 7**,** 11496.

Ni, T., F. Jiao, X. Yu, S. Aden, L. Ginger, S. I. Williams, F. Bai, V. Pražák, D. Karia, P. Stansfeld, P. Zhang, G. Munson, G. Anderluh, S. Scheuring & R. J. C. Gilbert (2020) Structure and mechanism of bactericidal mammalian perforin-2, an ancient agent of innate immunity. *Science Advances,* 6**,** eaax8286.

Nishiyama, S., A. Pradipta, J. S. Ma, M. Sasai & M. Yamamoto (2020) T cell-derived interferon-γ is required for host defense to Toxoplasma gondii. *Parasitol Int,* 75**,** 102049.

Olivera, G. C., E. C. Ross, C. Peuckert & A. Barragan (2021) Blood-brain barrier-restricted translocation of Toxoplasma gondii from cortical capillaries. *Elife,* 10.

Park, M., J. M. Salgado, L. Ostroff, T. D. Helton, C. G. Robinson, K. M. Harris & M. D. Ehlers (2006) Plasticity-induced growth of dendritic spines by exocytic trafficking from recycling endosomes. *Neuron,* 52**,** 817-830.

Parker, S. J., C. W. Roberts & J. Alexander (1991) CD8+ T cells are the major lymphocyte subpopulation involved in the protective immune response to Toxoplasma gondii in mice. *Clin Exp Immunol,* 84**,** 207-12.

Paterson, C., Y. Wang, T. M. Hyde, D. R. Weinberger, J. E. Kleinman & A. J. Law (2017) Temporal, Diagnostic, and Tissue-Specific Regulation of NRG3 Isoform Expression in Human Brain Development and Affective Disorders. *Am J Psychiatry,* 174**,** 256-265.

Peiseler, M. & P. Kubes (2019) More friend than foe: the emerging role of neutrophils in tissue repair. *The Journal of clinical investigation,* 129**,** 2629-2639.

Petri, W. A., G. Reichmann, W. Walker, N. Villegas Eric, L. Craig, G. Cai, J. Alexander & A. Hunter Christopher (2000) The CD40/CD40 Ligand Interaction Is Required for Resistance to Toxoplasmic Encephalitis. *Infection and Immunity,* 68**,** 1312-1318.

Pittman, K. J., P. W. Cervantes & L. J. Knoll (2016) Z-DNA Binding Protein Mediates Host Control of Toxoplasma gondii Infection. *Infect Immun,* 84**,** 3063-70.

Ploix, C. C., S. Noor, J. Crane, K. Masek, W. Carter, D. D. Lo, E. H. Wilson & M. J. Carson (2011) CNS-derived CCL21 is both sufficient to drive homeostatic CD4+ T cell proliferation and necessary for efficient CD4+ T cell migration into the CNS parenchyma following Toxoplasma gondii infection. *Brain, behavior, and immunity,* 25**,** 883-896.

Pott, H., Jr. & A. Castelo (2013) Isolated cerebellar toxoplasmosis as a complication of HIV infection. *Int J STD AIDS,* 24**,** 70-2.

Prandovszky, E., E. Gaskell, H. Martin, J. P. Dubey, J. P. Webster & G. A. McConkey (2011) The neurotropic parasite Toxoplasma gondii increases dopamine metabolism. *PloS one,* 6**,** e23866-e23866.

Prasad, K. M., K. V. Chowdari, L. A. D'Aiuto, S. Iyengar, J. A. Stanley & V. L. Nimgaonkar (2018) Neuropil contraction in relation to Complement C4 gene copy numbers in independent cohorts of adolescent-onset and young adult-onset schizophrenia patients-a pilot study. *Transl Psychiatry,* 8**,** 134.

Prevention, C. f. D. C. a. 2018. Parasites - Toxoplasmosis (Toxoplasma infection).

Radke, J. B., D. Worth, D. Hong, S. Huang, W. J. Sullivan, Jr., E. H. Wilson & M. W. White (2018) Transcriptional repression by ApiAP2 factors is central to chronic toxoplasmosis. *PLOS Pathogens,* 14**,** e1007035.

Resende, M. G., B. Fux, B. C. Caetano, E. A. Mendes, N. M. Silva, A. M. Ferreira, M. N. Melo, R. W. A. Vitor & R. T. Gazzinelli (2008) The role of MHC haplotypes H2d/H2b in mouse resistance/susceptibility to cyst formation is influenced by the lineage of infective Toxoplasma gondii strain. *Anais da Academia Brasileira de Ciências,* 80**,** 85-99.

Ridderbusch, I. C., J. Richter, Y. Yang, M. Hoefler, H. Weber, A. Reif, A. Hamm, C. A. Pané-Farré, A. L. Gerlach, A. Stroehle, B. Pfleiderer, V. Arolt, H. U. Wittchen, A. Gloster, T. Lang, S. Helbig-Lang, L. Fehm, P. Pauli, T. Kircher, U. Lueken & B. Straube (2019) Association of rs7688285 allelic variation coding for GLRB with fear reactivity and exposure-based therapy in patients with panic disorder and agoraphobia. *Eur Neuropsychopharmacol,* 29**,** 1138-1151.

Robert-Gangneux, F. & M. L. Dardé (2012) Epidemiology of and diagnostic strategies for toxoplasmosis. *Clin Microbiol Rev,* 25**,** 264-96.

Russo, R. C., C. C. Garcia, M. M. Teixeira & F. A. Amaral (2014) The CXCL8/IL-8 chemokine family and its receptors in inflammatory diseases. *Expert Rev Clin Immunol,* 10**,** 593-619.

Sa, Q., E. Ochiai, T. Sengoku, M. E. Wilson, M. Brogli, S. Crutcher, S. A. Michie, B. Xu, L. Payne, X. Wang & Y. Suzuki (2014) VCAM-1/α4β1 integrin interaction is crucial for prompt recruitment of immune T cells into the brain during the early stage of reactivation of chronic infection with Toxoplasma gondii to prevent toxoplasmic encephalitis. *Infect Immun,* 82**,** 2826-39.

Saab, A. S. & K. A. Nave (2017) Myelin dynamics: protecting and shaping neuronal functions. *Curr Opin Neurobiol,* 47**,** 104-112.

Sabin, A. B. & J. Warren (1942) Therapeutic effectiveness of certain sulfonamides on infection by an intracellular protozoon (Toxoplasma). *Proceedings of the Society for Experimental Biology and Medicine,* 51**,** 19-23.

Sas, A. R., K. S. Carbajal, A. D. Jerome, R. Menon, C. Yoon, A. L. Kalinski, R. J. Giger & B. M. Segal (2020) A new neutrophil subset promotes CNS neuron survival and axon regeneration. *Nature Immunology,* 21**,** 1496-1505.

Sasai, M. & M. Yamamoto (2019) Innate, adaptive, and cell-autonomous immunity against Toxoplasma gondii infection. *Exp Mol Med,* 51**,** 1-10.

Schneider, C. A., D. X. Figueroa Velez, R. Azevedo, E. M. Hoover, C. J. Tran, C. Lo, O. Vadpey, S. P. Gandhi & M. B. Lodoen (2019) Imaging the dynamic recruitment of monocytes to the blood-brain barrier and specific brain regions during Toxoplasma gondii infection. *Proc Natl Acad Sci U S A,* 116**,** 24796-24807.

Schultz, T. L., C. P. Hencken, L. E. Woodard, G. H. Posner, R. H. Yolken, L. Jones-Brando & V. B. Carruthers (2014) A thiazole derivative of artemisinin moderately reduces Toxoplasma gondii cyst burden in infected mice. *J Parasitol,* 100**,** 516-21.

Sellers, R. S., C. B. Clifford, P. M. Treuting & C. Brayton (2011) Immunological Variation Between Inbred Laboratory Mouse Strains: Points to Consider in Phenotyping Genetically Immunomodified Mice. *Veterinary Pathology,* 49**,** 32-43.

Serrano-Saiz, E., M. C. Vogt, S. Levy, Y. Wang, K. K. Kaczmarczyk, X. Mei, G. Bai, A. Singson, B. D. Grant & O. Hobert (2020) SLC17A6/7/8 Vesicular Glutamate Transporter Homologs in Nematodes. *Genetics,* 214**,** 163-178.

Shichita, T., M. Ito, R. Morita, K. Komai, Y. Noguchi, H. Ooboshi, R. Koshida, S. Takahashi, T. Kodama & A. Yoshimura (2017) MAFB prevents excess inflammation after ischemic stroke by accelerating clearance of damage signals through MSR1. *Nature Medicine,* 23**,** 723-732.

Shinjyo, N., H. Nakayama, L. Li, K. Ishimaru, K. Hikosaka, N. Suzuki, H. Yoshida & K. Norose (2021) Hypericum perforatum extract and hyperforin inhibit the growth of neurotropic parasite Toxoplasma gondii and infection-induced inflammatory responses of glial cells in vitro. *J Ethnopharmacol,* 267**,** 113525.

Sibley, L. D., E. Weidner & J. L. Krahenbuhl (1985) Phagosome acidification blocked by intracellular Toxoplasma gondii. *Nature,* 315**,** 416.

Simmons, L. J., M. C. Surles-Zeigler, Y. Li, G. D. Ford, G. D. Newman & B. D. Ford (2016) Regulation of inflammatory responses by neuregulin-1 in brain ischemia and microglial cells in vitro involves the NF-kappa B pathway. *Journal of Neuroinflammation,* 13**,** 237.

Solomon, W., N. O. Wilson, L. Anderson, S. Pitts, J. Patrickson, M. Liu, B. D. Ford & J. K. Stiles (2014) Neuregulin-1 attenuates mortality associated with experimental cerebral malaria. *Journal of neuroinflammation,* 11**,** 9-9.

Still, K. M., S. J. Batista, C. A. O'Brien, O. O. Oyesola, S. P. Früh, L. M. Webb, I. Smirnov, M. A. Kovacs, M. N. Cowan, N. W. Hayes, J. A. Thompson, E. D. Tait Wojno & T. H. Harris (2020) Astrocytes promote a protective immune response to brain Toxoplasma gondii infection via IL-33-ST2 signaling. *PLoS Pathog,* 16**,** e1009027.

Stirling, D. P., S. Liu, P. Kubes & V. W. Yong (2009) Depletion of Ly6G/Gr-1 Leukocytes after Spinal Cord Injury in Mice Alters Wound Healing and Worsens Neurological Outcome. *The Journal of Neuroscience,* 29**,** 753.

Strauss, R. E., L. Mezache, R. Veeraraghavan & R. G. Gourdie (2021) The Cx43 Carboxyl-Terminal Mimetic Peptide αCT1 Protects Endothelial Barrier Function in a ZO1 Binding-Competent Manner. *Biomolecules,* 11.

Sukhumavasi, W., C. E. Egan & E. Y. Denkers (2007) Mouse Neutrophils Require JNK2 MAPK for Toxoplasma gondii-Induced IL-12p40 and CCL2/MCP-1 Release. *The Journal of Immunology,* 179**,** 3570.

Suzuki, Y. (2002) Host Resistance in the Brain against Toxoplasma gondii. *The Journal of Infectious Diseases,* 185**,** S58-S65.

Suzuki, Y., F. K. Conley & J. S. Remington (1989) Importance of endogenous IFN-gamma for prevention of toxoplasmic encephalitis in mice. *J Immunol,* 143**,** 2045-50.

Swierzy, I., U. Händel, A. Kaever, M. Jarek, M. Scharfe, D. Schlüter & C. Lüder (2017) Divergent co-Transcriptomes of different host cells infected with Toxoplasma gondii reveal cell type-specific host-parasite interactions. *Scientific Reports,* 7.

Takamori, S., J. S. Rhee, C. Rosenmund & R. Jahn (2001) Identification of differentiation-associated brain-specific phosphate transporter as a second vesicular glutamate transporter (VGLUT2). *J Neurosci,* 21**,** Rc182.

Tan, G.-H., Y.-Y. Liu, X.-L. Hu, D.-M. Yin, L. Mei & Z.-Q. Xiong (2011) Neuregulin 1 represses limbic epileptogenesis through ErbB4 in parvalbumin-expressing interneurons. *Nature Neuroscience,* 15**,** 258.

Tanaka, S., M. Nishimura, F. Ihara, J. Yamagishi, Y. Suzuki & Y. Nishikawa (2013) Transcriptome analysis of mouse brain infected with Toxoplasma gondii. *Infection and immunity,* 81**,** 3609-3619.

Thiébaut, R., S. Leproust, G. Chêne & R. Gilbert (2007) Effectiveness of prenatal treatment for congenital toxoplasmosis: a meta-analysis of individual patients' data. *Lancet,* 369**,** 115-22.

Tomita, T., D. J. Bzik, Y. F. Ma, B. A. Fox, L. M. Markillie, R. C. Taylor, K. Kim & L. M. Weiss (2013) The Toxoplasma gondii cyst wall protein CST1 is critical for cyst wall integrity and promotes bradyzoite persistence. *PLoS pathogens,* 9**,** e1003823-e1003823.

Tsuda, Y., H. Takahashi, M. Kobayashi, T. Hanafusa, D. N. Herndon & F. Suzuki (2004) Three Different Neutrophil Subsets Exhibited in Mice with Different Susceptibilities to Infection by Methicillin-Resistant Staphylococcus aureus. *Immunity,* 21**,** 215-226.

Tsytsykova, A. V. & A. E. Goldfeld (2002) Inducer-specific enhanceosome formation controls tumor necrosis factor alpha gene expression in T lymphocytes. *Mol Cell Biol,* 22**,** 2620-31.

Ustyanovska Avtenyuk, N., G. Choukrani, E. Ammatuna, T. Niki, E. Cendrowicz, H. J. Lourens, G. Huls, V. R. Wiersma & E. Bremer (2021) Galectin-9 Triggers Neutrophil-Mediated Anticancer Immunity. *Biomedicines,* 10.

Valgardsdottir, R., I. Cattaneo, C. Klein, M. Introna, M. Figliuzzi & J. Golay (2017) Human neutrophils mediate trogocytosis rather than phagocytosis of CLL B cells opsonized with anti-CD20 antibodies. *Blood,* 129**,** 2636-2644.

Villard, O., B. Cimon, C. L'Ollivier, H. Fricker-Hidalgo, N. Godineau, S. Houze, L. Paris, H. Pelloux, I. Villena & E. Candolfi (2016) Serological diagnosis of Toxoplasma gondii infection: Recommendations from the French National Reference Center for Toxoplasmosis. *Diagn Microbiol Infect Dis,* 84**,** 22-33.

Villarino, A., L. Hibbert, L. Lieberman, E. Wilson, T. Mak, H. Yoshida, R. A. Kastelein, C. Saris & C. A. Hunter (2003) The IL-27R (WSX-1) Is Required to Suppress T Cell Hyperactivity during Infection. *Immunity,* 19**,** 645-655.

Virreira Winter, S., W. Niedelman, K. D. Jensen, E. E. Rosowski, L. Julien, E. Spooner, K. Caradonna, B. A. Burleigh, J. P. Saeij, H. L. Ploegh & E. M. Frickel (2011) Determinants of GBP recruitment to Toxoplasma gondii vacuoles and the parasitic factors that control it. *PLoS One,* 6**,** e24434.

Vogel, N., M. Kirisits, E. Michael, H. Bach, M. Hostetter, K. Boyer, R. Simpson, E. Holfels, J. Hopkins, D. Mack, M. B. Mets, C. N. Swisher, D. Patel, N. Roizen, L. Stein, M. Stein, S. Withers, E. Mui, C. Egwuagu, J. Remington, R. Dorfman & R. McLeod (1996) Congenital toxoplasmosis transmitted from an immunologically competent mother infected before conception. *Clin Infect Dis,* 23**,** 1055-60.

Vyas, A., S.-K. Kim, N. Giacomini, J. C. Boothroyd & R. M. Sapolsky (2007) Behavioral changes induced by Toxoplasma infection of rodents are highly specific to aversion of cat odors. *Proceedings of the National Academy of Sciences of the United States of America,* 104**,** 6442-6447.

Wang, F., Y. J. Yang, N. Yang, X. J. Chen, N. X. Huang, J. Zhang, Y. Wu, Z. Liu, X. Gao, T. Li, G. Q. Pan, S. B. Liu, H. L. Li, S. P. J. Fancy, L. Xiao, J. R. Chan & F. Mei (2018) Enhancing Oligodendrocyte Myelination Rescues Synaptic Loss and Improves Functional Recovery after Chronic Hypoxia. *Neuron,* 99**,** 689-701.e5.

Wang, Z.-D., H.-H. Liu, Z.-X. Ma, H.-Y. Ma, Z.-Y. Li, Z.-B. Yang, X.-Q. Zhu, B. Xu, F. Wei & Q. Liu (2017) Toxoplasma gondii Infection in Immunocompromised Patients: A Systematic Review and Meta-Analysis. *Frontiers in Microbiology,* 8**,** 389.

Watts, E., Y. Zhao, A. Dhara, B. Eller, A. Patwardhan & A. P. Sinai (2015) Novel Approaches Reveal that Toxoplasma gondii Bradyzoites within Tissue Cysts Are Dynamic and Replicating Entities In Vivo. *mBio,* 6**,** e01155-15.

Webster, J. P. & G. A. McConkey (2010) Toxoplasma gondii-altered host behaviour: clues as to mechanism of action. *Folia Parasitol (Praha),* 57**,** 95-104.

Wilson, E. H., U. Wille-Reece, F. Dzierszinski & C. A. Hunter (2005) A critical role for IL-10 in limiting inflammation during toxoplasmic encephalitis. *Journal of Neuroimmunology,* 165**,** 63-74.

Wu, M., O. Cudjoe, J. Shen, Y. Chen & J. Du (2020) The Host Autophagy During Toxoplasma Infection. *Front Microbiol,* 11**,** 589604.

Xiao, J., Y. Li, L. Jones-Brando & R. H. Yolken (2013) Abnormalities of neurotransmitter and neuropeptide systems in human neuroepithelioma cells infected by three Toxoplasma strains. *J Neural Transm (Vienna),* 120**,** 1631-9.

Xie, X., Q. Shi, P. Wu, X. Zhang, H. Kambara, J. Su, H. Yu, S.-Y. Park, R. Guo, Q. Ren, S. Zhang, Y. Xu, L. E. Silberstein, T. Cheng, F. Ma, C. Li & H. R. Luo (2020) Single-cell transcriptome profiling reveals neutrophil heterogeneity in homeostasis and infection. *Nature immunology,* 21**,** 1119-1133.

Xu, Z., G. D. Ford, D. R. Croslan, J. Jiang, A. Gates, R. Allen & B. D. Ford (2005) Neuroprotection by neuregulin-1 following focal stroke is associated with the attenuation of ischemia-induced pro-inflammatory and stress gene expression. *Neurobiology of Disease,* 19**,** 461-470.

Yang, J., Z. He, C. Chen, J. Zhao & R. Fang (2022) Starch Branching Enzyme 1 Is Important for Amylopectin Synthesis and Cyst Reactivation in Toxoplasma gondii. *Microbiol Spectr***,** e0189121.

Yap, G., M. Pesin & A. Sher (2000) Cutting Edge: IL-12 Is Required for the Maintenance of IFN- Production in T Cells Mediating Chronic Resistance to the Intracellular Pathogen, Toxoplasma gondii. *Journal of Immunology,* 1950**,** 628-31.

Yu, H.-N., W.-K. Park, K.-H. Nam, D. Song, H.-S. Kim, T.-K. Baik & R.-S. Woo. 2015. *Neuregulin 1 Controls Glutamate Uptake by Up-regulating Excitatory Amino Acid Carrier 1 (EAAC1)*.

Yuan, R., C. J. M. Musters, Y. Zhu, T. R. Evans, Y. Sun, E. J. Chesler, L. L. Peters, D. E. Harrison & A. Bartke (2020) Genetic differences and longevity-related phenotypes influence lifespan and lifespan variation in a sex-specific manner in mice. *Aging Cell,* 19**,** e13263.

Zhang, X., G. A. Horwitz, T. R. Prezant, A. Valentini, M. Nakashima, M. D. Bronstein & S. Melmed (1999a) Structure, expression, and function of human pituitary tumor-transforming gene (PTTG). *Mol Endocrinol,* 13**,** 156-66.

Zhang, Y. W., K. Kim, Y. F. Ma, M. Wittner, H. B. Tanowitz & L. M. Weiss (1999b) Disruption of the Toxoplasma gondii bradyzoite-specific gene BAG1 decreases in vivo cyst formation. *Molecular microbiology,* 31**,** 691-701.

Zhou, J. & L. Wang (2017) SAG4 DNA and Peptide Vaccination Provides Partial Protection against T. gondii Infection in BALB/c Mice. *Frontiers in microbiology,* 8**,** 1733-1733.

Zou, X., X. J. Yang, Y. M. Gan, D. L. Liu, C. Chen, W. Duan & J. R. Du (2021) Neuroprotective Effect of Phthalide Derivative CD21 against Ischemic Brain Injury:Involvement of MSR1 Mediated DAMP peroxiredoxin1 Clearance and TLR4 Signaling Inhibition. *J Neuroimmune Pharmacol,* 16**,** 306-317.